,

1

# Università Politecnica delle Marche

DIPARTIMENTO DI INGEGNERIA INDUSTRIALE E SCIENZE MATEMATICHE

Corso di Dottorato di Ricerca in Ingegneria Industriale – Curriculum Ingegneria Energetica

# Tools and Methods to study the integration of flexibility assets in the future Smart Grid

Advisor:
**Prof. Gabriele Comodi**

Ph.D. Dissertation of:
**Francesco Carducci**

Curriculum Supervisor:
**Prof. Ferruccio Mandorli**

To Alice, my beautiful 2 years old niece, which i hope one day will be curious enough to open this dissertation and laugh about the weird ideas of her uncle.

# Abstract

This dissertation presents tools and methodologies to support the research communities, as well as industrial entities and policy makers, understanding the role that flexibility assets and aggregators will play in the future Smart Grid.

A Virtual power plant framework for aggregators of flexibility resources is introduced, based on two operation levels: the "Local assets level", where the aggregator interacts with the end users collecting data to estimate and control their flexibility, and the "Flexibility Aggregator level", where it interacts with the energy market to buy/sell energy and provide different services. For each level, the aggregators objectives are presented , together with a list of the main open questions/challenges from both the research and industry communities.

A generalized modeling methodology is defined to describe and control the different flexibility assets as an equivalent energy storage. Using this formulation it is possible to aggregate the contribution of thousands of heterogeneous assets by evaluating the single time-variant parameters and summing their relative contribution.

A simulation methodology to test the impact of integrating a thermal energy storage with an existing HVAC system is presented, using the School of Art, Design and Media building, located within the NTU campus in Singapore, as case study. Results show how the extra flexibility granted by the energy storage can sensibly improve a building performances, reducing reducing operational costs while improving the cooling system efficiency.

The concept of equivalent storage model is introduced and applied to simulate a heterogeneous population of 1000 thermostatically controlled loads. The study demonstrates how moving from a dynamic setpoint strategy towards a dynamic deadband one, consumers could trade energy saving potential to increase their load flexibility. Relaxing the thermostats control deadband, aggregators can replace more storage capacity integrating the same number of residential costumers. Using the same simulation platform, a study on the impact of different climate areas on the aggregated flexibility is presented. Results show how temperate climates get

the most benefits from a dynamic deadband strategy, giving us precious indications to build targeting recommendations.

A novel modeling approach is defined to describe an aggregation of Electric Vehicles System Equipments (EVSEs) as an equivalent energy storage. The model is based on five parameters that can be estimated using historical charging data. These parameters depend on arrival and departure time, the energy consumed driving and the charging frequency. They should be evaluated for each single EVSE and summed up to aggregate their contribution.

Following our studies on flexibility assets modeling, the results from some experimental tests performed in an industrial microgrid are presented. A sensible heat thermal energy storage and the existing HVAC system are integrated to reduce the peak load during critical hours. Results show that, when the strategy is revoked and the original temperature setpoint is restored, a new peak is generated in terms of power demand. Also, data show that sampling the electricity consumption with a 15 minutes time granularity is adequate to identify the activation of a load shedding strategy.

The last part of the dissertation focuses on how to optimally manage the aggregated capacity gathered from an heterogeneous portfolio of flexibility assets.
A methodology is presented to address the optimal portfolio management problem for flexibility aggregators. The methodology integrates the equivalent storage models for flexibility assets in a convex optimization. The goal of the formulation is to optimally manage the available flexibility resources, leveraging the energy price variability to reduce operational costs, while producing valuable services for the national grid. The methodology is tested in two alternative scenarios. Results show that integrating controllable thermostatically controlled loads and electric vehicles in an urban district, we can reduce aggregators need for extra storage capacity by up to 30%, while providing the same level of service. Results highlight how integrating EVSEs can have a positive, negative or neutral effect depending on mobility schedules and the required service.

Finally, a multi-agent based control architecture is introduced with the scope of managing the flexibility assets of an industrial microgrid. The control architecture is tested using real data from an Italian industrial facility, simulating the interests of an aggregator which seek to optimally control the different flexibility assets of the microgrid to reduce operational costs and limit consumption peaks during critical hours. Different comparison metrics are introduced to highlight how the effectiveness of the control architecture is affected by the energy price variability.

# Acknowledgements

I do believe that our lives represent the weighted sum of all things that happen to us and, most importantly, of all the people we meet.

Looking back i realize today how lucky i have been. There are moments in life when you need to be in the right place, with the right person, having the right discussion. That very discussion will eventually trigger that something in you, that will change your life forever. I would like to say thanks here to some of these right persons that i have met, persons that without knowing it, contributed in their own way to this thesis.

I would like to thank my academic advisor, Gabriele Comodi, who shared with me his vision of the research world, without ever imposing it. He entrusted me completely, giving me the opportunity to learn my way, exploring my own ideas and intuitions. He pushed me to travel, allowing me to growth as a person and as a researcher.

I would like to thank Cristina Cristalli, Antonio Giovannelli and Gino Romiti which for an extended period of time acted as parents figures, advisors and great sources of inspiration for the passion and the energy they demonstrate every day at work.

Thanks to Sila Kiliccote and Emre Can Kara, my technical and spiritual advisors for the period i spent at SLAC, in Silicon Valley. I don't think they fully realize what they did to me, when they granted me the opportunity to join their research group and work with them. They made me realize one of my life dreams, having the chance to work at Stanford, one of those legendary places that we sometimes hear about in movies and books. Not only that. Through their passion and their advices, they made me realize how much i love doing research and how much i would like to be good at my job. For all of this and much more, i will be eternally grateful to them.

I would like to thank Alessandro Romagnoli, an extremely passionate and skilled researcher, who accepted me in his group in Singapore, giving me the unique opportunity to confront myself with a completely different culture.

# Contents

# List of Figures

# List of Tables

# Chapter 1

# Introduction

The way we generate, control and distribute energy has always been one of the pivotal problems for the human race. Men in caves used fire to generate heat and satisfy their primary demands: heating their caves and cooking their food. Along the centuries we evolved, together with our lifestyle and the nature of our necessities: we need light to work and study at night; cooling energy to maintain food for longer periods; mechanical power to move complex machineries. The industrial revolutions first, and the discovery of electricity later, represented a paradigm shift that change the way we thought about energy generation and consumption. These pivotal moments set the cornerstones of the XX century society. All over the world, countries started investing in fossil fuel power plants, in transmission and distribution networks to sustain the growth of energy demand coming from industries and the new cities.

The XX century power grids requirements are quite simple: deliver cheap, reliable electrical power to everyone. XX century power grids are mostly based on big thermal power plants, powered by fossil fuels, and unidirectional transmission/distribution networks, designed to reliably transmit power from generation sites towards final users [87]. This paradigm, that worked fine for over a century, is now challenged by a new set of requirements. The future power grids need to deliver clean, cheap and reliable electrical power to everyone [56]. To make human presence in this planet sustainable, we need our power generation and distribution systems to be sustainable. This means shifting from fossil fuels towards alternative, clean source of energy.

In the last two decades we have seen renewable generation technologies, such as PV solar and wind turbines, getting introduced into every nation's energy mix, in both centralized, large power plants in the order of decades of mega-Watts, and

distributed way, rooftops solar in the order of decades of kilo-Watts. This trend is now stronger than ever, thanks to the ambitious goals that many countries of the world are posing to reduce GHG emissions and record low auction prices, which are making renewable generation every day more competitive. A recent report from the International Energy Agency shows how solar PV installed capacity grew by 50%, about 74 GW, in 2016 alone [55].

The 2016 Paris agreement goes towards this direction, committing industrialized nations to reduce GHG emissions 80% below 1990 levels by 2050. A recent study from E3 indicates a possible pathway to achieve these goals, highlighting how we need to decarbonize the energy generation mix and push for the electrification of our services, from the residential to the mobility sector [86]. Our services' demand is already becoming more and more dependent from the electrical grid, due to novel technologies which are gradually being introduced. Highly efficient Heat pumps use electricity to generate both cooling and heating energy, substituting natural gas that was used for heating purposes. Plug-in electric vehicles aim to contribute to the electrification of both private and commercial mobility sector, reducing our dependency from fossil fuels while affecting the air quality in our cities. These transformations, which are widely recognized as positive first steps towards our path to decarbonization and a more sustainable future, also represent serious challenges for the energy distribution network. They are forcing us to rethink the way we design and operate power grids, which as today are not ready to cope with many of these new technologies.

Power grids are designed to work under balanced supply and demand at all times. This hard constraint is increasingly challenged by uncertain and intermittent renewable generation sources. Historically, grid balance was maintained by operating the controllable thermal generators, dispatching the so called peaker plants which can be ramped up and down at will. These power plants, which remain idle for the majority of the time, are used to balance the demand, sustain power reliability, compensate for grid's frequency and voltage oscillations. This is what we call a "demand following" paradigm: we operate the available peaker plants to cope with the energy demand variance at all time. If the peak demand grows, we build new peaker plants to cope with it.

This paradigm is being challenged by the growth of the peak demand to respect with the average demand. The combined effect of residential loads electrification and the adoption of distributed PV generation, generate a stiff ramp in the national net-load demand during late afternoons, when people goes home from work and

PV production start decreasing. We can see this happening around the world. In California this issue is referred as the Duck Curve problem: CAISO (Californian Independent System Operator) estimated that California's late afternoon ramp needs will increase up to 13 GW by 2020 [18]. Therefore, the system requires a flexible resource mix that can react quickly and balance the fast changes in electricity net demand, avoiding reliability issues. However, an MIT study, based on 2005-2009 data, demonstrates how peaker plants are not anymore a sustainable solution. The study shows how in the states of New England and Washington, the national demand of energy exceeded 70% of its peak for only about 1000 hours per year, so that more then 30% of the installed capacity was in use less then 12% of the time [73]. Leaving aside the environmental standpoint, this trend makes peaker plants less and less appealing also from the economic perspective.

The Smart Grid paradigm offers an alternative solution to this problem by shifting part of the control burden from the generation to the demand side. The Smart Grid combines advancement in information technology, power systems, energy systems engineering and data analysis to increase the power grid reliability. It works by leveraging data to better manage grids' resources, remotely controlling a portfolio of distributed technologies so that they can actively respond to changing grid conditions [58].
The Smart Grid implies a Copernican revolution from the perspective of the old paradigm: we operate on the energy demand to cope with the variability of our energy mix. Technically, we move part of the control burden from the centralized generation systems to end users, incentivizing a diverse use of energy to reduce the need for extra peaker plants. In this new paradigm, consumers play a more active role, which is now possible thanks to the diffusion of low cost advanced metering infrastructure and distributed technologies, such as remotely controllable inverter, rooftop PV solar and electric energy storage systems.

Demand response programs were designed to engage end users and promote this new paradigm. They aim to increase the distribution network flexibility using a bottom up approach, aggregating distributed energy resources (DER) to maintain the grid balance during critical hours. In exchange for using their resources, end users get rewarded with economic benefits or services [82]. In this dissertation, we use the term "Flexibility assets" to indicate DERs which can be coordinated and controlled to reshape the energy demand at distribution level, providing extra flexibility and services to the national grid (e.g. electric energy storage systems (EES), distributed generation plants, as well as interruptible residential and industrial loads).

These flexibility assets are characterized by their relative small capacities with respect to the centralized generation, and they are connected to low and medium voltage electricity distribution grids. Thus, while they have huge untapped potential, they need to be aggregated to functionally replace peaker plants in delivering valuable electricity services. The Aggregation process is defined as the effort of grouping distinct agents in a power system (i.e. consumers, producers, storage assets) to act as a single entity when interacting with an energy market [15]. This effort is coordinate by a new player in the energy market, the aggregator. Aggregators are companies who act intermediary between end users and DER owners that are willing to offer their capacity in exchange for benefits, and the power grid participants which are willing to pay for the extra capacity [51].

Throughout this dissertation we will talk about flexibility assets, developing models, methodologies and tools that can help us imagine their role in the future energy distribution system. We will look at the problems from the prospective of an aggregator, addressing some of the open questions that must be answered before the Smart Grid vision becomes a reality.

## 1.1 Goals and main contributions

**The main goal of this dissertation is to introduce tools and methods to support the research community, as well as industrial entities and policy makers, understanding the role that flexibility assets and aggregators will play in the future Smart Grid.**
This research field, while being in constant expansion and evolution, is already extremely wide and complex. For this reason we decided to narrow the scope of this work, defining our own vision for flexibility aggregators and focusing on three specific types of flexibility assets: energy storage systems, thermostatically controlled loads (TCLs) and electric vehicles (EVs).
The aggregator we envisioned is interested in the direct load control approach to demand response, as opposed to the indirect one. The Direct load control paradigm sees the aggregator as a central entity developing and enforcing automated control strategies to dispatch the distributed assets which are part of its portfolio of resources; on the other hand, the indirect control approach wants to trigger behavioral changes in the end users by setting an exogenous stimulus, e.g. a new energy price tariff that penalizes specific hours of the day. We believe the former approach to be more interesting due to its characteristics, which make it suitable for a wide

range of grid services and demand side management applications, from slow ones (e.g. price arbitrage in the day ahead market) to really fast one (e.g. grid primary regulation) [59].

Our main contributions to the state of the art are the following:

- We introduce a Virtual Power Plant architecture for Aggregators interested in performing direct load control of flexibility assets.

- By simulating an heterogeneous population of 1000 TCLs, we demonstrate how a control strategy based on deadbands relaxation can significantly increase the aggregated demand flexibility at the expense of energy efficiency.

- We define a modeling approach to describe and control an aggregate of EVs charging stations as an equivalent energy storage.

- By performing tests in an industrial microgrid, we demonstrate that it is possible to identify the activation of a peak reduction strategy using electricity consumption data collected with a 15 minutes time granularity

- We define a methodology to solve the optimal portfolio management problem for flexibility aggregators, using the equivalent energy storage models developed for the different flexibility assets within a convex formulation

- We present a multi-agent based control mechanism tailored over the necessities of an industrial microgrid.

## 1.2 Dissertation Overview

In chapter 2, we introduce the Virtual Flexibility Plant framework for aggregators. We distinguish between two operation layers for the aggregator. Each layer brings its own open questions to be answered and challenges to be handled. Also, in this chapter we present four different categories of flexibility assets, highlighting the importance of introducing a general modeling formulation.

In chapter 3, we present a study on the effect of a thermal energy storage when coupled with an existing Heating Ventilating and Cooling (HVAC) system. In particular we show how we can use the extra system flexibility to better manage the heat pumps and increase the overall system efficiency.

In chapter 4, we implement a methodology to estimate the technical potential of an aggregation of heterogeneous TCLs in providing demand response (DR) services.

We use this methodology to assess the effect of different control strategies, and different climate conditions, on the flexibility estimation.

In chapter 5, we focus on EV. We first discuss about risks and opportunities related to a potential shift from fossil fuel based mobility towards EV. Then we introduce an equivalent storage model for aggregations of EV charging stations.

In Chapter 6, we present some preliminary results obtained by introducing some advanced demand management strategies in an industrial building. These strategies aim to control the HVAC system and the local thermal energy storage to reduce the building load during peak hours of the day.

In chapter 7, we introduce an optimal portoflio management strategy for flexibility aggregators. We use it to optimally size the flexibility assets in the portfolio or, given a fixed portfolio, to obtain the optimal dispatch profile. The framework uses an equivalent energy storage approach to model the different assets of a potential portfolio (Energy storages, EVs, TCLs). We present a general convex formulation to address the optimal dispatch problem.

In chapter 8, we introduce a multi-agent based control architecture to efficiently dispatch the flexibility assets of an industrial microgrid, based on DER availability and time-of-use rates (TOU). We use actual consumption and generation data from an Italian industrial microgrid and energy prices from different markets. The study aims at highlighting the potential of such a control architecture and the impact of the energy price.

In chapter 9, we conclude discussing the results we obtained and the impact we expect for our research. We also suggest some future research path that can potentially develop from our work.

# Chapter 2

# The Virtual Flexibility Plant for Aggregators

## 2.1 Preface to Chapter 2

In this chapter we introduce the Virtual Flexibility Plant framework for aggregators of flexibility assets. We first present the related literature on the topic, then we introduce the framework to describe the different tasks that the aggregator faces at both the end users and aggregate levels. We use the last portion of the chapter to introduce the general idea of equivalent storage formulation, explaining its crucial role when modeling the different flexibility assets. Many of the concepts introduced here will be referenced later throughout the thesis.

## 2.2 Introduction

The electrical distribution system is facing significant changes from both the generation and the demand prospectives. From the generation side we introduced new distributed generation capabilities, intermittent renewable sources and new, more and more affordable, ways to store energy. From the demand side we are seeing a new electric loads coming from the residential, industrial and even the mobility sector. Distributed energy sources (DERs) are connected to the low and medium voltage distribution grids and are characterized by smaller capacity with respect to the centralized units. Their primary goal is to provide reliable, stable, power to local users, however their distributed nature enables a new set of services towards both the final user and, once aggregated and coordinately controlled, the entire distribution grid. Many studies from recent literature focus on the technical po-

tential of DERs, energy storage systems and demand response strategies that, once aggregated, can generate benefits for the distribution grid and value streams for the end user. In [71] authors describe a method to estimate the technical potential that California could leverage aggregating residential TCLs to provide frequency regulation and spinning/nonspinning reserve. In [61] authors estimate the potential benefits of aggregating large numbers of electric vehicles charging stations to optimally coordinate their charging strategy based on a time of use (TOU) rate structure. To untap the full potential of these controllable distributed resources, to make them observable and controllable, we must integrate them with smart sensors and information technologies. Aggregators play a critical role as enablers, being both the technology providers and the ones interested in using the untapped potential to contract services with the grid. Aggregators are service and technology providers, facilitating an active participation of end users and DER owners with the energy market. They form a portfolio of consumers, distributed generation systems and controllable assets (e.g. DERs, energy storage) that must be optimally managed with respect to an energy market. In [15] authors explore the value of aggregation, distinguishing among different categories of them, showing how different regulatory and market frameworks can be leveraged by aggregators to generate value for them-self, for end-users and the entire distribution system. For example, they can assume the basic role of retailers for their end users, while creating a value stream for all the flexible assets and prosumers who wants to act as distributed grid resources [14]. From the national grid prospective, the aggregator portfolio of consumers, generators and storage represents a virtual power plant: an additional backup resource that can be dispatched for a price. Virtual power plant (VPP) aggregate distributed generation units, consumers and energy storage systems creating an ICT infrastructure to allow the continuous exchange of data. VPP main goal is to optimally manage the distributed resources by trading the overall capacity in an energy exchange platform. In recent years this vision of Virtual Power Plants made by the aggregated contribution of many distributed assets have been garnering interest in the research community. We suggest the interested reader to refer to the work of Nosratabadi et al. [79]. They present a comprehensive review of the concept of virtual power plant in relation to the one of microgrid and distributed resources. They also study the optimal scheduling problem, analyzing the state of the art in all its aspects: modeling techniques, solving methods, objectives. In this chapter we introduce a VPP framework for flexibility aggregators. We refer to it as the Virtual Flexibility Plant (VFP). The VFP represents the aggregation

mechanism we envisioned. We distinguish between two operational layers for the aggregator, Each one with its own open questions to be answered and challenges to be handled. Also, in this chapter we present four different categories of flexibility assets, highlighting the importance of introducing a general modeling formulation.

## 2.3 Framework description

Figure 2.1 shows our framework for aggregators of flexibility assets, we call it Virtual Flexibility Plant (VFP). We need to introduce four entities to describe it. The aggregator has a central lore. It represents the company, or institution, which works as facilitator between the distributed flexibility assets, that can provide distributed flexibility increasing/reducing the consumption capacity, and the energy market which requires such extra capacity. We refer here to energy market as a generic entity which is representative of one or more market frameworks. The aggregator can interact with all of them to buy energy, bid its virtual capacity and price its services. The Minimum flexibility units represent grid nodes over which the aggregator has observability and, in specific cases, direct control. These nodes represent point of connection between the end users and the main grid. Each Minimum flexibility unit is associated to one smart meter. The aggregator has no observability over anything that happens behind this meter. The flexibility assets represent the different kinds of resources that can provide extra flexibility to the end user demand and, through the aggregator, to the distribution network. Throughout this dissertation we are going to focus on three kinds of flexibility assets: energy storage systems, controllable TCLs and electric vehicles. The VFP is a combination of distributed generation units, controllable load and energy storage systems that are aggregated to trade their flexibility for money and reduce their cost of operation. The aggregator, which control the VFP, can coordinate its assets to arbitrage the energy price, by buying more energy during low price hours and bidding its extra capacity during peak hours. Alternatively, it can use its resources to sell specific services to the grid. For example, the fast reactive assets of the portfolio (such as TCLs and energy storage) can be dispatched to provide frequency regulation services. The aggregator we envision operates at two distinguished levels: the "Local assets level", where it interacts with the end users collecting data to estimate and control their flexibility, and the "Flexibility Aggregator level", where it interacts with the energy market to buy/sell energy and provide different services.
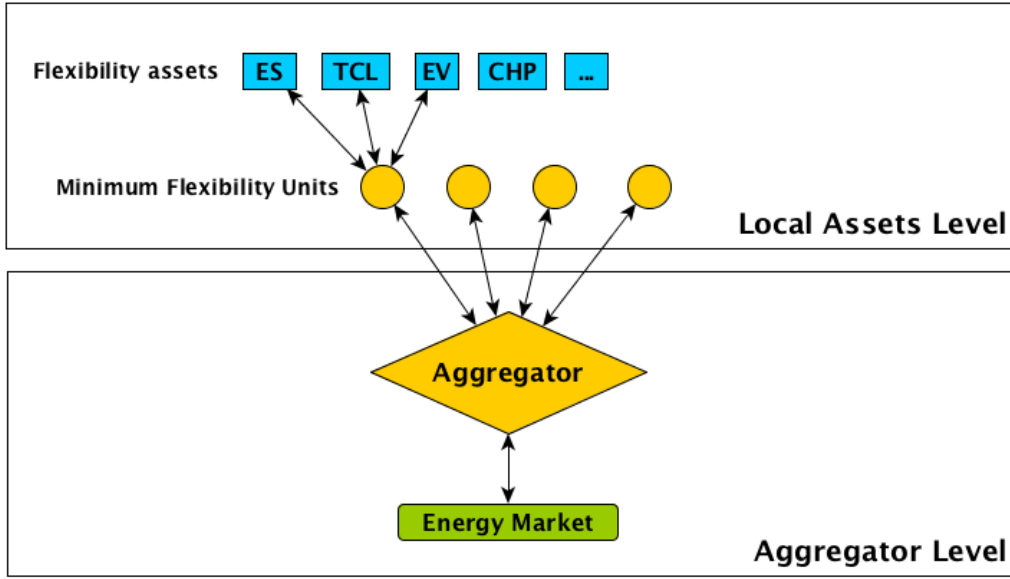
FIGURE 2.1: The Virtual Flexibility Plant architecture for aggregators

### 2.3.1 Local assets level

At the "local assets level", the aggregator establish a peer-to-peer communication channel with each Minimum flexibility unit. From the aggregator prospective each Minimum flexibility unit corresponds to an asset of its portfolio of resources. The aggregator needs observability and controllability over these nodes of its network, thus each of them requires an appropriate advanced metering and communication infrastructure. At any given time, the aggregator needs data on nodes' net-load, which represents the amount of power exchanged with the grid through the metering points. Throughout this work we consider positive net-load when the power is flowing from the main grid towards the end user, which means that behind the meter the demand is greater then the local generation; we consider negative net-load when the power is flowing from the end user towards the main grid, which means that local generation is exceeding the demand. The "Minimum flexibility unit" is an abstraction that represents different types of resources as nodes of the aggregator's portfolio. The Minimum flexibility unit is always associated to a single meter but, depending on the aggregation level, it can be representative of a single flexibility asset (e.g. an energy storage system, a cogeneration plant), a single end user (e.g. an household), multiple end users (e.g. an urban district) or an industrial microgrid. With the "minimum flexibility unit" abstraction, the aggregator is not interested in how complex is the energy network behind a specific meter. Using

historical data, the aggregator evaluates the natural behavior, the baseline, of each node. The baseline is then used as a reference to estimate nodes' flexibility in terms of how much they can variate their power consumption with respect to their natural behavior.

At the Local assets level the aggregator is interested in the following actions:

1. Enable the different Minimum flexibility units by providing the necessary advanced metering infrastructure to ensure observability and control

2. Estimate the baseline behaviour of each Minimum flexibility unit

3. Estimate the flexibility that each Minimum flexibility unit can provide

Both the academic and industrial research communities are working on solving a series of challenges in relation to these services. To begin with, aggregators need data from the Minimum Flexibility Units. It is critical to define standards and protocols to install the appropriate advanced metering infrastructure at the local level. This problem involves different fields. The required set of sensors and communication devices should be advanced enough to ensure observability and control, while being affordable to allow aggregators to build a business model out of their services [57]. Moreover, it is crucial to define safety protocols and communication standards to ensure end users privacy and cyber-security [64].

Once data is obtained, aggregators can move further and estimate, for each minimum flexibility unit, the baseline behavior and the potential flexibility that can be provided. This process involves a modeling effort to transform, for each node, historical and real time data into flexibility insights. All these modeling tasks are necessary to build simulations, define and tests management strategies at both the local assets' and aggregator's levels. These simulations can also be used for targeting purposes, analyzing alternative sets of locations and end users to find the optimal location for the aggregator to invest and propose its services. In this dissertation we choose to focus on the modeling and simulation tasks, defining specific methodologies to study the impact of different flexibility assets at both local and aggregate level. To limit the scope of the research we choose to focus on three kinds of flexibility assets. Chapter 3 is dedicated to energy storage systems, chapter 4 to thermostatically controlled loads and chapter 5 to electric vehicles. We briefly introduce the topic of the metering infrastructure in chapter 6, when we talk about data granularity in demand side management applications, referring to some experimental tests we performed in an industrial microgrid.

### 2.3.2 Aggregator level

At the "Flexibility Aggregator level", the aggregator exchanges data with all the "Minimum flexibility units" of its portfolio to estimate the available flexibility, send control signals and observe the assets response. At the same time, it interacts with the energy market to buy/sell energy and value its aggregated flexibility. The aggregator final goal is to generate value for itself and to the end users which are part of its portfolio by optimally managing their flexibility resources. Aggregating multiple controllable assets, the aggregator accumulates flexibility which can be leveraged to change its market position and provide different kind of services to the national grid. For example, in the case of a residential district, by asking the final users to reduce their net-loads the aggregator dispatches virtual positive capacity; from the national grid prospective the overall energy demand decreases momentarily. By asking to the final users to reduce their net-load the aggregator dispatches virtual negative capacity; from the national grid prospective the overall energy demand increases momentarily. At the Local assets level the aggregator is interested in the following actions:

1. Estimate the aggregated flexibility that its portfolio of assets can provide

2. Identifie the optimal portfolio management strategy using energy price and resource availability forecast to make inform decisions

3. Once identified the optimal strategy, send control signals to the single Minimum flexibility units to dispatch them

4. Verify that each Minimum flexibility unit is actually able to follow the control strategy using real time data and the baseline model

Also at this operational level, there are many challenges that need to be addressed to enable the vision we have for large scale aggregators. Research need to define the necessary data infrastructure, which mean a generalizable data model, data exchange protocols and a functional, scalable and secure database architecture. Aggregators are also interested in how to build and optimally manage their resource portfolios depending on the aggregation scale, market conditions, technical constraints and required services. Another interesting series of problems are related to the development of business strategies to generate value for the end users, while providing a service for the national grid and ensuring a profit for the aggregator. Here, researcher in the field of multi-agent programming and game theory are working to simulate how different remunerative strategies could work to incentivize the

aggregation of end users in coalition, so that they could be willing to offer their flexibility in exchange for money or extra services. For example, Chalkiadakis et al. adopted a similar approach to design a pricing mechanism to incentive fair and efficient cooperative Virtual Power Plants [22].

In this dissertation we focus on how to optimally manage a portfolio of flexibility assets. In particular we introduce and apply two alternative approaches, tailoring them over the requirements of different aggregation levels. In chapter 7, we define a convex formulation to solve the optimal portfolio management problem, applying it to an urban district. In chapter 8, we present a multi-agent based control mechanism to manage the assets of an industrial microgrid.

## 2.4 The equivalent storage formulation

As we discussed in the previous paragraphs, Aggregators want to observe the status, aggregate and control the different flexibility assets of its portfolio. The nature of aggregator's portfolios could be extremely heterogeneous, integrating together different kinds of flexibility assets: office loads through smart plugs, air conditioners through thermostats, EVs through the relative charging stations. Furthermore, depending on the aggregation level the portofolio could refer to the aggregated resources of a local microgrid with a single point of connection with the national grid, an urban district or a regional area with lots of points of connection. For each asset of the portfolio, the aggregator needs to evaluate the relative flexibility, in terms of how much the energy demand of the asset can increase/decrease in respect with the baseline, and the associated cost for the resource dispatch. The Virtual Flexibility Plant Framework introduces an higher abstraction layer in order to model different flexibility assets, and refer to different aggregation levels, using the same formulation. An energy storage system is a machine which stores energy in different forms to increase the level of control over a system. From the grid prospective, it can be considered as a flexibility generator. We can completely define its behavior by knowing its state of charge (the internal energy content to respect with its maximum capacity), its dissipation rate and the amount of power which is being charged/discharged (figure 2.2).
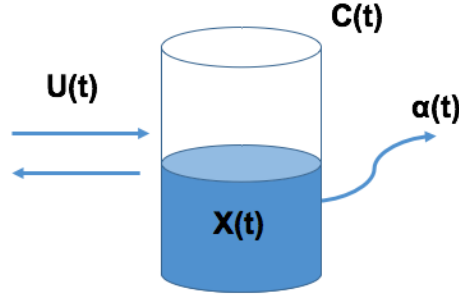
FIGURE 2.2: The equivalent energy storage model.

It seems natural to imagine every other flexibility asset as a particular case of an energy storage system, described by the same parameters while constrained to follow different sets of physical rules. Our Virtual Flexibility Framework uses a general equivalent energy storage formulation to model the contributions of all the different flexibility assets. In doing so we extend the generalized battery concept presented in [49]. Our equivalent storage model is defined by a set of signals $U_{(t)}$ that satisfy the following equations:

$$-\eta_- <= U_{(t)} <= \eta_+ \qquad \dot{x}_t = -\alpha x_t - U_{(t)} \qquad |x_{(t)}| <= C \qquad (2.1)$$

Where $\eta_+$ and $\eta_-$ represent respectively the maximum charging and discharging rates of the equivalent energy storage system; the state variable x represents the internal energy of the system; $\alpha$ is the dissipation rate, the amount of energy naturally lost due to storage inefficiencies, and C the total energy capacity of the equivalent system. We can use this formulation to model and control a generic flexibility resource as a storage. To describe a generic flexibility resource using its equivalent storage form, we need to define how to extrapolate the four equivalent storage parameters (energy capacity, maximum charging/discharging power, dissipation rate) using real time and historical data. This task can be more or less straightforward depending on the flexibility resource nature. As an example, in the case of residential air conditioners the equivalent storage capacity is related to the thermal mass within the thermostat deadband; the state of charge can be associated to the relative distance between the indoor temperature and the comfort limits; the maximum charging rate is equivalent to the maximum cooling capacity of the machine; the dissipation rate is related to internal and external heat gains. Using this formulation, we can aggregate the contribution of thousands of heterogeneous assets by simply summing the equivalent storage parameters. Thus, we are able to describe and control radically different kinds of portfolio using the same set of modeling

and optimization tools. Later in this dissertation we are going to present how to estimate the equivalent storage parameters for an aggregation of controllable TCLs and EVs, respectively chapters 4 and 5.

## 2.5    Conclusion

In this chapter, we introduced the virtual flexibility plant framework for aggregators. The framework is based on two operation levels: the "Local assets level", where the aggregator interacts with the end users collecting data to estimate and control their flexibility, and the "Flexibility Aggregator level", where it interacts with the energy market to buy/sell energy and provide different services. For each level we presented the aggregators objectives, its activities and a list of open questions/challenges from both the research and industry worlds. We explained the reasons behind the need for a generalized modeling methodology and presented the equivalent storage formulation for flexibility assets. Using this formulation, we can aggregate the contribution of thousands of heterogeneous assets by simply summing the equivalent storage parameters. Thus, we are able to describe and control radically different kinds of portfolio using the same set of modeling and optimization tools. In the next chapters we will talk about different flexibility assets, showing how they can be integrated at different levels of the distribution grid and provide different kinds of services.

# Chapter 3

# Energy storage systems as flexibility resources

## 3.1 Preface to Chapter 3

In the last chapter we talked about the Virtual Flexibility Plant framework for aggregators. We used the framework to introduce the main research questions that we will face throughout this dissertation. With this chapter we begin discussing about the different flexibility assets. Specifically, we focus on energy storage systems, showing how they can be integrated with existing HVAC plants to increase the flexibility of the system and produce economic benefits. This chapter has been published as follows: "G.Comodi, F.Carducci, N.Balamurugan, A.Romagnoli; Application of Cold Thermal Energy Storage (CTES) for building demand management in hot climates. Applied Thermal Engineering (2016), V. 103 pp. 1186-1195". I undertook the majority of work related to this chapter, including all the modeling tasks, the development of a simulation platform and the interpretation of results. Mr. Balamurugan provided some preliminary analysis on the dataset. Assistant professors Comodi and Romagnoli contributed with comments on the ideas presented and editorial assistance.

## 3.2 Introduction

Climate change is unequivocal. Each of the last three decades has been successively warmer than any preceding decade since 1850, and the concentration of Greenhouse Gases have increased. Society can reduce the carbon intensity of energy services, pushing the transition toward low-carbon and/or carbon-neutral technologies [39].

Buildings will play an important role since they represent around 40 percent of world energy demand and 25 percent of global water demand, while producing one third of total GHG emissions [36]. Energy demand for building cooling will be one the main causes of the growing energy consumption of developing countries located in hot/tropical climates, hence major efforts are necessary to limit their energy demand. Demand Side Management is a mean to increase the efficiency of an entire power system, from generation to the end use, optimizing resources allocation, limiting the peak demand, shaping the loads depending on the necessity of the grid [94]. In this context, Thermal Energy Storage (TES) is becoming more and more interesting, since it currently represents one of the most cost-effective solutions to enable demand management strategies [4]; TES enables storing thermal energy (either heat or cold) through a storage medium capable to release the required amount of energy when needed [34]. Several studies demonstrated the effectiveness of such systems in different contexts. Cabeza et al. [16] showed the CO2 mitigation potential of TES systems for different applications (refrigeration, solar power plants, passive system in buildings, greenhouses, dishwashers) and countries. They emphasize the importance of analysing each scenario separately, since different applications impact the energy system in different ways and the results can be heavily affected by the energy mix of the reference country. Arteconi et al. [5] described an existing installation of TES in Italy and performed simulations to prove the potential of different Demand Side Management strategies. Their results showed that the use of TES leads to an increase in energy demand, while costs decrease proportionally with the difference between peak and off-peak energy rates. Schreiber et al. [90] reported the performance of absorption thermal energy storage combined with cogeneration for industrial applications: they proved that, when appropriately integrated with low grade heat sources, TES has the potential to increase the energy efficiency of the industrial process, reducing the primary energy consumption up to 25%. Chvala [25] presented a technical assessment of TES technology to investigate the potential in U.S. federal buildings sector, concluding that TES is a feasible solution for this category of buildings: thus, TES should be taken into consideration when retrofitting and/or replacement of chillers is carried out. Ora et al. [80] proved the benefits, both energetic and economical, of using a combination of TES and direct air free cooling to satisfy the energy demand of a 1250 kW data centre. The use of direct free cooling is shown to be feasible by itself, however, when using TES in combination with an off-peak electricity tariff, the operational cooling cost can be further reduced. Deforest et al. [32] investigated the economic benefits of sensible

heat thermal energy storage by simulating its application, for an office building, in four different locations spread across the world (Miami, Lisbon, Shanghai and Mumbai). Their results showed the potential of TES systems in reducing the annual electricity costs (5-15%) and peak electricity consumption (13-33%). All these studies concur to establish that the feasibility of TES applications is related to economic and climatic conditions such as electricity rates/regulations and duration of cold/hot seasons respectively. In this chapter we focus only on cold thermal energy storage (CTES) applied in hot climate. In particular, we propose a techno-economic methodology to size CTES according to different management strategies: peak load management, price arbitrage and replacement of chillers' partial load operations. The last strategy is particularly interesting since it demonstrates how, under certain conditions, CTES can be used to increase the overall efficiency of the cooling system. We investigate the viability of CTES for building demand management purposes in hot climates. We propose a case study using data from the School of Art, Design and Media (SADM), located within the Nanyang Technological University (NTU) campus in Singapore. We develop and apply a deterministic model to evaluate the impact of integrating the CTES with the existing cooling system. In the first part of the chapter, we outline the case study, describing the building, cooling plant, energy demand and enhancement opportunities in terms of cooling system efficiency. In the second part, we describe the sizing methodology, the modeling technique, and the different scenarios of interest. Finally, we discuss the results of the techno-economic analysis.

## 3.3 Materials and Methods

### 3.3.1 Energy audit

**The climate in Singapore**

Singapore lies just north of the Equator near Latitude 1.5 deg N and Longitude 104 deg E. Due to its geographical location and maritime exposure, Singapore climate is characterized by uniform temperature and pressure, high humidity and abundant rainfall. There is not a distinct wet or dry season: maximum rainfall occurs in December and April, while the drier months are usually February and July. Daily temperature usually ranges between a minimum of 23-26C and a maximum of 31-34C with extremes of minimum of 19.4C and maximum of 36C. With regards to ambient relative humidity (R.H.), the daily R.H. spans between 90% (and above) in
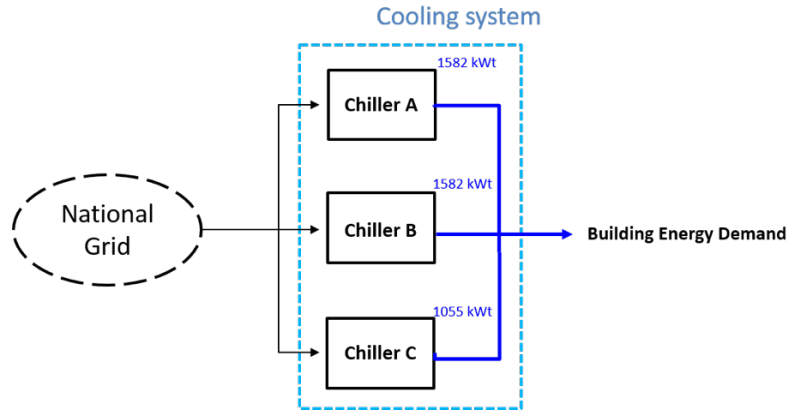
FIGURE 3.1: Model of the building's cooling system

the early morning and 60% in the mid-afternoon; the mean value is 84% but during prolonged heavy rain, relative humidity often reaches 100%.

**Cooling system description**

The School of Art, Design and Media (SADM) was built in 2007 as an institutional building with offices, laboratories, libraries, studios and lecture theaters. The building is located inside the Nanyang Technological University campus. Air conditioning for the building is provided by three water chillers, as represented in figure 3.1. Chillers (CH) A and B are fitted with centrifugal compressors, using R-123 refrigerant, having a cooling capacity of 1582 kW each. Chiller C is fitted with a screw compressor, using R-134a refrigerant, having a cooling capacity of 1055 kW. Each chiller has its own dedicated chilled water pump, condenser water pump and cooling tower. Each pump and cooling tower are fitted with a variable speed drive. The speed of the chilled water pumps (CHWP) and cooling towers (CT) varies from 30 to 50 Hz, while the condenser water pumps (CWP) are operated with fixed speed at 31Hz. All the air handling units are fitted with electronic air filter and CO2 sensor. A building management system (BMS) is in place to monitor and control the systems operation. During weekdays, Chiller C is in operation from 7.30 am to 10.30 pm and from 7.30 am to 1.30 pm on Saturdays. Chiller B usually provides the cooling energy demand exceeding the capacity of chiller C. Chiller A is usually used as backup unit. The building is closed on Sundays and Public Holidays (PH), therefore none of the chillers operates during these periods.

TABLE 3.1: Chillers specs

| Parameter | CH (A-B) | CH(C) |
|---|---|---|
| Refrigerant | R-123 | R-134A |
| Cooling Capacity | 1582 kWc | 1055 kWc |
| Year of Manufacture | 2006 | 2003 |
| Chiller related electric power | 270 kW | 169 kW |
| Chilled water supply temperature | 6.7 °C | 6.7 °C |
| Chilled water mass flow | 68.5 l/s | 45.2 l/s |
| Condenser water supply temperature | 29.5 °C | 29.4 °C |
| Condenser water return temperature | 35.0 °C | 34.6 °C |
| Condenser water mass flow | 85.7 l/s | 56.78 l/s |
| Rated COP | 5.8 | 6.2 |

TABLE 3.2: Chilled water pumps specs

| Parameter | CHWP A - B | CHWP C |
|---|---|---|
| Design flow rate | 68.5 l/s | 45.5 l/s |
| Design pump head | 28.1 m | 35.0 m |
| Design motor power | 37.0 kW | 30.0 kW |

TABLE 3.3: Cooling towers specs

| Parameter | CHP A - B | CHP C |
|---|---|---|
| Design flow rate | 85.7 l/s | 58.3 l/s |
| Design pump head | 27.0 m | 25.0 m |
| Design motor power | 37.0 kW | 30.0 kW |

TABLE 3.4: Cooling towers specs

| Parameter | CT |
|---|---|
| Cooling capacity | 1973kW |
| Design flow rate | 85.71 l/s |
| Design condenser water supply temperature | 29.5 °C |
| Design condenser water return temperature | 35.0 °C |
| Design wet bulb temperature | 26.7 °C |
| Design motor power | 3x7.5 kW |

**Cooling load and compressor operating efficiency**

The present study utilizes real data obtained by monitoring the chillers system over 4 months. Since there is no real alternation in climate between summer and winter in Singapore, the measured cooling load is almost steady throughout the year. Thus, the behavior of the building over 4 months can be considered representative of a whole year cooling demand. Data were collected with a 1-minute time-step and then aggregated to obtain 15-minute cooling load and COP profiles. Figures 3.2 to 3.5 show both the variability and the non-elasticity of the daily cooling load profile of each month. Figures highlight a regular pattern for the cooling load during the four monitored months: the compressors starts operating at 07:00 and turns off at 23:00. Three different operating phases can be identified for the cooling system. A peak-load phase in the morning between 07:00 and 09:00, due mostly to the high quantity of cooling energy necessary to overcome the rise of building temperature occurring during nights and week-ends. Indeed, since the BMS is programmed to switch-off during both night time and week-ends, the indoor temperature of the building increases because of the high minimum outside temperature (usually around 26C). A maintaining phase, between 09:00 and 19:00, when the cooling load ranges between 1000-1200 kWc. A partial load phase, between 19:00 and 23:00, in which there is a reduction of cooling demand due to both the lower occupancy of the building and, to a lesser extent, to the lower outside temperature. Figure 3.6 shows the measured coefficient of performance of the system as a function of the cooling demand. The average COP of the chiller system is 5.3 (during office hours between 08.30 and 17:30).
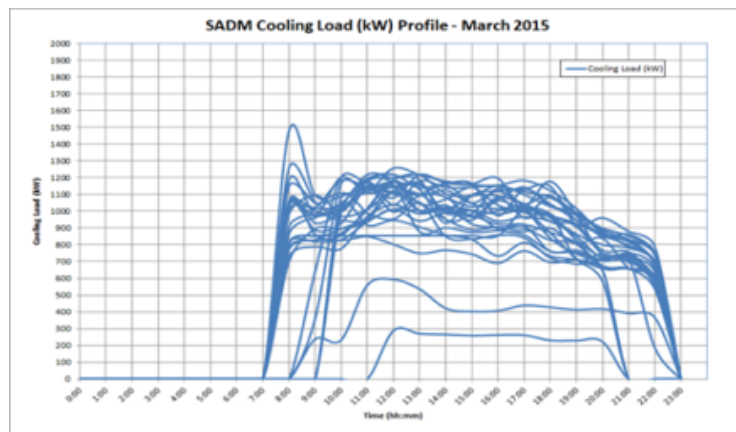


FIGURE 3.2: Cooling load profiles in March 2015
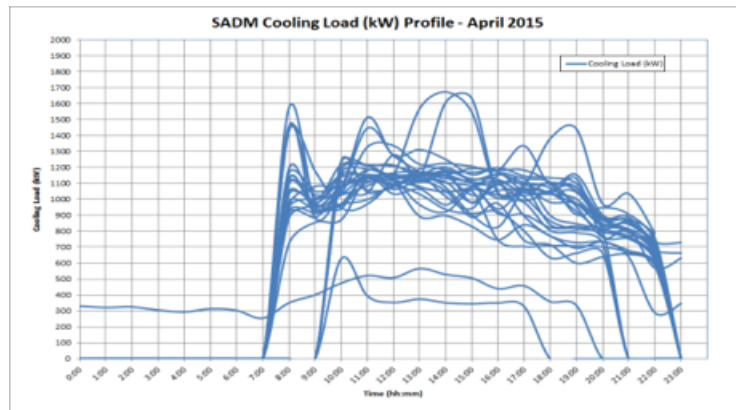
FIGURE 3.3: Cooling load profiles in April 2015
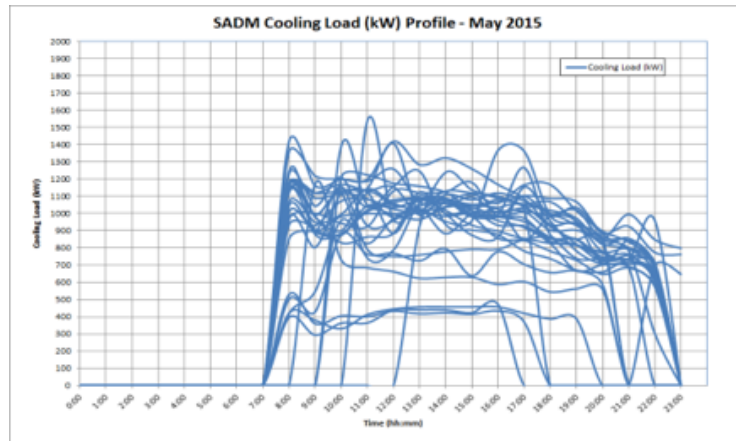


FIGURE 3.4: Cooling load profiles in May 2015
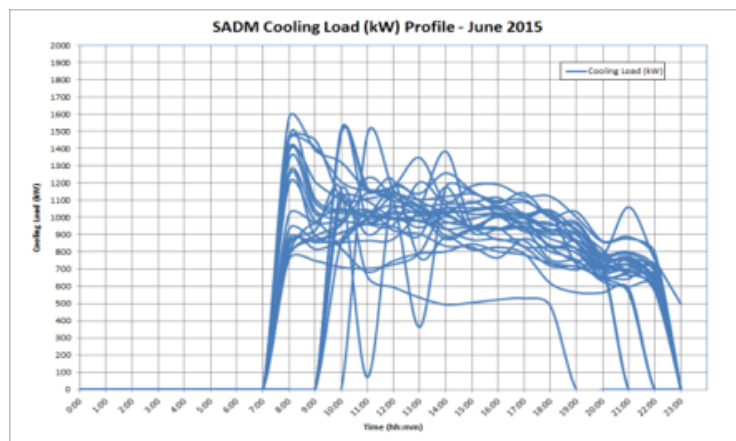


FIGURE 3.5: Cooling load profiles in June 2015
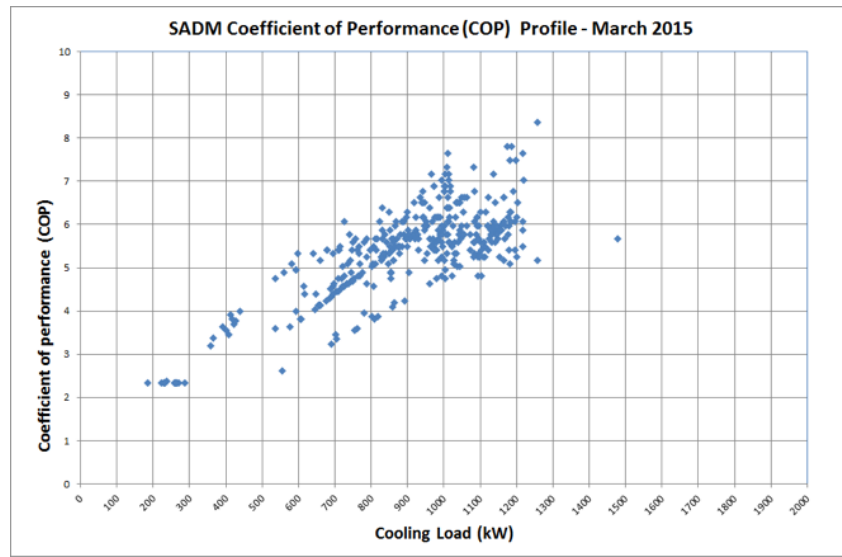
FIGURE 3.6: Coefficient of Performance of the cooling system

**Opportunities for demand side management**

The energy audit highlights some opportunities to improve the cooling systems techno-economic performance. In particular, starting from the data presented in Figures 3.2 to 3.5, three area of intervention have been identified. Figure 3.7 shows the cooling load profile for a typical working day as measured over the 4 months monitoring period.
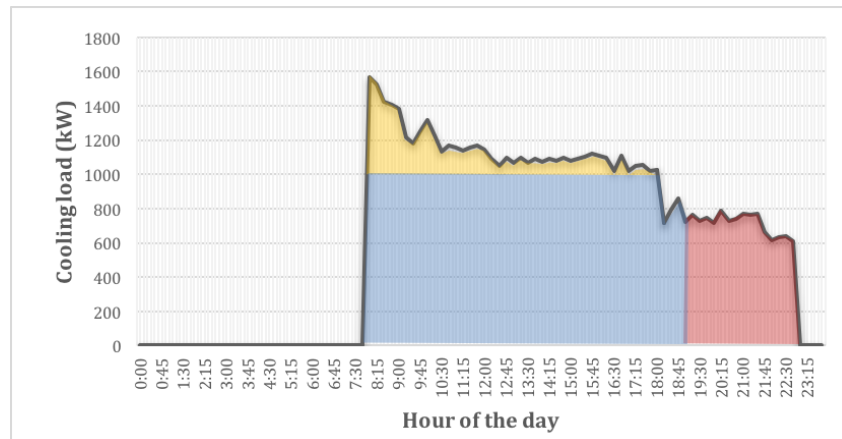


FIGURE 3.7: Cooling load profile for a normal operative day

First area of intervention, Partial load operation (red area)

The audit showed that Chiller C has the highest rated COP (refer to Table 3.2); the datum is confirmed by the experimental data (refer to figure 3.6) which show

that the cooling system performs better (COP around 5.5) in the range of 1000-1100 kWc, whereas its performance decreases at partial load with COP dropping down to 4.9 at around 700 kWc. A possible intervention, hence, consists of exploiting storage technologies to avoid chiller partial load operations.

Second area of intervention, Peak-load management (yellow area)

At the present time, the BMS automatically manages the three chillers (refer to Table 3.1) to supply the exact quantity of cooling energy required. As already emphasized, the cooling system works most of the time in the maintaining phase supplying around 1000-1200 kWc of cooling energy which is very close to the 1050 kWc cooling capacity of chiller C ( refer table 3.1). Hence, a second possible area of intervention should address the opportunity of exploiting demand side management in order to reduce the peak load so that only the most performing chiller (chiller C, Table 3.1) is operated, with the two others serving as backup units.

Third area of intervention, Price arbitrage

This intervention is strictly economic and relates to the exploitation of the price arbitrage potential due to the difference between peak and off-peak electricity tariff in Singapore. The larger the spread between the peak and off-peak electricity tariff, the larger could be the economic benefit. In Singapore, the off-peak energy tariff is about 65% of the peak one. The peak period is between 07:00 and 23:00, which matches the daytime working schedule of the SADM building. Hence, the third area of intervention is to evaluate the techno-economic opportunity of shifting most of the cooling load from peak to off-peak hours.

The goal of this work is to assess the viability of using Cold Thermal Energy Storages (CTES) to implement demand side management strategies in order to increase the overall efficiency of the whole cooling system. In particular, the following actions are assessed:

### 3.3.2 Energy storage Modeling and design methodology

**Energy Storage Model**

For the techno-economic analysis, a deterministic model is adopted to simulate the behavior of the storage. The purpose of the model is to evaluate the amount of electrical energy consumed to charge the storage when in operation. The first step consists in defining the amount of cooling energy to be shifted by means of the storage depending on the type of action to be implemented. Once defined the amount of energy to be shifted, the amount of cooling Energy-To-Charge is
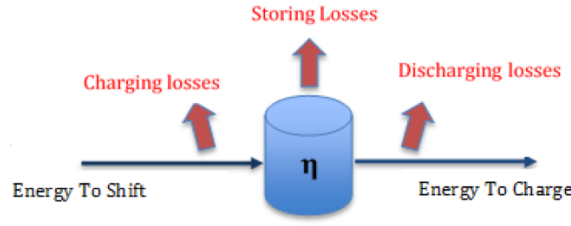
FIGURE 3.8: Energy storage model

calculated. The Energy-To-Charge can be easily calculated as:

$$E_{Charge} = \frac{E_{Shift}}{\eta} \qquad (3.1)$$

Where is the charge/discharge efficiency of the storage, also called round trip efficiency. The storage efficiency is approximated as a constant parameter, evaluated considering the average charging, discharging and storing losses. The steady-state model does not account for the change in external conditions (e.g. temperature, humidity) which, in the real case, would affect the storage efficiency. This simplified model is particularly suited for a preliminary techno-economic feasibility study in Singapores climate characterized by almost steady ambient conditions along the day and across the year.

**Cooling energy demand of the building**

The assessment of the cooling energy demand of the building is essential for the techno-economic analysis of a CTES. Table 3.5 shows a list of parameters used to define the daily cooling energy demand of the building. For each month, the daily average cooling energy consumption of the building, the daily average COP ($COP_{DA}$) of the chillers, the daily AVG electricity consumption (Daily AVG Electricity Consumption) and the monthly cooling energy consumption (Monthly load) were calculated referring to the real load profiles, obtained by monitoring the cooling system for four months. In order to assess the effect of CTES on the performance of the cooling system, the COP of the system was also calculated for three different periods of the day: the Daily AVG COP, the Daily AVG COP between 07:00-18:00 and the Daily AVG COP between 19:00-23:00. Table 3.5 also reports the monthly surplus and the daily average surplus calculated from real acquired data. These values were calculated in order to address Action 2 (yellow area in Figure 3.7) in which only the most efficient chiller (chiller C) is operated during peak hours. The

TABLE 3.5: Cooling energy demand of the building

| Month | Monthly load (kWhc) | Daily AVG load (kWhc) | Daily AVG elec load (kWhe) | Daily AVG load 19-23 (kWhc) | Daily AVG COP | Daily AVG COP 19-23 | Monthly sur-plus (kWhc) | Daily AVG sur-plus (kWhc) |
|-------|---------|---------|---------|---------|---------|---------|---------|---------|
| March | 344801 | 12771 | 2425 | 2714 | 5 | 5.2 | 4.3 | 9242 |
| April | 390061 | 14447 | 2744 | 2742 | 5.4 | 5.5 | 5.1 | 18273 |
| May | 359861 | 12409 | 2357 | 2547 | 5.3 | 5.4 | 5.1 | 6941 |
| June | 344000 | 11862 | 2253 | 2559 | 5.4 | 5.4 | 4.9 | 7332 |
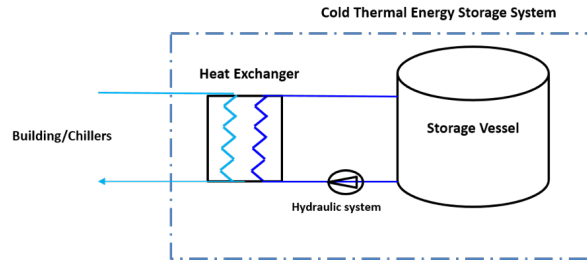


FIGURE 3.9: Typical CTES system's configuration

monthly surplus represents the sum of all the hourly surplus of a specific month. The daily average surplus is calculated as the Monthly Surplus divided by the number of operative days. The hourly surplus ($E_{surplus}$) is defined as the difference between the hourly energy demand and the rated capacity of chiller C ($C_{chillerC,i}$) and it is calculated for the ith hour as:

$$E_{surplus,i} = E_{demand,i} - C_{chillerC,i} \qquad (3.2)$$

**Storage technology and charge/discharge management**

The medium considered in the CTES system is water (sensible heat storage) at atmospheric pressure operating with a temperature of 5°C (temperature range between 7°C when fully charged and 12 °C when fully discharged). Figure 3.9 shows the proposed schematic diagram of the CTES.

The storage efficiency of the CTES system depends on its components such as the insulation material, the water diffusion mechanism inside the vessel, the auxiliary systems (pumps, heat exchanger). The thermal energy storage technology review

from Irena, indicates that TES systems have an efficiency which spans between 50% and 90% [108]. However, specific tests and experimental analysis carried out by some of the authors of this paper on a real sensible heat thermal energy storage located in Italy, have ascertained a storage efficiency of 85% [5]. The capital cost for the whole system was also calculated as $212\,US\$/m^3$, including the cost for vessel, hydraulic system, compact heat exchanger and civil works. With regard to the operating strategies, TES system usually operates in full storage or partial storage mode. Full storage systems are designed to cover the whole energy demand during peak hours. On the contrary, partial storage systems shift the excess demand from a pre established threshold and can be used to shave the peaks, to stabilize the variable load of the energy demand or to partially replace the chillers system. CTES operating in full storage mode results in a larger and more expensive design since it aims to completely replace the cooling system during peak hours; this operating mode is usually suitable for large peak/off-peak spreads.

**Comparison metrics**

The main parameters utilized to assess costs and potential benefits of each proposed solution are the following: storage size, electricity to charge, percentage of electricity saved, economic savings, savings per energy unit (specific savings), estimated capital costs and payback period. The Storage size is calculated using the following relation:

$$Q = mc_p\delta T \tag{3.3}$$

Where Q represents the daily energy quantity to shift (based on the average working day and on the type of action addressed), expressed in kJ; m is the total mass of water stored in the vessel in kg; cp is specific heat of water at constant pressure, expressed in kJ/kgK; is the maximum temperature difference to which the storage medium is subjected. The Daily Electricity to Charge (kWh/day) represents the amount of electricity consumed to charge the storage. It is related to the Energy to Charge (Equation 3.1) and the chillers average COP during charge ($COP_{charge}$). As an example, when addressing the first area of intervention, the charge operations occurs during off-peak hours, with chillers operating at rated capacity and rated COP (see Table 3.1).

$$E_{charge\_daily} = \frac{E_{charge}}{COP_{charge}} \tag{3.4}$$

The new Daily Electricity Consumption ($E_{daily\_cons}$)after the CTES introduc-

tion is calculated according to Equation 3.5, being a function of the Daily Electricity to Charge ($E_{charge\_daily}$), the Daily Energy to Shift ($E_{shift\_daily}$) and the COP ($COP_{phase}$) of the chillers in the phase considered (peak load, maintaining, partial load).

$$E_{daily\_cons} = E_{daily\_con} - \frac{E_{shift\_daily}}{COP_{phase}} + E_{charge\_daily} \tag{3.5}$$

The performance of the chillers can be represented by the Daily AVG COP, either the Daily AVG COP 7-18 or the Daily AVG COP 19-23, depending on which portion of the energy demand is being shifted. As an example, when addressing the first area of intervention, shifting the energy to avoid partial load operations (red area, figure 3.7), the average COP considered is the Daily AVG COP 19-23. The Annual electricity savings ($Savings_{ele}$), measured in kWh, are calculated as the difference between the Daily electricity consumption of the cooling system before and after the CTES introduction, multiplied by the Number of Operative Days per Year (Nd).

$$Savings_{ele} = (E_{daily\_cons} - E_{daily\_charge}) * Nd \tag{3.6}$$

The Economic savings ($Savings_{eco}$), measured in US dollars, are calculated as the difference between the yearly operative costs before and after the introduction of the energy storage. When evaluating the yearly operative costs the Energy-to-Shift per day, the Energy-To-Charge per day, the spread between peak (PT) and offpeak tariffs (OPT) and the number of operative days per year are taken into account.

$$Savings_{eco} = (\frac{E_{shift\_daily}}{COP_{avg}} - E_{daily\_charge})(PT - OPT) * Nd \tag{3.7}$$

The Savings per energy unit (US\$/kWhc) is obtained by dividing the economic savings by the energy capacity of the storage. This is a measure of the overall effectiveness of the solution. The Payback period ($PBP$) (years) represents the main parameter to assess the economic feasibility of an investment: it is evaluated considering the capital costs (Capex) and the annual Economic savings.

$$PBP = \frac{Capex}{Savings_{eco}} \tag{3.8}$$
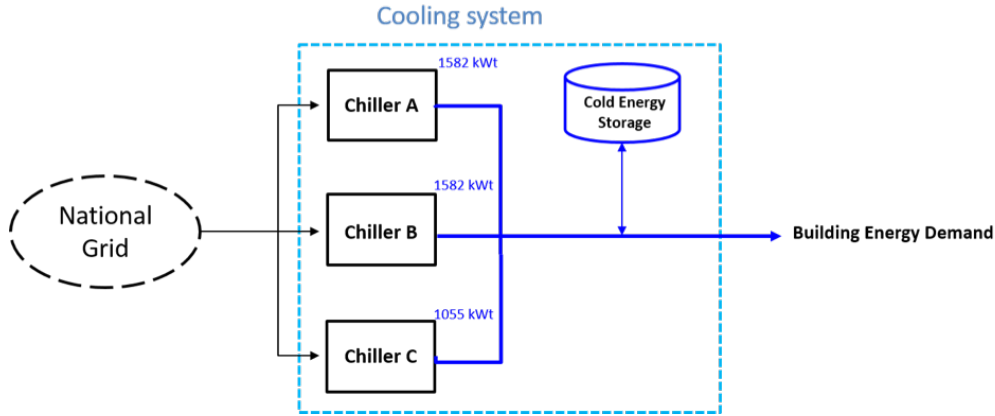
FIGURE 3.10: The new cooling system integrating the CTES

## 3.4 Results and considerations

This section presents the main results of the techno-economic study carried out in order to find the optimal sizing of the CTES according to its use in the cooling system management strategy. It was assumed that the new cooling system (Figure 3.10), integrating the cold storage and the present chillers, had to satisfy a daily average cooling energy demand of 12872 kWhc , considering 275 operative days per year. In particular, 12872 kWhc was calculated as the average cooling energy demand in the four monitored months and it represents the 100% of the design daily average cooling energy demand. Figure 3.10 shows the simplified scheme of the new cooling system integrating CTES.

### 3.4.1 Integrating a storage to avoid partial load operations

In this case, the storage was sized to manage the average cooling energy demand of the SADM building between 7 and 23 period, which corresponds to 2800 kWhc (Energy-to-shift) of cooling energy during an average working day. The cold storage works in total storage mode: during off-peak hours the most efficient chiller (chiller C, Table 3.1) charges the storage; from 8 to 19 the existing chillers supply the cooling energy required, with an average COP of 5.4; from 19 to 23 the energy demand is completely satisfied by the cold storage (Figure 3.11). Indeed, without the CTES, the chillers worked during peak hours in the red zone of Figure 3.11, with an average COP of 4.8. Using the CTES, 2800 kWh of cooling energy can be shifted in off-peak hours, with chillers operating at rated capacity with a higher average COP of 6.2. The new cooling system does achieve more than 11 MWh of
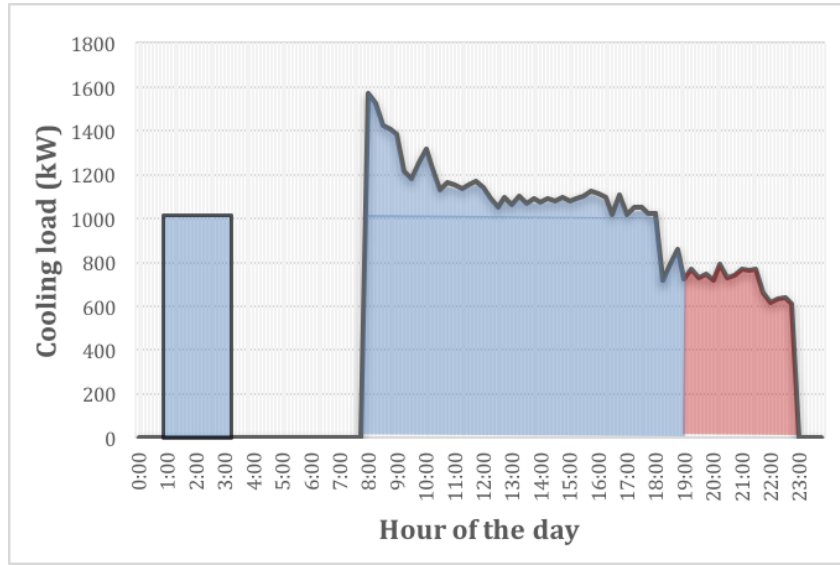
FIGURE 3.11: New cooling load obtained ntegrating a storage to avoid partial load operations

electricity savings per year. In order to store 2800 kWh of cooling energy a $482m^3$ vessel is necessary. The investment cost can be estimated as $212US\$/m^3$ while the economic savings are calculated as 11480 US\$ (that is a 4.1 US\$/kWh). The estimated payback period is 8.9 years (Table 3.6).

### 3.4.2 Integrating a storage to replace the backup chillers

In this case, the storage was designed to shift the daily average surplus in the average working day. In this scenario CTES works in partial storage mode: during

TABLE 3.6: Main results obtained using a storage to avoid partial load operations

| Parameter | Value |
| --- | --- |
| Energy To Shift | 2800 kWh |
| Annual electricity savings | 11520 kWh |
| % of the daily demand stored | 21.7% |
| Storage size | 482 m3 |
| Economic Savings | 11480 US\$/year |
| Savings per energy unit | 4.1 US\$/kWh |
| Estimated cost | 102184 US\$ |
| Payback | 8.9 years |
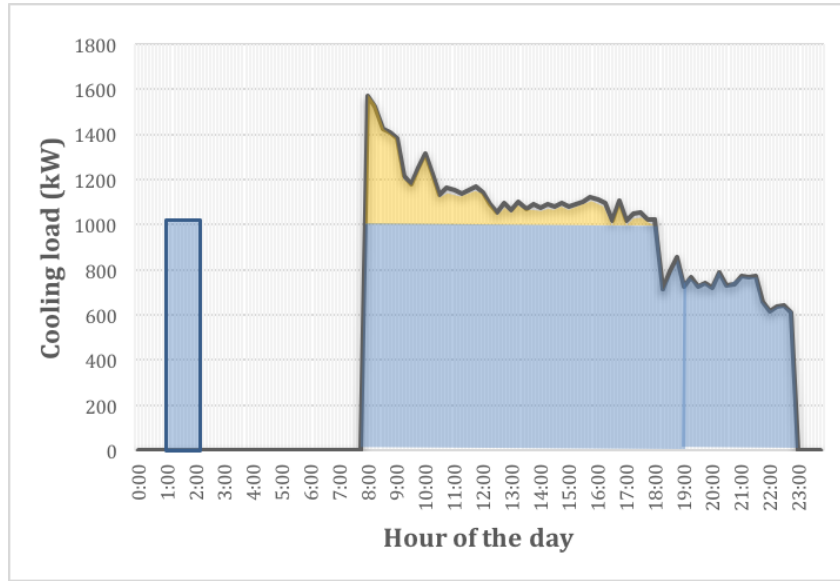
FIGURE 3.12: New cooling load obtained using a storage to replace the backup chillers

off-peak hours chiller C charges the storage at rated capacity, with a COP of 6.2; from 8 to 19 chiller C supplies the cooling energy required to the building at its maximum capacity (1050 kW); whenever the energy demand exceeds the 1050 kW limit, the cold storage provides the surplus energy required (Figure 3.12). The improvements in the overall cooling system efficiency are limited: the benefits of charging the storage during night, at rated COP, are almost completely lost in the storing process. Under the economic point of view this scenario entails a shifting of 731 kWh of cooling energy for a volume of the storage of $126m^3$ and an estimated investment cost of 102184 US$. The yearly Economic savings are calculated as 1660 US$ (2.27 $/kWh), for a payback period of 16 years.

### 3.4.3 Integrating a storage to arbitrage the energy price

This sizing scenario is meant to exploit the price arbitrage potential due to the difference between peak and offpeak electricity tariffs in Singapore. The proposed operating schedule is a sort of hybrid storage mode, which is a combination of the two previous operating strategies: during off-peak hours the chillers work to charge the storage; from 08 to 19 the storage works in partial storage mode, using the stored energy to compensate the daily average surplus (yellow area in Figure 3.13); from 19 to 23 the storage works in total storage mode so that the cooling energy demand relies uniquely on the cold storage (red area in Figure 3.13). This scenario was

TABLE 3.7: Main results obtained ntegrating a storage to replace the backup chillers

| Parameter | Value |
|---|---|
| Energy To Shift | 731 kWh |
| Annual electricity savings | 20 kWh |
| % of the daily demand stored | 5.7% |
| Storage size | 126 m3 |
| Economic Savings | 1660 US$/year |
| Savings per energy unit | 2.27 US$/kWh |
| Estimated cost | 26653 US$ |
| Payback | 16 years |

evaluated for four different percentage of the daily energy demand: 27%, 50%, 75% and 100%. The 27% of the total energy demand represents the minimum storage capacity necessary to address both the first and the second area of intervention (red and yellow areas in Figure 3.11). Regardless of the percentage of the daily energy demand being shifted, priority is always given to the period between 19 and 23 to avoid the chillers working at lower COP (red area in Figure 3.13). Using the hybrid storage operating strategy, shifting the 100% of the daily demand, 32180 US$ of savings per year were estimated, with a $2.5 US\$/kWh$ rate. To shift this quantity of cooling energy a $2214 m^3$ vessel is necessary for an estimated investment cost of $469371 US\$$. Table 3.8 shows the model outputs related to the other suggested designs.

### 3.4.4 Results discussion

The results, showed in Table 3.6 to 3.8, demonstrate that the introduction of CTES entails a reduction of the electricity consumption of the cooling system for most of the suggested scenarios. At a first sight, this result could be unexpected since the energy storage introduces an inefficiency in the whole cooling system. This result is explained by the fact that, in these two scenarios, the CTES allows the optimal management of the cooling system achieving a higher average COP able to compensate the inefficiency introduced by the storage itself. In the 75% and 100% scenarios, Chillers A, B and C have to work together, thus the AVG COPcharge is much lower (Daily AVG COP between 7 and 18, table 3.5) than in the other scenarios in which the cooling system can work with the COP of the most performing chillers. The Savings per energy unit gives an indication of which design

FIGURE 3.13: New cooling load obtained Integrating a storage to arbitrage the energy price

TABLE 3.8: Main results obtained integrating a storage to arbitrage the energy price

| Parameter | 27% daily demand | 50% daily demand | 75% daily demand | 100% daily demand |
|---|---|---|---|---|
| Energy To Shift (kWh) | 3531 | 6436 | 9654 | 12872 |
| Annual electricity savings (kWh) | 10505 | 6932 | -72144 | -101092 |
| Storage size (m3) | 608 | 1107 | 1661 | 2214 |
| Economic Savings (US$/year) | 14124 | 23427 | 24811 | 31180 |
| Savings per energy unit (US$/kWh) | 4 | 3.64 | 2.57 | 2.5 |
| Estimated cost (US$ ) | 128896 | 234685 | 352132 | 46937 |
| Payback (years) | 9.1 | 10 | 14.2 | 14.6 |

is the most effective. The sizing scenario described in Table 3.6 is the best with savings of 4.1 US$/kWh. In this case the whole amount of Energy-To-Shift exploits both the peak/off-peak price spread and the cooling efficiency enhancement moving from the lower COP value due to partial load operations (Daily average COP 19-23, table 3.5), to the rated COP of chiller C (6.2). Table 3.7 describes the suitable CTES size to replace chillers A and B in addressing the demand surplus from 7 to 19; the results show that the Savings per energy unit (2.27 US$/kWh) and Annual electricity savings are negligible. Indeed, this scenario is the only one that does not address the partial load operations, thus offering much less potential improvement of the cooling system performances. However, it still manages to produce savings and once the existing system starts getting older or less efficient, such a design can be taken into consideration to replace the chillers, downsizing the installed equipment. The 27% case is of particular interest since it represents the minimum investment to address both the first and second area of intervention described in Section 3.3.1. This design is able to exploit both the profitable aspects discussed before, proving itself extremely effective (2.76 US$/kWh of savings per energy unit). The 75% and 100% cases, as already mentioned, are the most inefficient designs, since they need the three chillers to work together to charge the storage, resulting in a lower average COP: the introduction of the storage actually increases the energy consumption of the cooling system which leads lower Savings per energy unit (2.57 and 2.50 US$/kWh). From a purely economic point of view, the results shown in Tables 3.6, 3.7 and 3.8 demonstrate the viability of the suggested solutions. The payback periods stand between a minimum of 8.9 years and a maximum of 16 years. An expected good result considering that the case study presents some of the ideal conditions for CTES applications: a large, steady, cooling demand throughout the year. Moreover, the cooling demand profiles perfectly match with the peak period of Singapore electricity tariff. On the other hand, the spread between peak and off-peak tariff is not particularly large and it does not represent an adequate economic incentive to shift the loads to off-peak hours. All considered, CTES applications seem appealing in Singapore. The main limit of CTES technology with sensible heat is the low energy density value, which results in large amount of space requirements. This work showed that the storage volume ranges from 482 $m^3$ to 2214 $m^3$ in the case of complete day-night shifting of the cooling energy demand. A large amount of space in direct proximity of the building is necessary and, especially in highly populated cities like Singapore, is not always available.

## 3.5 Conclusions

This work has demonstrated the feasibility of CTES for building demand management in hot climate. The School of Art, Design and Media building, located within NTU campus in Singapore, served as case study. In the first part, the building characteristics and the demand profiles were analyzed to search for energy efficiency improvement opportunities. Three possible areas of intervention were identified: (i) to reduce/remove partial load operations; (ii) to exploit demand management strategies in order to reduce peak loads, so that only the most performing chiller needs to operate; (iii) to perform price arbitrage, exploiting the difference between peak and off-peak electricity rate in Singapore. Six scenarios were described, addressing different percentage of the average daily demand. For each scenario the appropriate size of CTES and the key performance indicators were evaluated. Results indicate that it is possible to enhance the efficiency of the whole system, achieving, for most of the cases, both energy and economic savings. In particular, the most effective solution is that with the CTES replacing the cooling system partial load operation. The payback periods of the different scenarios stand between a minimum of 8.9 years and a maximum of 16 years. All these aspects make CTES applications appealing. However, sensible heat technology is characterized by a low energy density value, which results in large amount of space requirements. For the case study, the storage volume ranges from $482m^3$ to $2214m^3$, thus a lot of space in direct proximity to the building is necessary and, especially in highly populated cities like Singapore, is not always available.

# Chapter 4

# Thermostatically controlled loads as flexibility resources

## 4.1 Preface to Chapter 4

In the last chapter we talked about energy storage systems showing how, when correctly integrated with an existing plant, they can provide extra flexibility to the system and value to the final user. In this chapter we introduce another category of flexibility assets, the thermostatically controlled loads (TCLs). Specifically we focus on the intrinsic flexibility of the residential cooling energy demand. The aim of this chapter is to introduce a new methodology to evaluate the impact of end users' comfort preferences in their demand flexibility. The proposed methodology is designed from the prospective of an aggregator which seeks to evaluate the flexibility potential, and eventually control, an aggregate of residential air conditioner units. We also present, and test, a new thermostat control strategy based on deadband relaxation, highlighting its impact on the aggregate demand response potential. I undertook the majority of work related to this chapter, including part of the modeling tasks, the development of a simulation platform and the interpretation of results. Dr. Emre Can Kara, Dr. Michaelangelo Tabone and Sila Kiliccote provided help with technical support, ideas and editorial assistance.

## 4.2 Introduction

Many nations have set ambitious goals to increase energy production from renewable sources. The European Union (EU) set a target of 33% share of renewable electricity by 2020 among its member states [81]. In the U.S., 29 states committed to some

form of Renewable Portfolio Standards (RPS). These combined RPSs require an additional 60 GW of renewable capacity by 2030 [9]. This trend poses a challenge to power distribution systems in terms of reliability, maintenance costs, and service quality. Power grids are designed to work under balanced supply and demand. Intermittent generation disturbs this balance, making it more challenging to operate the system reliably, maintain service quality, and reduce costs [56] [76]. Specifically, the state of California is concerned with balancing supply and demand in evening hours, when solar generation is decreasing and residential loads are increasing (i.e. the duck curve problem) [18]. Demand response (DR) offers a solution to mitigate some of these issues, by controlling the demand. Thermostatically controlled loads (TCL) in residential buildings, such as refrigerators, air conditioners, heat pumps and electrical boilers, are among most studied DR resources [62]. Often, these loads operate via hysteresis, modulating the indoor air temperature between upper and lower bounds around a setpoint, which are defined by users' preferences. By changing these bounds and controlling the setpoints, TCLs are able to rapidly adjust their demand. These characteristics make them ideal candidates to provide fast responding ancillary services [12]. TCLs have been studied extensively in literature and we refer the interested reader to [19]. Recent studies focus on new methods to model an aggregation of TCLs and evaluate their DR potential. In [60], authors suggest an autoregressive method to quantify the potential of an aggregation of TCLs in supplying automated DR services. They use lagged values of setpoint adjustments, outdoor air temperature, solar insulation and auxiliary power as regressors to predict the cumulative shed capability during a DR event. In [49], authors describe the flexibility of an aggregation of TCls as a stochastic battery. The model key parameters, such as power limits, energy capacity and dissipation rate, are defined by TCLs characteristics, outdoor air temperature and end user setpoint preferences. In [24], authors introduce a new control strategy for residential TCls, designed to provide fast DR resources. The discomfort degree hour method is used to estimate the DR strategy impact over end users comfort. In [71] authors describe a method to estimate the energy storage capabilities, and the associated revenue potential of an aggregation of residential TCLs. They estimate that the technical resource potential of residential TCLs in CA is in the order of 10-40 GW and 8-12 GWh, and it would alone satisfy the 2020 statewide energy storage mandate [71]. In [102], the authors use a large set of simulated buildings to develop a new framework to estimate TCLs' DR potential using Energy Plus and two-state models. In [43] the authors explore the flexibility of heat pumps, accounting for different energy de-

mands, heat sources and distribution systems. Their results show that flexibility is strongly dependent on ambient temperature and system size. Most of these works analyze the impact of a limited set of exogenous variables on TCLs flexibility, such as buildings' physical characteristics and the weather. Furthermore, these works often report a trade-off between energy savings and flexibility. However, with the increasing penetration of renewables, wind and solar generation are likely to be curtailed at times when they exceed consumer demand. At these times, it becomes appropriate to use this excess energy at the expense of efficiency in order to enable flexibility [99]. In addition, the role of user behavior on DR potential is often overlooked, partly because it is hard to accurately model user behavior in physical models used in these papers. Nevertheless, it is critical to define the boundaries within which TCls flexibility can be stretched. In [83], the authors demonstrate the importance of having accurate models to capture users' occupancy patterns and avoid energy savings over-estimations, stressing the need for further research about user behavior. In this study, we investigate the impact of human behavior on the DR potential of residential cooling load estimates and flexibility. Specifically, we focus our attention to regulation and load shifting flexibility. Regulation is an ancillary service that accounts for the short-term variability in supply and demand that might affect the stability of the power system control area. It is a service that is provided throughout the day. The providing load and generation units adjust their load or generation based on a 4 second signal. We define load shifting flexibility to address the afternoon ramping problem facing California under increased renewable generation scenarios. We estimate the potential of residential cooling loads to shift their consumption to less critical times of the day. In both cases, we analyze the changes in DR potential estimates when human behavior is incorporated as temperature setpoint schedules and temperature deadband width adjustments. We use the TCL model suggested in [71] to simulate the cooling load of a heterogeneous population of air conditioners in three different climate zones. We test several simulation setups. Specifically, we incorporate dynamic deadband width and dynamic setpoint adjustment scenarios to assess the impact of each parameter on the DR potential estimates for regulation services and addressing the duck curve problem. Finally, we present insights for customer targeting.

## 4.3 Methodology

### 4.3.1 Individual TCL model and flexibility

In this work, we build a simulation framework from the discrete-time model presented in [71]. We believe that his model represents a good trade-off between estimation accuracy and computational complexity. Indoor temperature $\theta$ of each household $i$ is calculated for each time step $k$ using:

$$\theta^i_{k+1} = a^i \theta^i_k + (1 - a^i)(\theta^i_{a,k} - q^i_k \theta^i_g). \tag{4.1}$$

where $\theta^i_{a,k}$ represents the outdoor air temperature; $\theta^i_g$ is the temperature heat gain, which depends on the household thermal resistance $R$ and the air conditioning machine characteristics (rated power $P$ and coefficient of performance $\eta$). $a$ is a non-dimensional parameter regulating the sensitivity of the model to an internal/external heat gain. We implement the thermostatic hysteresis using the binary activation variable $q$ to maintain the internal temperature within the upper $\theta_{+,k}$ and lower $\theta_{-,k}$ comfort boundaries as follows:

$$\theta^i_g = R^i P^i \eta^i \tag{4.2}$$

It is given as follows:

$$a^i = e^{(-h/R^i C^i)} \tag{4.3}$$

We assume a constant coefficient of performance ($\eta$), while in reality it should change in relation to the outdoor air temperature. Comfort boundaries are defined by the user's indoor temperature setpoint and thermostat deadband width. We use them to implement different preferences and behavior in our model. For default users we use constant setpoint (CS) and deadband preferences $\theta_{defS}$ and $\delta_{defD}$. We then implement two different control strategies using $\theta_{adjS}$ and $\delta_{adjD}$. We change the setpoint and deadband width with respect to default users, as given in 4.4 for the lower boundary. A similar formulation can be given for $\theta_{+,k}$.

$$\theta_{-,k} = (\theta_{defS} + \theta_{adjS,k}) - \frac{(\delta_{defD} + \delta_{adjD,k})}{2} \tag{4.4}$$

$$\theta_{+,k} = (\theta_{defS} + \theta_{adjS,k}) + \frac{(\delta_{defD} + \delta_{adjD,k})}{2} \tag{4.5}$$

These two control strategies are *dynamic setpoint* (DS) and *dynamic deadband* (DD). The DS case represents users with defined setpoint schedules based on their

daily routine, relaxing the setpoint constraints when they are away, thus reducing the daily energy requirement. The DD case maximizes the cooling load flexibility by enlarging the deadband when the users are away. The constant setpoint case represents the user which is unable, or does not care, to adjust the setpoint temperature when is not home. While this profile is obviously bad from the point of view of the consumer, which is going to pay a higher bill for the extra energy consumption, the aggregator has guaranteed a certain amount of flexible load. During the day, when nobody is home, load variability is completely dependant on external heat gain sources. The dynamic setpoint case represents the commonly-used, energy-saving control strategy based on thermostat's setback. The end-user defines a setpoint schedule based on his daily routine, relaxing the setpoint constraints when nobody is home, thus reducing the daily cooling energy requirement. From the prospective of the aggregator, this strategy reduces the amount of curtailable load in certain hours of the day, reducing the potential for down regulation services. The dynamic deadband case is designed to maximize the cooling load flexibility. We assume that DR will not violate the user's comfort settings. Thus no DR is available if the indoor temperature is outside of temperature deadband. As in [71], we quantify the DR potential by modeling air conditioners as a virtual energy storage, constrained by aggregated energy capacity $E_{cap}$ and power capacity $P_{cap}$. $E_{cap,k}$ represents the additional amount of additional energy required by all ($N_a$ available air conditioning systems to traverse their deadbands in ON mode compared to the expected energy use under normal operation. Mathieu et al. define $E_{cap}$ as $E_{cap,k} = \sum_{i=1}^{N_a} P^i h_{p,k}^i (1 - D_k^i)$.

$$D_k^i = \frac{h_{p,k}^i}{h_{p,k}^i + h_{u,k}^i}. \tag{4.6}$$

$h_p$ represents the amount of time it takes for the air conditioner to traverse the deadband in ON mode and is given as follows:

$$h_{p,k}^i = -R^i C^i \ln \frac{\theta_{-,k}^i - \theta_{a,k}^i + \theta_g^i}{\theta_+^i - \theta_{a,k}^i + \theta_g^i}. \tag{4.7}$$

The amount of time required in OFF mode, $h_u$, is evaluated using a similar formulation. In our model, both $h_p$ and $h_u$ are time dependent, since they are subjected to comfort boundaries and outdoor temperature variations. The duty cycle $D$ is the faction of time the air conditioner is on, which is the ratio of $h_p$ to $h_p + h_u$. The power capacity $P_{cap}$ represents the maximum charging and/or discharging rate of the virtual energy storage and can be evaluated as $P_{cap,k} = \sum_{i=1}^{N_a} P^i$.

$P_m$ is the average power consumption of the aggregation and can be estimated as $P_{m,k} = \sum_{i=1}^{N} P^i D_k^i$. We use these parameters to quantify the potential of our aggregation to provide frequency regulation services or load shifting services. In both cases, we assume that $\theta^i$ is equal to the expected indoor temperature value (i.e. halfway between $\theta_{-,k}^i$ and $\theta_{+,k}^i$). In CAISO, the regulation market clears every 15-minutes [17] and the aggregator bids the maximum power capacity it is able to sustain. For each 15-minute block, we calculate the aggregated regulation potential as $P_{reg,k} = min(\frac{E_{cap,k}}{2 \times 3}, P_{cap,k} - P_m, P_m)$. $P_{reg}$ is constrained by energy and capacity limits. $E_{cap}$ is divided by 2 because the expected indoor temperature is halfway between the deadband limits, and divided by 3 to account for the difference between the simulation timestep and the market clearing timestep (i.e. 5 minutes vs. 15 minutes). Furthermore, $P_{reg}$ is constrained by the up and down power capacity of the equivalent virtual storage.

$$P_{reg,k} = min(\frac{E_{cap,k}}{2 \times 3}, P_{cap,k} - P_m, P_m) \tag{4.8}$$

For the load shifting problem, we are interested in evaluating the amount of energy that the AC population can shift from evening to less critical hours of the day, $E_{shift,k}$. For this purpose, we evaluate the load shifting potential starting at 6pm, when the power grid starts requiring more capacity to balance between the increasing residential demand and the decreasing renewable generation. The energy shifting potential represents the amount of energy that the aggregator is able to curtail for three straight hours, from 6pm to 9pm, using cooling load flexibility. Similar to $P_{reg}$, $E_{shift,k}$ could be written using a set of constraints:

$$E_{shift,k} = min(\frac{E_{cap,k}}{2 \times 12}, 3P_m) \tag{4.9}$$

In (4.9), $E_{cap}$ is divided by 12 to convert the energy value from the simulation time step of 5 minutes to an hourly time step; i.e., kWh.

### 4.3.2 TCLs characteristics

We simulate a population of 1000 households. The characteristics of each household are defined by R, C, P and $\eta$. For each household in the population, we sample these parameters from the distributions given in [71]. For the CS case, the indoor temperature setpoint is 22.5 C and the constant deadband width is 0.5 C. When assessing the regulation potential using the DS and DD cases, we assume that the users are away from home between 7am and 6pm. For the evening shifting problem, we extend the flexible range to 7am and 9pm. Figure 4.1 shows the
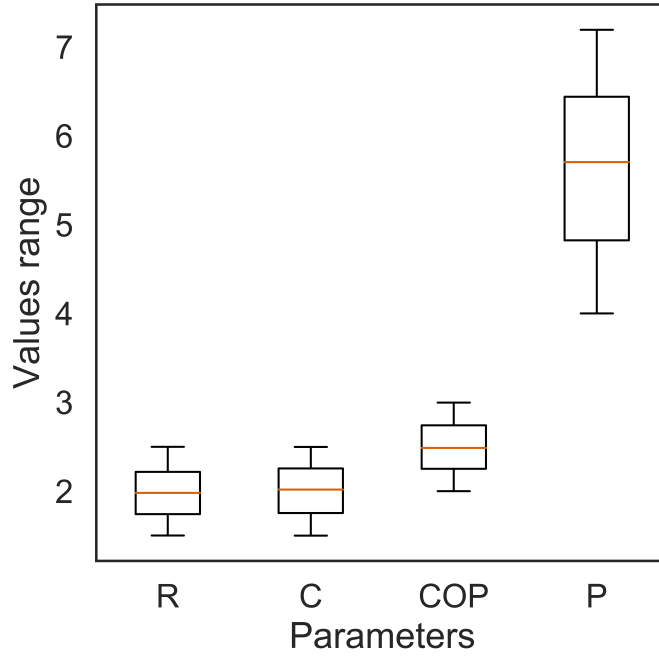
FIGURE 4.1: The boxplots represent the parameters distribution for the simulated population of households.

resulting parameters distribution from our population of households. Another set of assumptions is related to the thermostat setpoint temperature and the relative deadband width. We arbitrarily choose the indoor temperature setpoint to be 22.5C for the entire population of simulated households, considering a deadband width of 0.5 C. We refer to these values as "default temperature" and "default deadband", since in our simulations they represent the comfort boundaries for the constant setpoint case, or whenever the end user is home. We also define the daily schedule of the consumers living the simulated households. We want their schedule to be representative of a typical working day, thus we arbitrarily assume that nobody is home from 7am until 6pm.

### 4.3.3 Simulation setup

Using hourly outdoor air temperature data from 2016 [44], we evaluated the median temperatures for each hour in summer for three cities that represent different climate zones: Sacramento, Los Angeles and Las Vegas. We use these temperature profiles, depicted in Figure 4.2, as an input to the TCL model. For each city, we assess the impact of the different control strategies in terms of both daily regulation potential
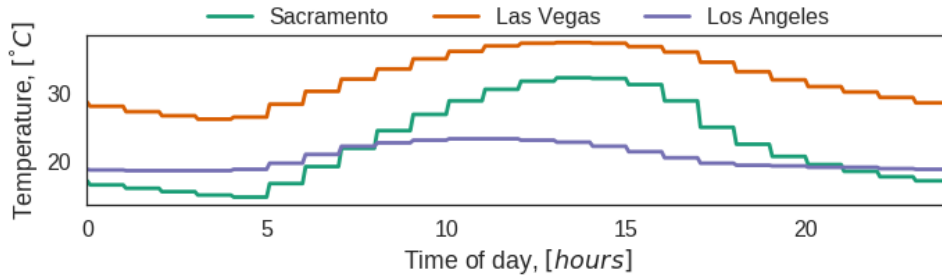
FIGURE 4.2: Median temperature profiles for Sacramento, Los Angeles and Las Vegas

and load shifting potential. We use the CS case (identical to [71]) as a benchmark for all the other cases, we then simulate different DS and DD scenarios, testing a range of $\theta_{adjS}$ and $\delta_{adjD}$ values between 0.5C and 3C .

Specifically, for *dynamic setpoint* we increase the setpoint by 0.5, 1,1.5,2 and 2.5 C and for *dynamic deadband* we increase the deadband width by 0.5, 1,1.5,2 and 2.5 C, respectively.

### 4.3.4 Thermostat control strategies

TCLs operate maintaining the indoor temperature between upper and lower bounds which are defined by consumer's setpoint preferences and the control deadband area. A deadband area is necessary to guarantee some hysteresis to the control loop. Without it, TCLs would be switching their on/off state as soon as the established setpoint temperature is crossed. For an aggregation of TCLs, the control strategy represents the way to translate consumer's behavior into action. In this work, we investigate the overall impact of different control strategies on flexible cooling loads, while analyzing the implications for both aggregator and end users.

- The constant setpoint case represents the user which is unable, or does not care, to adjust the setpoint temperature when is not home. While this profile is obviously bad from the point of view of the consumer, which is going to pay a higher bill for the extra energy consumption, the aggregator has guaranteed a certain amount of flexible load. During the day, when nobody is home, load variability is completely dependant on external heat gain sources.

- The dynamic setpoint case represents the commonly-used, energy-saving control strategy based on thermostat's setback. The end-user defines a setpoint schedule based on his daily routine, relaxing the setpoint constraints when nobody is home, thus reducing the daily cooling energy requirement. From the

FIGURE 4.3: Power and indoor air temperature profiles generated using different thermostat control strategies.

prospective of the aggregator, this strategy reduces the amount of curtailable load in certain hours of the day, reducing the potential for down regulation services.

- The dynamic deadband case is designed to maximize the cooling load flexibility. The consumer is still defining a schedule to modify his comfort constraints when nobody is home. However, instead of setting back the internal temperature setpoints, it relaxes the dead band width around the same setpoint. As a result, the dead band area increases, which means that the TCL has a larger energy buffer to consume before switching to a new state.

## 4.4   Results

Figure 4.3 shows sample air conditioning load profiles and the respective indoor air temperatures for a single household, generated using the different control strategies presented in this chapter.The CS and DS cases have similar power consumption patterns in terms of switching frequency and periodicity. The DD strategy has a significant effect on the load. The main difference is represented by the longer signal period, which is the direct consequence of an increased deadband. The larger the deadband, the longer it takes for the indoor temperature to reach the comfort boundaries. While the end user is in the house the three curves are perfectly superimposed. During working hours, the indoor temperature profiles diverge considerably. With the DS, after a transition period in which the air conditioning

system is not available, the indoor temperature starts modulating around the new setpoint. This strategy produces considerable cooling energy savings in all cities as depicted in the left panel of Figure 4.5. However, as shown in the middle panel of Figure 4.5, the regulation flexibility is impacted negatively. In the DD scenario, the air conditioners modulates around the same temperature, even during working hours. However, the expanded deadband width allows the system to maintain the operating status for a longer period. This increases the regulation flexibility in all the cities and the model seems to be sensitive to the outdoor air temperature conditions. Specifically, we observe that the added value of an expanded deadband width is more pronounced in milder climates. The DD increases the average regulation flexibility per day per household by almost 11 kWh (600%) in Sacramento, by 12 kWh (250%) in Las Vegas and by 3 kWh (260%) in Los Angeles (Figure 4.5). Sacramento and Las Vegas show comparable results in absolute terms, however, in Sacramento, the DD control strategy is able to increase the available flexibility by almost six times with respect to the DS case. Indeed, in milder climates households are subjected to lower heat gains, which means that it takes more time for the indoor temperature to cross the deadband and reach its upper limit with a relaxed duty cycle. As a result, we obtain more capacity to dispatch DR services. On the downside, the DD strategy increases the average daily energy consumption per household by around 5 kWh (75%) in Sacramento, 6 kWh (15%) in Las Vegas and 0.6 kWh (80%) in Los Angeles. (Figure 4.5). From the load shifting perspective, there is no flexibility in Los Angeles regardless of the control strategy adopted. In the CS case, we observe the same level of flexibility for both Sacramento and Las Vegas. However, when switching to a DS, Sacramento's potential is largely reduced, while Las Vegas' remains unaltered. This reduction is driven by the outside temperature when thermostat setback occurs, making cooling already unnecessary for 6 pm at Sacramento. The DD strategy increases the flexibility potential in both Sacramento and Las Vegas. Figure 4.5 shows that all homes under CS shift about 0.2 kWh of cooling away from evening hours into afternoon hours. Our study shows that if consumers were to be able to do DD instead of DS, they could shift an extra 1 kWh of cooling load during the same period. Overall, our results highlight the importance of capturing human behavior and preferences when estimating demand response potential. These preferences impact the model's response to the same set of inputs significanly. Using the *dynamic setpoint* strategy, consumers can achieve a substantial reduction in terms of cooling energy consumption, however, the aggregator who would be interested in selling grid services, find itself with a scarcer
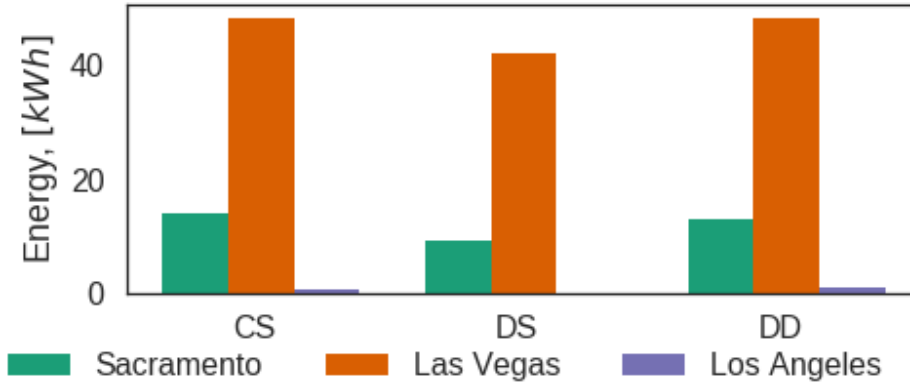
FIGURE 4.4: The effect of different control strategies over 1000 simulated households in terms of cooling load.

share of controllable loads. Relaxing the deadband width, we trade energy savings potential for a boost in terms of cooling load flexibility. Depending on how valuable this flexibility become in the future, one or the other strategy could become more or less interesting to pursuit from the aggregator's prospective. The impact of these control strategies is amplified in certain climate conditions. Specifically, temperate climates get both the most benefits out of the *dynamic deadband* strategy, in terms of a flexibility boost, and drawbacks, in terms of increased cooling energy consumption. Thus, aggregator companies which are willing to build a portfolio of flexible cooling loads portfolio, should take into account in their evaluations both the climate conditions and consumers preferences, considering the full range of implementable control strategies, to avoid a misleading representation of the actual potential of their assets. They should target costumers in specific locations and implement different control strategies depending on the kind of service they want to provide, taking into account all the possible value streams. It is worthy to note that, a house in Las Vegas provides more cooling load flexibility than the same house in Sacramento if both use dynamic or constant setpoint control strategy. However, if we implement a dynamic deadband control in Sacramento, the relative benefit is much larger than a house in Las Vegas.

## 4.5   Conclusions and next steps

In this work, we used a well-studied TCL model to simulate the cooling load of 1000 residential air conditioner units and analyze the impact of human behavior on their DR potential. Specifically, we tested three different control strategies to
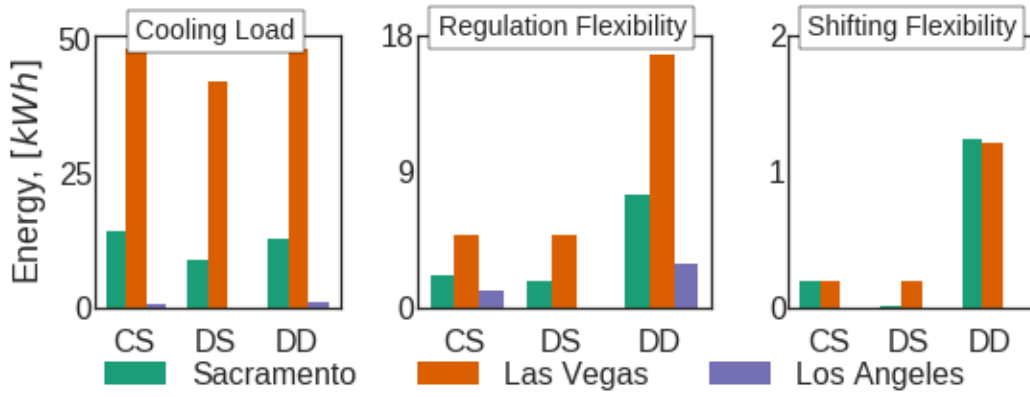
FIGURE 4.5: The impact of different control strategies on cooling load, regulation flexibility, and shifting flexibility.

capture human behavior and preferences: the thermostat is not programmed at all and a constant setpoint temperature is maintained throughout the day (*constant setpoint* strategy); the setpoint temperature is set back during working hours (*dynamic setpoint* strategy); instead of setting back the setpoint during unoccupied times, we expand the deadband around the setpoint (*dynamic deadband* strategy). Specifically, the *dynamic deadband* strategy increased the average regulation flexibility per day per household in Sacramento by 10.8 kWh (591%) and by 11.9 kWh (247%) in Las Vegas. On the downside, it also increased the average daily energy consumption by 5.3 kWh (76.5%) and 6.0 kWh (14%) per day per household respectively. Results showed the same trend when addressing the ramping problem: households using the *dynamic deadband* strategy were able to shift extra 1 kWh of cooling load away from evening hours, into afternoon hours. We modeled a heterogeneous population of 1000 households using a specific set of parameters sampled from uniform distributions. Using this population, we ran 33 different simulations, testing the effect of different climate conditions and setpoint/deadband variations. We observed that human behavior, expressed through thermostat control preferences, has a critical effect on the estimated demand response potential. Using the *dynamic setpoint* strategy, consumers achieve substantial cooling energy savings while sacrificing a share of their load flexibility. On the other hand, by relaxing the deadband, consumers trade energy savings potential for an increase in flexibility. While the trading efficiency for flexibility may seem wasteful, models of high penetration renewable energy systems suggest that significant curtailment of PV generation may be required during daytime [99]. Thus consuming excess energy during the day to prevent consumption in the evening may be very beneficial. The

impact of the different control strategies is amplified in certain climate conditions. Specifically, temperate climates get the most benefits from a *dynamic deadband* strategy in terms of flexibility. A house in Las Vegas provides more load flexibility than the same house in Sacramento if both use a DS or CS control strategy. However, the relative benefit of implementing DD in Sacramento is much larger than in Las Vegas. Future strategies for enabling DR will benefit from focusing on human behavior. Aggregators can target specific combinations of costumers and locations to maximize flexibility. They may also encourage consumers to alter their comfort limits instead of their set points, and then offer to optimize cooling energy consumption to either reduce costs or to best support the integration of renewables.

# Chapter 5

# Electric vehicles as flexibility resources

## 5.1 Preface to chapter 5

In the last two chapters we analyzed two kinds of flexibility assets, respectively thermal energy storage and thermostatically controlled loads, that can be integrated in residential or commercial buildings to enable advanced energy demand control strategies. In this chapter we talk about electric vehicles (EVs) as a distributed flexibility resource. As our main contribution, we present a modeling approach to describe an aggregation of Electric Vehicles System Equipments (EVSEs) as an equivalent energy storage. We describe the different parameters governing the model, explaining how they can be estimated from historical charging patterns. Finally, we talk about the importance of mobility patterns and EVSEs characteristics, as they influence the aggregate ability to shift the energy demand and provide extra flexibility. The equivalent energy storage model we present here is part of a study on EVs flexibility and Aggregation, lead by Mr. Michael Pertl, PhD candidate at Denkmark Technishe University (DTU). I undertook the majority of work related to this chapter, including the definition of an equivalent energy storage model. Mr. Pertl contributed to the modeling tasks and realizing the use case in section 5.4.1. Doctors Emre Can Kara, Michaelangelo Tabone, Mattia Marinelli and Sila Kiliccote provided help with technical support and ideas.

## 5.2   Introduction

The progressive rollout of electric vehicles (EV), which is concurrent with the decarbonization of the power sector, can bring environmental benefits in terms of global $CO_2$ emissions reduction and air quality in our urban centers [54]. For such reasons, many international institutions and governments are setting ambitious targets to foster a rapid growth for this technology. By the end of 2015, 1.26 million electric cars were on the road worldwide. The Paris declaration on Electro-Mobility and Climate Change sets a global goal of 100 million electric cars by 2030 [53]. The European Union aims at achieving by 2050 a 60% reduction in its GHG emissions levels compared with those of 1990 [27]. At the same time, California set its own target to deploy 1.5 million electric vehicles on the road by 2025 [96]. These are ambitious goal that will force people to reconsider the very idea of mobility, having an impact not only on the environment but on our day-to-day lives too. Such a rapid growth for this technology introduces a number of challenges from the infrastructural point of view. The mass diffusion of EVs will affect the way we design parking lots and gas stations, modify urban mobility patterns and considerably affect the electricity demand of our cities. Martinenas et al. [69] study the effects of uncontrolled EV charging at distribution level, analyzing the risks for obsolete electrical infrastructures. This latter aspect its particularly critical since todays power system is already under stress due to the combined effect of residential electrification and distributed renewable generation, which is increasing the peak demand in late afternoons, pushing the system to invest massive resources to match the demand ramp [18]. Research is focusing on ways to model and simulate the effect of EV charging at both transmission and distribution levels, to develop guidelines and strategies to have a smoother integration between EVs and power grids. Many recent studies have focused on the potential benefits of controlled charging as oppose to uncontrolled charging. Specifically, these studies demonstrate how aggregated Electric Vehicles charge offer some degrees of flexibility that could potentially be leveraged to increase districts resiliency, redistribute part of the energy demand towards convenient periods of the day and even offer ancillary services to the grid, such as frequency regulation [63]. This flexibility can be leveraged by installing an appropriate Electric Vehicle System Equipment (EVSE) which enables remote visibility and control of a charging station. Thus, an aggregator, which can be a third party organization or the owner of the EVSEs, is able to cluster an control a large number of charging stations, implementing either a direct and centralized, or indirect and fully decentralized, smart charging strategy [45]. Many studies have

proposed alternative approaches to model an aggregate of EV, tailored over the needs of specific applications. Saber et al. designed a methodology to leverage EVs flexibility to participate in the wholesale market with the purpose of maximizing the utilization of RES, reducing operational costs and emissions [88]. Bessa et al. formulated an optimization problem for EV aggregators which are willing to participate in the day-ahead and secondary reserve market sessions [13]. Their methodology is based on a a centralized aggregator which, for each of the aggregated final users, has information related to the preferred state-of-charge for up to the following day. Their results highlight the impact of variables uncertainties on the optimal strategy. Kara et al. [61] developed a methodology to study the potential benefits of centralized smart charging from the perspective of different stakeholders. Their model assume that, for each EVSE, arrival times, departure times and the energy demand profile is known by the aggregator. Their results show that optimizing charging schedules over both energy and demand charge it is possible to achieve a reduction of almost 25% in the aggregated monthly bills. Daina et al. defined a model to integrate activity-based demand modeling systems for the analysis of integrated transport and energy systems'[31]. Specifically they suggested a methodology to empirically capture end users behavioral choices in smart grid contexts. Their results show significant heterogeneity in end users behavior which implies that fixed charging behavioral scenarios could be misrepresentative of the reality. furthermore, heterogeneity could represent an opportunity for DSO and service providers to incentivize more flexible charging choices with targeted actions for the so called "inflexible drivers". In this chapter, we talk about how EVs can be considered as flexibility resources. We present the potential benefits and challenges related to EV integration, using real data from the PecanStreet dataset [72] to show the impact of EV penetration in urban districts. We introduce a new, general purpose, modeling approach to represent EV's flexibility as an equivalent energy storage. We define 9 time-varying parameters that fully characterized the equivalent storage model and that can be inferred from available historical charging patterns. In the last section of the chapter, we discuss about mobility patterns and EVSEs characteristics, highlighting how they affect the aggregate ability to shift the energy demand and provide extra flexibility to the grid.

## 5.3 Controlled vs uncontrolled charge

In this section, we use data from the Pecan Street open dataset to give context and introduce the need for a modeling strategy to enable EV charging stations aggregation and centralized control. Pecan Street Dataset consists of 1000, fully monitored, residential households in Austin, Texas. Many of these households have smart thermostats, distributed generation sources, EV charging stations and advanced metering infrastructures to collect high granularity data for each load and generation source. Figures 5.1 to 5.3 show data from a single household within the dataset. Figure 5.1 shows the original load of the household which consists of classic appliances (eg. freezer, TVs, coffee machine) as well as the air conditioning. The figure is a good representation of a typical residential load profile. Besides the baseline load, we can distinguish two peaks: the first pick in correspondence with the morning routine (from 6 to 9 am), and a higher one in the late afternoon when people arrive home from work. Figure 5.2 adds a second curve which represents the households net-load, obtained by subtracting the PV generation from the energy consumption. Due to the effect of PV generation, the households find itself self-consuming energy and selling portion of it back to the grid during the central hours of the day, when the PV production is maximum and consumption is limited to the baseline loads. The updated net-load shape highlights even more the importance of late afternoon peak, when the building starts importing energy from the national grid again, after being a generator for hours. The mass rollout of EVs is going to further accentuate this problem. Figure 5.3 adds a third curve which represents the actual household net-load, obtained by adding to the previous curve the consumption monitored from the level-2 charging station. The EV start charging as soon as the resident arrives home and plug the car, at around 6 pm. The figure shows how this effects the household net-load by further increasing the late afternoon peak by a large margin. In this specific case, the peak power increases up to 200% after the integration of an electric vehicles.
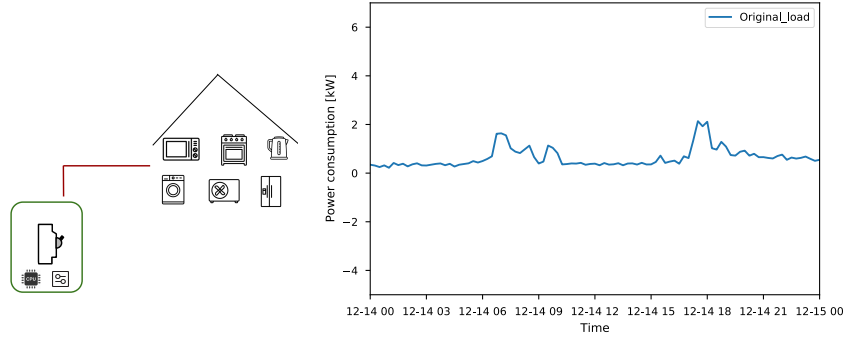
FIGURE 5.1: Net-load profile from Pecan Street Dataset
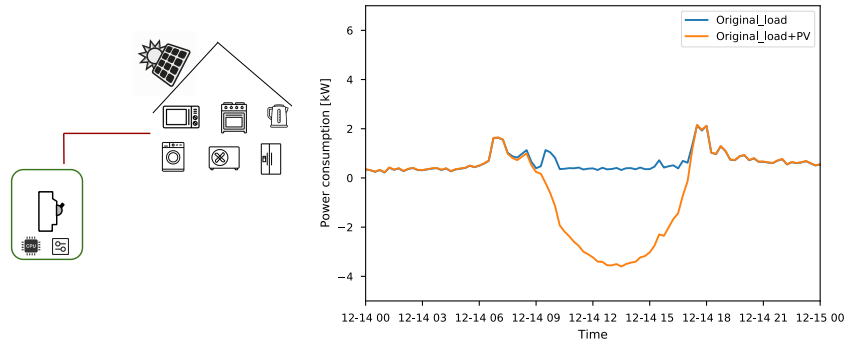


FIGURE 5.2: Net-load profile from Pecan Street Dataset considering PV generation
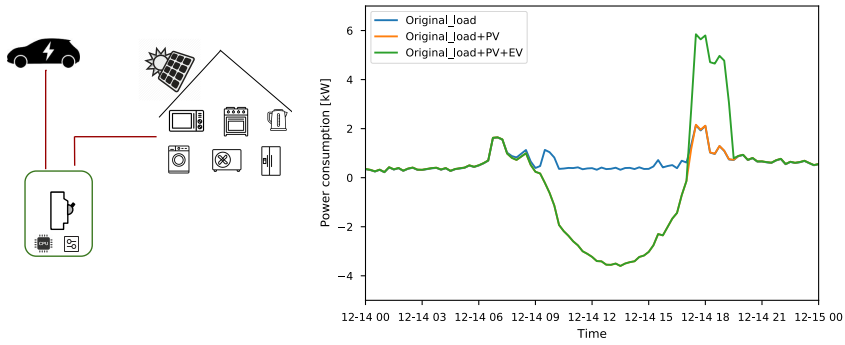


FIGURE 5.3: Net-load profile from Pecan Street Dataset considering PV generation and EV charge

These figures demonstrate how a sudden paradigm shift from fossil fuel based towards electric mobility, would drastically change the load profile of our districts. Due to the limited heterogeneity of residential patterns, which are based on working people habits, the aggregated demand peak during late afternoon becomes a

serious issue for the national grid which has to ramp its generation capabilities, tapping into expensive, and pollutant, peaker plants [33] [18]. Thus, a mass integration of uncontrolled EVs could create a series of issues at both distribution and transmission grid levels. However, as shown in the literature, EVs demand inherently has some degrees of flexibility that can be leveraged to control the charging profile. EV charging can be controlled, slow down or shifted in time, to provide services to the grid while taking into account users preferences and operational constraints. In this case, the load flexibility can be defined as the ratio between the time a car is plugged but not charging to the overall session duration [61]. The bigger the difference between the actual charging duration and the overall session duration, the higher the potential flexibility that that specific EV is bringing to the system. To evaluate these quantities we need to know, or estimate, the arrival and departure times, which make the session duration, as well as the initial and expected final state-of-charge of the vehicle's battery.

## 5.4  EV equivalent energy storage model

In chapter 2, we introduced the general equivalent energy storage model, showing how every flexibility asset can be described as a particular case of an energy storage system, defined by the same parameters while constrained to follow different sets of physical rules. We already introduced equation 5.1, which describes the equivalent energy storage model, based on the work of Hao et al. [49]. The equivalent storage model is defined by a set of signals $U_{(t)}$ that satisfy the following equations:

$$ -\eta_- <= U_{(t)} <= \eta_+ \qquad \dot{x}_t = -\alpha x_t - U_{(t)} \qquad |x_{(t)}| <= C \qquad (5.1) $$

Where $\eta_+$ and $\eta_-$ represent the maximum charging and discharging rates of the equivalent energy storage system respectively. The state variable $x$ represents the internal energy of the system; $\alpha$ is the dissipation rate, the amount of energy naturally lost due to storage inefficiencies, and C the total energy capacity of the equivalent system. For the EV equivalent energy storage model, the flexibility signal $U^{ev}$ is defined as the overall charging requirements of a collection of electrical vehicles supply equipment (EVSE). For each EVSE, the flexibility is achieved by redistributing the charging schedule. By default, EVSEs use a constant power charge strategy that aim at fully charge the battery as fast as possible. By knowing the expected final user's departure time, EVSE can delay the completion of the charging process acting on the charging schedule, still ensuring that the battery is fully charged by

the expected departure time. The flexibility signal $U^{ev}$ is obtained by the sum of the rescheduled charging profile of each of the EVSEs of the collection. It is function of a series of 5 parameters which can be predicted by studying the historical charging sessions of the aggregated EVSEs collection $U^{ev} = f(E^{ev}, \delta_a^{ev}, \delta_d^{ev}, P_+^{ev}, P_-^{ev})$ Equations 5.2 to 5.5 show how these parameters are related to each other and to historical charging patterns.

$$C^{ev}(t) = C^{ev}(t-1) + \alpha_E^{ev}(t) + \beta_E^{ev}(t) \tag{5.2}$$

$$\eta_+^{ev}(t) = \eta_+^{ev}(t-1) + \sum_{i=1}^{M} P_{+,i}^{ev} \cdot \delta_{a,i}(t) + \sum_{i=1}^{M} -P_{+,i}^{ev} \cdot \delta_{d,i}(t) \tag{5.3}$$

$$\alpha_E^{ev}(t) = \sum_{i=1}^{M} E_i^{ev} \cdot \delta_{a,i}(t) \tag{5.4}$$

$$\beta_E^{ev}(t) = \sum_{i=1}^{M} -E_i^{ev} \cdot \delta_{d,i}(t) \tag{5.5}$$

The storage capacity $C^{ev}$ represents, at each time step, the amount of energy that should be collectively delivered by the distributed EVSEs to satisfy the charging requirements of all the EVs plugged into the system (equation 5.2). $\eta_+^{ev}$ and $\eta_-^{ev}$ are the equivalent storage maximum charging and discharging rates, they are estimated summing the maximum charging rates $P_+^{ev}$ and discharging rates $P_-^{ev}$ over each active EVSE. Equation 5.3 shows how to estimate the maximum charging rate; a similar expression can be derived for the the maximum discharging rate substituting $P_+^{ev}$ with $P_-^{ev}$. Using this formulation a non-zero $\eta_-^{ev}$ value assumes a EVSE with vehicle-to-grid (V2G) capabilities. While this storage model can be applied to study V2G interactions, we consider V2G applications and value discussion beyond the scope of this work. $\alpha_E^{ev}$ and $\beta_E^{ev}$ are respectively the capacity boosting and dissipation rate (equations 5.4 and 5.5). $\alpha_E^{ev}$ is the amount of capacity added to the equivalent storage at time $t$. This capacity represents the sum of the energy requested during the whole session by each EV plugged into the system at time $t$. $\beta_E^{ev}$ is the amount of capacity removed from the equivalent storage at time $t$, representative of the amount of energy leaving the system when a car is unplugged. For each EVSE, $E^{ev}$ represents the amount of energy to charge during each charging session. $\delta_a$ (equation 5.6) and $\delta_d$ (equation 5.7) are Kronecker impulse functions respectively centered at the EV arrival and departure times.

$$\delta_{a,i}(t) = \begin{cases} 1 \text{ at arrival time of EV i} \\ 0 \text{ otherwise} \end{cases} \tag{5.6}$$

$$\delta_{d,i}(t) = \begin{cases} 1 \text{ at departure time of EV i} \\ 0 \text{ otherwise} \end{cases} \tag{5.7}$$

The state-of-charge (SOC) is defined as the ration between the instantaneous energy content of the equivalent storage $C^{ev}(t)$ divided by its total capacity $C(t)$, calculated summing the capacity of each plugged vehicle's battery 5.8. In the case that the total capacity drops to zero, then the SOC is also considered to be zero.

$$SOC(t) = \begin{cases} \frac{C^{ev}(t)}{C(t)} \cdot 100 \ \% \ \text{for} \ C(t) \neq 0 \\ 0 \ \text{else} \end{cases} \tag{5.8}$$

This equivalent energy storage model is extremely flexible and can be applied to different market context and any aggregation level. The parameters of an aggregate of heterogeneous EVSEs can be estimated by summing the parameters evaluated for the single EVSEs. These parameters can be estimated through conventional methods such as autoregressive models, trained using historical EVSEs sessions data (e.g. arrival times, departure times, session energy).

### 5.4.1 Using the equivalent energy storage model

In this section, we use a trivial case to explain how the equivalent storage model can be implemented to describe an aggregation of EVSEs. Figure 5.4 shows the storage parameters evolution over a 24 hour period for two EVSEs. The example is taken from original measurement data and presents current practice of uncontrolled charging. The top subplot shows the evolution of the total/instantaneous storage capacity as new EVs approach and leave the system. At $t = 5.45$ the first EV arrives and adds about 20 kWh to the system, i.e. the total storage capacity at that time is equal to $\alpha_E$ as the capacity is a function of the previous capacity plus $\alpha_E$ and $\beta_E$ as shown in (5.2). At the same time the maximum charging rate of the storage increases from zero to 6.6 kW (level 2 EVSE) as seen in the middle subplot. The two EVSEs do not have vehicle-to-grid (V2G) capability, hence, no discharging is possible and the minimum charging power is 0. At 06.45 a second EV arrives and plugs to the second EVSE. The second EV adds extra capacity $\alpha_E$ to the system, the total capacity increases as well as the maximum charging power. Also the second car starts immediately to charge and $P_{act}$, which represent the equivalent storage instantaneous charging power, increases up to 10 kW. As the second EV connect the equivalent storage SOC drops due to the sudden increase in the total storage capacity. At 13.30 the first EV leaves and the total storage capacity is reduced by the same amount that was added at 05.45. From this point on, no charging happens anymore as the plugged EV is fully charged. The second EV leaves at 17.30 and all parameters drop to zero since the two EVSEs are now vacant.
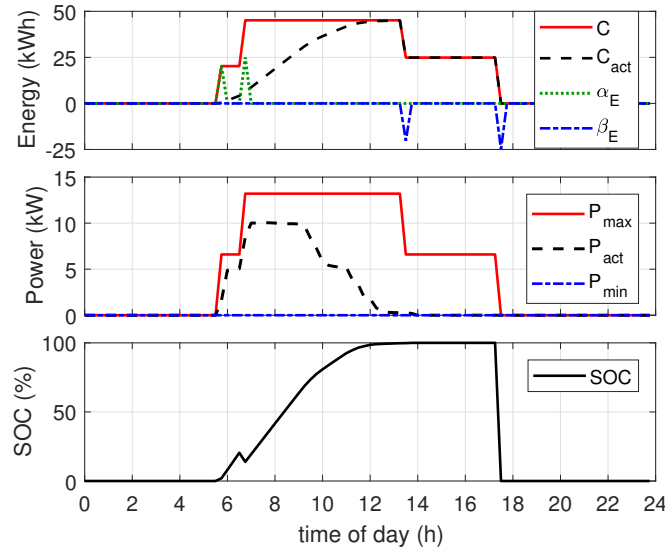
FIGURE 5.4: Storage parameter evolution for two EVSEs over 24 h period.

## 5.5 The impact of mobility patterns on the aggregate flexibility

As we saw in the last chapter, the EV equivalent storage parameters, which allow us to describe and control the flexibility granted by an aggregation of EVSEs, depend on the characteristics of the charging sessions (e.g. arrival times, departure times, energy demand). Therefore, end users behavioral patterns, as well as their mobility schedules, affect the ability of EVs to offer flexibility by altering their charging profiles. Specifically, the flexibility associated with each EV driver depend on arrival and departure time, the energy consumed driving and the charging frequency. Hence, mobility patterns and EVSEs positioning matters. Figure 5.5 reports three charging patterns. Top subplots show the charging rates in terms of power, while the session length is highlighted by the pink area. Bottom subplots show the evolution of the equivalent storage parameters: the black line indicated the evolution of the equivalent storage instantaneous capacity, while the grey area represents the energy that can be stored in the system, its flexibility. The Intermittent charging pattern is typical of an EVSE which is visited by cars throughout the whole day, which can be representative of a charging station located in the parking lot of a shopping mall or along the highway. The Workplace charging pattern is characterized by a long session, lasting from the beginning of the working day until the end of it. Due to the non-perfect homogeneity in employees schedule, we expect the equivalent storage parameters to change a lot throughout the day. This pattern is typical of EVSEs

which are installed directly at the workplace, thus sessions characteristics (begin, end, charge frequency, demand) are extremely related to exogenous variables such as working schedules, facility position, number of employees or shifts. The Evening charging pattern is characterized by a long session, lasting from late afternoon, at the end of the working day, until the next morning, before the beginning of the new working day. This pattern is typical of residential EVSEs. Again, aggregating different residential EVSEs we expect the resulting equivalent storage capacity to change a lot depending on EVs arrivals/departures distribution. For this reason, EVs integration in a virtual resource portfolio can have either positive, neutral or even negative effect depending on the smart charging strategy and the kind of service we seek to provide. Given EVSEs characteristics, inferred from historical charging patterns, the aggregator can seek to create a perfect portfolio of EVSEs by selecting and clustering them depending on the service it seeks to provide. For example, if the aggregator aims to play in the balancing market and sell capacity in the peak hours of the morning, it should integrate controllable workplace EVSEs in its portfolio and delay the charging schedule playing with employees flexibility.
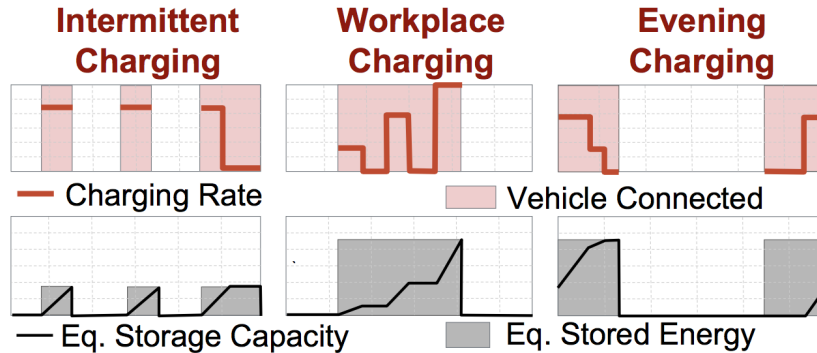


FIGURE 5.5: Mobility patterns and storage parameters

## 5.6 Conclusions

In this chapter, we talked about how EVs can be considered as flexibility resources. We presented the challenges and the potential opportunities related to a mass EV rollout, using real data from the Pecan street dataset to show the effect of EV integration in a urban district. We introduced a new, general purpose, modeling approach to represent EV's flexibility as an equivalent energy storage. We defined the different parameters showing how they can be estimated from historical charging data. We explained how the model can be used by referring to a trivial case of

an aggregation of two EVSEs. In the last section, we discussed about the impact of mobility patterns and EVSEs positioning in the aggregate flexibility, highlighting how aggregators should build their portfolios of resources, clustering different kinds of EVSEs, depending on their necessity and the kind of services they want to provide. With the next chapter, we move from the modeling tasks to the optimal management of a portfolio of heterogeneous flexibility assets. We will see how the equivalent storage model we presented can be used to model and capitalize EVs flexibility.

# Chapter 6

# Flexibility resources in an industrial microgrid

## 6.1 Preface to chapter 6

In the last chapters, we defined methodologies to model and simulate different flexibility assets, showing how they can be integrated to provide demand response services and, in general, to acquire a better control over the energy demand. In this chapter, we show some preliminary results obtained by integrating controllable TCLs and energy storage in an industrial microgrid. Specifically, we test a peak reduction strategy in an industrial microgrid, leveraging a sensible heat thermal energy storage and the existing HVAC system. This chapter allow us to discuss some of the challenges related to the actual implementation of a demand side management in an industrial environment, using off the shelf components and 15-minutes granularity data. This chapter has been presented in the 9th International Conference of Applied Energy, in Cardiff, as follows: "F.Carducci, Antonio Giovannelli, Massimiliano Renzi, G.Comodi; Improving flexibility of industrial microgrids through thermal storage and HVAC management strategies". I undertook the majority of work related to this chapter, including the design of experiments, data collecting and analysis and the interpretation of results. Mr. Giovannelli, Dr. Renzi and Dr. Comodi contributed with comments on the ideas presented and editorial assistance.

## 6.2 Introduction

In many countries, a large share of the national energy portfolio is now made from non-programmable renewable energy sources, thus is becoming harder to assure

the balance between the national energy demand and the offer given todays grid flexibility. Demand side management (DSM) programs are going to play a role in enhancing grids capability to cope with this problem, shifting part of the burden from control to demand [40]. Due to the nature of their loads, and the interest in investing in distributed generation, industrial microgrids are perfect candidates to provide services to the grid or actively playing in balancing the electricity market [7]. In [92], authors presented a methodology to identify interesting industrial applications for demand response. Alcazar-Ortega et al. [3] investigated the demand response potential in a meat industry in Spain, finding that the peak power demand in certain periods could be reduced by 50Having in mind these possibilities, research is focusing on new ways to assess how much power can be shifted, or cut, with respect to the traditional electric consumption patterns and for how long. Energy storage systems (ESS), thermostatically controlled loads (TCL) and Electric vehicles (EV) can be all used to enhance a microgrid flexibility and its potential in providing grid services. Thermal energy storage is a key technology to improve flexibility of final users. Several studies have demonstrated their potential in reducing peak loads or arbitraging price [29] [28] [6]. Thermostatically controlled loads (TCL), from residential refrigerators up to complex industrial scale heat pump units, can be managed to shift their electricity consumption away from peak times. Mathieu et al. [71] estimated that the technical resource potential for Californian residential TCLs is approximately 10-40 GW/8-12 GWh. In this chapter, we present the results achieved by implementing a set of load management strategies in an Italian microgrids. A thermal energy storage and the building HVAC system are used to leverage the thermal inertia of the industrial building and the synergy with the microgrids renewable generation. This studys central contributions are a set of indications on how these assets can be individually exploited to increase the microgrid flexibility in terms of net-load management, and a discussion over the limits of a metering infrastructure sampling with a 15-minutes granularity.

## 6.3 Methodology

In this section we present the industrial microgrid, the different flexibility assets and the demand side management strategies implemented.

### 6.3.1   The industrial microgrid

Our testbed is the industrial microgrid of Loccioni in Angeli di Rosora, Italy. In particular, we perform tests using both the thermal energy storage and HVAC system of one of the industrial buildings connected to the microgrid, the Leaf lab. It is a two storey building consisting of two distinct areas: the factory (total area of about 2400 m2) in the inner part of the building and the offices (total area of about 5200 m2) in the outer parts. The building is equipped with PV generation, with a nominal power of 236.5 kW. The cooling and heating demands are satisfied by three heat pumps, for a total capacity of 430 kW. A thermal energy storage is integrated with the HVAC system to store the excess of PV production during weekends. When the factory electricity demand is negligible and PV production is available, the thermal energy storage is charged by means of heat pumps. This thermal energy is then used during weekdays to reduce the peak load consumption. An advanced metering infrastructure is present in the building, collecting data on the electricity consumption, as well as internal comfort parameters (e.g. internal/external temperature) with a 15 minutes granularity.

### 6.3.2   The HVAC system

The HVAC system consists of chilled beams and air handling units as emission systems and of three water-to-water heat pumps (HP1, HP2, HP3) as production units. The AHUs are used for the whole building, including factory and offices, while the chilled beams are used for the offices only. These two systems can work together or separately. Two of the heat pumps (HP2, HP3), which have a nominal cooling capacity of 280 kW each (when supplying water at 7°C), are used for the AHUs. The smaller heat pump (HP1) has a cooling capacity of 150 kW (when supplying water at 15°C) and is used for the chilled beams only. Their capacity can be regulated according to the cooling demand by partializing the compressors usage between 20% and 100% of the total capacity and varying the supply temperature between 5°C and 15°C. The water source for the heat pumps is represented by a well at a constant year-round temperature of about 13°C. The water from the well can also supply the chilled beams directly in passive cooling mode for reduced cooling demands.

### 6.3.3 The thermal storage

The thermal energy storage consists of an insulated concrete water tank of $460m^3$. It has a rectangular base and its dimensions are $12.3 \times 11 \times 3.4m$. Each wall has a thickness of 0.25 m and is insulated by means of 0.16 m of xps polyfoam c350 (thermal conductivity 0.032 W/m K). The tank is buried below the ground to reduce heat losses as much as possible. In summer the storage tank can be charged by the heat pumps (HP2, HP3) outside the working hours (when PV electricity is available or during off peak hours, as better explained in the following) and it can supply then cold water to the AHUs when cooling is required during the working hours.

### 6.3.4 Demand side management strategies

We test two demand side management strategies. The first strategy aims to enhance the microgrid flexibility by the coordinated use of PV, heat pumps and thermal energy storage. During weekdays, PV generation is almost entirely absorbed by the building demand. On the other hand, during weekends PV generation exceeds the building energy demand: we can use this excess of energy to drive the electric compressors of the heat pumps and charge the thermal storage; then, during weekdays, we can discharge the thermal storage to reduce the electricity consumption during peak hours. The second strategy aims to enhance the microgrid flexibility by controlling the HVAC system. In particular, we regulate the heat pumps temperature set point in order to reduce the electricity demand during peak hours of the day, exploiting the thermal inertia of the building to maintain the internal comfort. This can be referred as a load shedding strategy. After we change the set point, the heat pumps shut down until the temperature reaches the new one.

## 6.4 Results

In this section we report the main results obtained implementing the DSM strategies described in the previous paragraph. Figure 6.2 shows the effect on the electricity demand of using the thermal energy storage for two weeks, in April 2017. Figure 6.1 shows the building net-load with 15 minutes granularity. The net-load becomes negative when the rooftop PV generation exceeds the energy demand of the building. The PV production is mostly self-consumed during working days, while it largely exceeds the energy demand during week-ends (9th and 16th of April). When this happens, the produced electricity is fed back into the main grid. Thanks to the thermal energy storage part of the electricity produced by the PV plant can be used
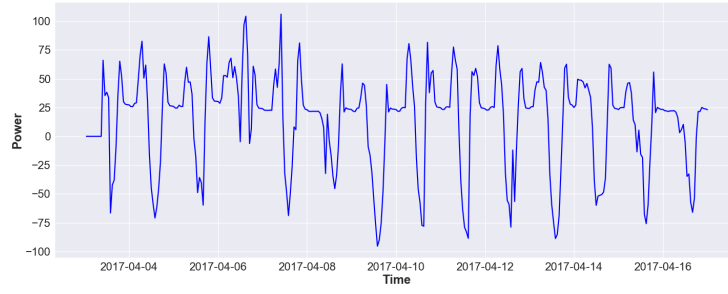
FIGURE 6.1: Building net-load with 15 minutes granularity
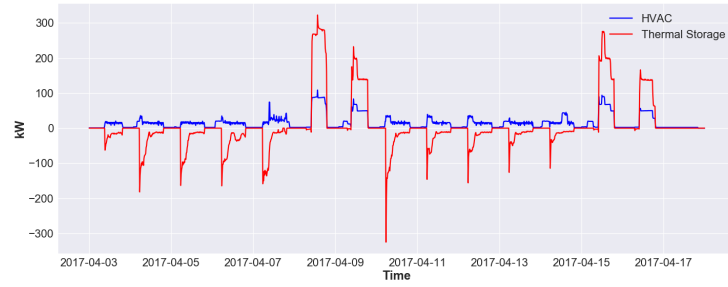


FIGURE 6.2: Effect of the thermal energy storage on the electricity demand

to drive the heat pumps and accumulate thermal energy. Figure 6.2 shows in blu the electricity demand from heat pumps, and in orange the thermal energy storage dispatch profile. We can abstract more insights from figures 6.1 and 6.2. First, the thermal energy storage is indeed charging during week-ends, using the PV over production. Nevertheless, part of the PV production is still exceeding and sold to the grid. The monitored period showed in Figure 6.1 includes the Easter weekend: Saturday (15th of April), Easter Sunday (16th of April)and Easter Monday (17th of April). As in other weekends, the energy produced by the PV plant drives the heat pump until the thermal energy storage is fully charged. The thermal energy storage discharging phase usually starts on Monday, during regular working hours, however on the Easter Monday it does not happen. Due to the festivities there is no cooling energy demand from the building. At the same time, the thermal energy storage is fully charged and the HVAC system is not operating, therefore all the PV production flows to the national grid. During working days, the energy discharged from the thermal energy storage allows us to reduce the power consumption during critical hours. Considering the thermal energy that can potentially be accumulated in the storage and the average measured heat pumps COP, which is set around 2.8, the thermal energy storage can help shred up to 40 kWe of power for three hours. We tested the load shedding strategy the 16th of November during a working day,
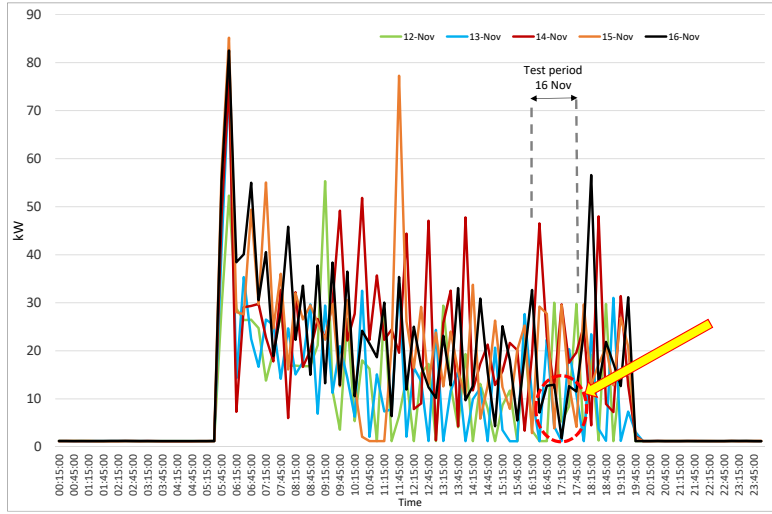
FIGURE 6.3: Heat pumps' consumption profile during five working days

between 16:45 and 17:45. Figure 6.3 shows the heat pumps consumption time series of five different working days. We highlight in black the one relative to November 16. Figure 6.4 windows the consumption time series around the testing time. In this case, the time series are all showed in gray except for the one relative to November 16, highlighted in black. The load shedding test started at 16:30. Figure 6.4 shows that the heat pumps electricity demand is indeed reduced by a sensible margin until 17:45, when the new set point is reached and the heat pumps starts working again (Figure 6.4). The consumption pattern showed during the test is noticeably different from the rest of the week: the on-off cycle, typical of thermostatically controlled loads, is clearly recognizable in gray curves. However, the black curve shows that during our test the cycle is interrupted by a longer off period. As expected, we register a high consumption peak after the heat pumps start working again. This peak is noticeably higher that the ones registered during the other days, over normal operation regimes. This recovery phase is well known in the literature: after a load shedding period, heat pumps are forced to work extra hard to maintain the desired thermal comfort ending up creating a new peak in electricity consumption. Thus, while the load shedding strategy provides a temporary reduction of around 20 kW in power consumption, it also generate a new higher consumption peak (57 kW at 18:15) and increase the overall energy consumption. Figure 6.4 shows a similar consumption peak the 14th of November (48 kW at 18:30). However, looking at
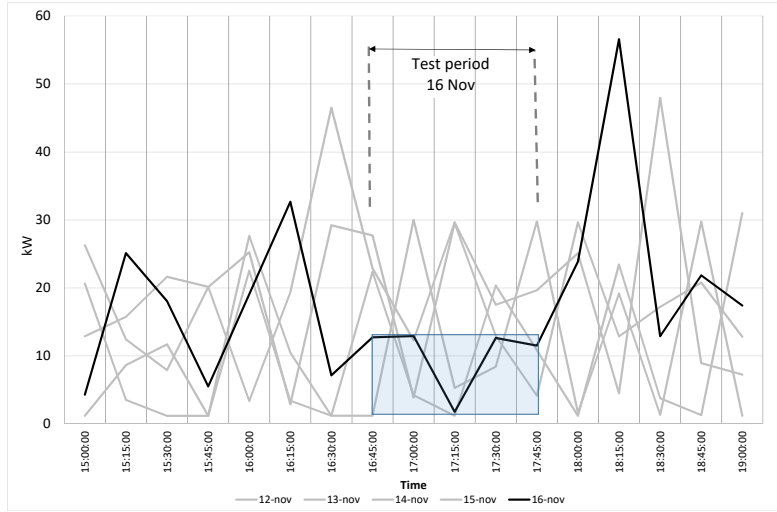
FIGURE 6.4: Heat pumps' consumption profile windowed around the testing time

TABLE 6.1: Data from November tests

| Day | Electricity consumption 16-18.30 [kWh] | Peak Demand 16-18.30 [kW] | Daily Avg External Temperature [°C] |
|-----|------------------|-----------------|------------------|
| 12-Nov | 31 | 30 | 8 |
| 13-Nov | 32 | 28 | 6 |
| 14-Nov | 62 | 48 | 5 |
| 15-Nov | 49 | 30 | 8 |
| 16-Nov | 51 | 57 | 8 |

the daily average external temperature values in Table 6.1, where peak demand and total energy consumption data are reported for each analyzed weekday, we notice how the 14th of November was in average a much colder day, a 3 °C difference in terms of daily average, which directly results in extra effort for the heat pumps, hence extra consumption.

These results confirm that load shedding strategies can contribute to provide a sudden reduction in power absorption and potentially enable a wide range of grid services. However, their effect at the building level is to shift part of the energy demand, generating new consumption peak and causing overall worst performances in terms of energy efficiency. This test also proves that sampling electricity consumption data with a 15 minutes time granularity is sufficient to identify the activation

of a load shedding strategy and, given a consumption baseline, to analyze its impact in terms of energy consumption. However, if the nature of the application requires precise estimates over the power consumption, higher granularity would be necessary to capture the actual consumption peaks within the on-off cycles.

## 6.5 Conclusions

In this study we showed how the HVAC system and a thermal energy storage can be used as flexibility assets in an industrial microgrid. Two demand side management strategies were implemented using a thermal energy storage and the HVAC system. Tests were carried in the industrial microgrid of Loccioni group, in Italy. The first strategy aimed at assessing the reserve of power that could be achieved by the integrated use of PV, heat pumps and thermal energy storage: the excess of PV generation during weekends was used to drive electric heat pumps and charge the thermal energy storage then, during weekdays, the same storage was discharged reducing the electricity consumption during critical hours. Results showed that thermal energy storage can, in mild seasons, contribute to curtail the peak load consumption by up to 40 kWe for three hours. The second strategy aimed at assessing the reserve of power that can be controlled using the HVAC system. Heat pumps temperature set points were regulated to reduce the electricity demand during peak hours of the day, exploiting the thermal inertia of the building to maintain the internal comfort. Results showed that load shedding via HVAC control can provide a temporary reduction in power consumption by up to 20 kWe, while a new consumption peak is generated right after the tests. When the strategy is revoked, and the original temperature setpoint is restored, the chillers turn on again at maximum power to push the temperature within the acceptable deadband, generating a new peak in terms of energy demand. The data we collected also proves that sampling electricity consumption with a 15 minutes time granularity is adequate to identify the activation of a load shedding strategy, giving us an important feedback when it comes to choose the appropriate metering infrastructure for such applications. Future studies will focus on how to evaluate the potential flexibility granted by the combination of all available micro grids assets, while exploring the integration of new assets and different demand management strategies.

# Chapter 7

# An Optimal Portfolio Management Framework for Flexibility Assets Aggregators

## 7.1 Preface to chapter 7

In chapter 5, we introduced a modeling approach to describe the behavior of an aggregate of electric vehicles charging stations as an equivalent energy storage system. Electric vehicles, battery energy storage systems and thermostatically controlled loads are different assets that aggregators can use to form their portfolio of flexibility resources. With this chapter, we move our attention from the modeling tasks, to the optimal management of a portfolio of flexibility resources. Specifically, we define a methodology to i) integrate the equivalent storage models we introduced in the previous chapters to estimate the aggregate flexibility resources available in a generic urban district; and ii) produce an optimal portfolio management strategy for flexibility aggregators that aim to optimally manage these resources, leveraging the energy price variability while producing valuable services for the national grid. The optimal portfolio management task is modeled and solved as a convex optimization problem, using the Python CVXopt library [75]. We apply the methodology in two alternative scenarios. The first scenario is related to aggregators bidding problem, while the second suggests a distributed approach to address national grid's ramping problems in critical hours of the day. I undertook the majority of work related to this chapter, including all the modeling tasks, the development of a simulation platform and the interpretation of results. Mr. Bennet Mayers contributed to the convex formulation. Dr. Michaelangelo Tabone, Dr. Emre Can Kara, Sila Kilic-

cote and professor Gabriele Comodi contributed with comments on the ideas and editorial assistance.

## 7.2   Introduction

Power grids are designed to work under balanced supply and demand at all times. This hard constraint is increasingly challenged by uncertain and intermittent renewable generation sources. Historically, grid balance was maintained by operating controllable thermal generators that relied on fossils fuels, which could be ramped up and down at will, within mechanical system constraints. However, the intermittent nature of renewable generation, such as wind and solar energy, puts an increase amount of stress in terms of power balance, system stability and ramp requirements [84]. Therefore, increasing the power system flexibility becomes a priority if we want to pursue our renewable integration goals towards a more sustainable future [8]. Many nations have set ambitious goals to increase the share of renewable resources in their energy mix [81], thus we are facing a future where it will be more difficult to maintain balance between supply and demand and thus maintain service quality [1]. Information technology with the grid (often referred to as the "Smart Grid") addresses some of these issues by collecting data and remotely controlling distributed technologies such that they can observe and actively respond to changing grid conditions [58]. The Smart Grid implies a Copernican revolution to the current electricity system: placing distributed infrastructure (some owned and operated by consumers) at the center of the control paradigm instead of generators. In this new paradigm, consumers must play a more active role, which will be facilitated by demand response and behind-the-meter resources like distributed solar and energy storage. Energy storage systems are machines designed to provide flexibility, given the ability to store energy under different forms and through different conversion system depending on the adopted technology [30]. Energy storage systems can be integrated at different scales and locations: in a distributed manner behind the meter, up to bulk applications at generation level. Depending on their scale and positioning they can be used for different kind of applications: frequency regulation, capacity deferral, intermittent generation integration, peak-shaving, demand management and price arbitrage [105]. Through Demand response (DR) final users can actively participate to the system balance using their flexibility, modulating their loads to provide services to the grid. Depending on the nature of the final user, different kind of flexible loads can be integrated with the grid. Thermostatically

controlled loads (TCL) in residential buildings, such as refrigerators, air conditioners, heat pumps and electrical boilers, are among most studied DR resources [62]. TCLs operate via thermostats based hysteresis control, modulating the indoor air temperature between upper and lower bounds around a setpoint. By controlling the setpoint, TCLs can be operated to rapidly adjust their demand. These characteristics make them ideal candidates to provide ancillary services [12].TCLs have been studied extensively in literature and we refer the interested reader to [19]. Electric vehicles (EV) can be valuable flexible assets too. Studies show how EV can provide a range of services by controlling their charging rate. EV charging stations can be integrated in a district to reduce local congestion problems or to implement distributed voltage control [63]. In [61] authors estimate the potential benefits of performing price arbitrage using a smart charging strategy based on a time of use (TOU) rate structure. Aggregators play a critical role as enablers of these technologies. Aggregators are service and technology providers, facilitating an active participation of end users and DER owners with the energy market. They can assume the basic role of retailers for their end users, while creating a value stream for all the flexible assets and prosumers who wants to act as distributed grid resources [14]. In [15] authors explore the value of aggregation showing how different regulatory and market frameworks can be leveraged by aggregators to generate value for them-self, for end-users and the entire electricity system.It is in the best interests of aggregators to optimally act on the energy market either when trading at the whole sale level or deciding how to dispatch their flexibility resources. In this work we refer to this as the optimal portfolio management problem. Depending on the level of aggregation and the range of services that the aggregator is interested in, both the definition of optimal and problem's constraints can be different. An aggregator interested in managing an individual industrial microgrid has to face a different set of challenges from one who wants to use the flexibility from California's residential TCLs as a virtual power plant. In this chapter, we present a framework for the optimal management of aggregators' flexible assets portfolio, focusing on three main sources of flexibility: thermostatically controlled loads, electrical vehicles charging, and battery energy storage systems. We model the different flexibility assets as equivalent energy storage, mapping their behaviour into a set of convex and affine constraints. We demonstrate the capabilities of the framework proposing two different case studies. In the first, that we call the ramp rate management problem, we want to optimally reshape the district net-load to reduce the aggregated ramp rate below a predetermined threshold. In the second one, that we call the

aggregator bidding problem, we we want the real time district net-load to track a profile bid by the aggregator in the day-ahead market. Many recent studies have focused on how to estimate the technical potential and optimally dispatch aggregate resources, targeting different levels of aggregation and specific service requirements. In [20] authors suggest a mixed-integer linear programming optimization model to maximize the profit of an aggregator which has to manage a portfolio of DER, solving for both planning and operation schedule. They explore both a stochastic and deterministic approach to the problem formulation and assess how the former one is more robust to price change and results in different strategic choices. In [48] authors suggest an near-optimum heuristic framework to perform an economic based optimization of the consumption schedule for 5555 residential costumers and more then 55 thousands schedulable loads. Their results show how such methods could benefits all the involved stakeholders: the aggregator can make profit by arbitraging in the spot market, costumers enjoy reduced bills, while at system level peak loads are lowered.In [103] a method based on linear programming for optimal scheduling and operation of a load aggregator's electric energy storage (EES) is presented. The flexibility granted by the energy storage capabilities is used to optimally bid into the day-ahead market. During real-time operation, the discrepancy between the bid capacity and the actual load requirements are compensated in a balancing market. Reported results show that it is possible to achieve energy cost savings, even if they are not enough to justify investing in EES. In [47] authors model the problem of an aggregator participating in the day-ahead market to optimally bid the energy requirements of a fleet of plugin electric vehicles as a MPEC (mathematical problem with equilibrium constraints), using a bilevel optimization approach: the upper level problem aims at minimizing operational costs, while the lower level represents the market clearing process.Reported results obtained using realistic driving patterns show that, for a relatively large aggregation of EV, the uncertainty related to drivers schedule has only a minor impact on the optimal solution. Moreover, even at low aggregation level, the aggregator can have a significant impact on market clearing prices depending on the EV population charging schedule. In [98] a robust mixed integer linear programming model is proposed to solve to optimal dispatch problem for microgrids, given the opportunity to work in both the energy and ancillary services markets. The formulation take into consideration aggregate loads, DER and energy storage, which can be leveraged as flexible ramping resources. With respect to the cited works our framework is able to manage an heterogeneous portfolio of flexible assets, integrating TCLs and EVs as equivalent energy storage systems.

We also propose a convex formulation to solve the flexible assets optimal dispatch problem which ensure reliability, high performance and potential for scalability. We use this framework to analyze the role of flexible loads in an aggregator portfolio, showing how this could change depending on the type of asset, the deliverable services and the technical requirements. We want to define an approach to optimally build and manage a portfolio of flexible loads depending on the services we want to provide and the technical potential of the different assets. The main contributions of this work are:

1. A general framework to build and manage a portfolio of flexible loads depending on the services to provide, the aggregation scale and the technical potential of the different assets

2. A convex formulation to solve the optimal dispatch problem, modelling EES, TCls and EVs as equivalent energy storage systems

3. A methodology to assess the economic value of flexible loads

The rest of the chapter is organized as follows. Section 7.3 is dedicated to the methodology: Section 7.3.1 describes the portfolio management framework, the modeling approach pursued for the different flexibility assets; Section 7.3.2 presents the convex formulation, analyzing the cost function and the general set of constraints; Section 7.3.3 is dedicated to an in depth description of the data-set and Section 7.3.4 describes the different case studies we implemented. Finally, Section 7.4 includes the results obtained in the two case studies and a discussion of future research objectives.

## 7.3    Methodology

### 7.3.1    The portfolio management framework

The flexible assets portfolio management framework for aggregators consists of three main components (Figure 7.1). The input module consists of a set of functions that pre-process inputs before the analysis, performing checks for dimension consistency and missing value detection. The flexibility estimation modules evaluate the equivalent energy storage parameters for both the EVs and TCLs assets. The optimal resource dispatch module consists of the convex optimization problem that uses the time series inputs to build the constraints. The final outputs of the framework are the time series related to the optimal dispatch of the single available asset. In
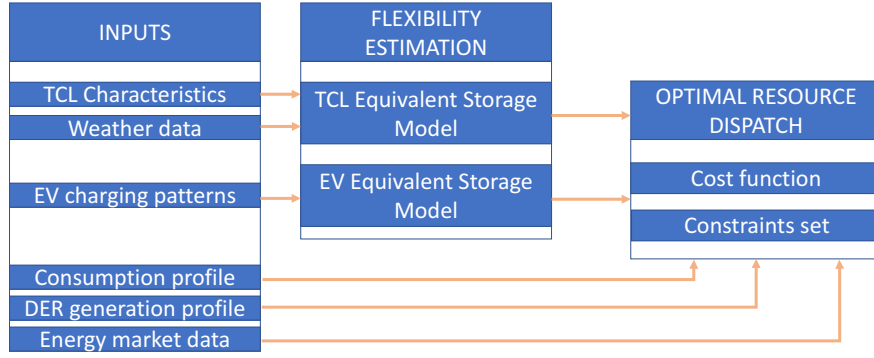
FIGURE 7.1: The Flexible Assets Portfolio Management Framework in its three main components.

the following sections, we are going to describe in details how the modeling and optimization components work.

### 7.3.2 Flexibility estimation

An energy storage system is a machine which stores energy in different forms to increase the level of control over a system. For this reason, it comes natural to imagine every other flexibility asset as a particular case of an energy storage system, described by the same parameters while constrained to follow different sets of physical rules. In this work, we follow the definition of generalized battery model presented in [49]. Our equivalent battery models are set of signals $U_{(t)}$ that satisfy the following set of equations:

$$-\eta_- <= U_{(t)} <= \eta_+ \qquad \dot{x}_t = -\alpha x_t - U_{(t)} \qquad |x_{(t)}| <= C \qquad (7.1)$$

Where $\eta_+$ and $\eta_-$ represent respectively the maximum charging and discharging rate of the equivalent energy storage system; the state variable $x$ represents the internal energy of the system; $\alpha$ is the dissipation rate and C the total energy capacity of the equivalent system. In the next two paragraphs we are going to describe how these equivalent storage parameters can be evaluated for aggregations of TCLs and EVs.

**TCL equivalent storage model**

To model and control the aggregate flexibility of a collection of TCLs we use the formulation described in [49]. The flexibility signal $U^{tcl}$ is defined as the sum of the perturbations that each of the N TCL of the collection can accept around
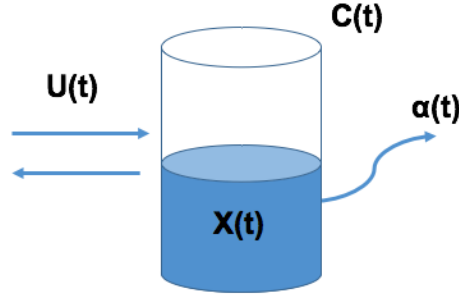
FIGURE 7.2: The equivalent energy storage model.

the nominal power consumption $P_0$ while still meeting the user specified comfort requirements.Equation 7.2 shows how to estimate the equivalent storage parameters using TCLs parameters.

$$C^{tcl} = \sum_{i=0}^{N} \frac{\delta^{tcl}}{b_i^{tcl}}, \qquad \eta_-^{tcl} = \sum_{i=0}^{N} P_{0,i}^{tcl}, \qquad \eta_+^{tcl} = \sum_{i=0}^{N} P_{m,i} - P_{0,i}^{tcl} \qquad (7.2)$$

$$a^{tcl} = \frac{1}{R^{th}C^{th}}, \qquad b^{tcl} = \frac{cop}{C^{th}}, \qquad P_0^{tcl} = \frac{a^{tcl}(\theta_a - \theta_r)}{b^{tcl}}$$

For each controllable TCL: $\delta^{tcl}$ represents the relative deadband width,$P_m$ the rated power,$C^{th}$ and $R^{th}$ represent the household thermal capacitance and resistance, finally $\theta_a$ and $\theta_r$ represent respectively the outdoor air and setpoint temperatures. The dissipation rate $\alpha$ is equivalent to the time constant $a_{tcl}$. Therefore, recalling the relations from equations 7.1, the flexibility signal is function of 7 parameters: $U^{tcl} = f(\delta^{tcl}, P_m, P_0^{tcl}, R^{th}, C^{th}, \Theta_a, \Theta_r)$. To estimate the parameters described in equation 7.2 we need actual data for each TCL of the aggregation. In this work, we obtain this data building a simulation from the discrete-time model presented in [71]. We believe that this model represents a good trade-off between estimation accuracy and computational complexity. Indoor temperature $\theta$ of each household $i$ is calculated for each time step $k$ using equation (7.3), where $\theta_{a,k}^i$ represents the outdoor air temperature; $\theta_g^i$ is the temperature heat gain, which depends on the household thermal resistance $R$ and the air conditioning machine characteristics (rated power $P$ and coefficient of performance. We assume a constant coefficient of performance, while in reality it should change in relation to the outdoor air temperature. $a$ is a non-dimensional parameter regulating the sensitivity of the model to an internal/external heat gain.

$$\theta_{k+1}^i = a^i\theta_k^i + (1 - a^i)(\theta_{a,k}^i - q_k^i\theta_g^i). \qquad (7.3)$$

We implement the thermostatic hysteresis control using equation (7.4): the binary activation variable $q$ control the system to maintain the internal temperature within the upper $\theta_{+,k}$ and lower $\theta_{-,k}$ comfort boundaries.

$$q_{k+1}^i = \begin{cases} 0, & \theta_{k+1}^i < \theta_{-,k} \\ 1, & \theta_{k+1}^i > \theta_{+,k} \\ q_k^i, & otherwisee \end{cases} \tag{7.4}$$

Comfort boundaries are defined by the user's indoor temperature setpoint and thermostat deadband width. The lower boundary is defined as $\theta_{-,k} = (\theta_r) - \frac{\delta}{2}$. A symmetric formulation can be derived for the upper boundary $\theta_{+,k}$. The simulation procedure requires local outdoor temperature data in time series format and a set of parameters for each TCL to work: machines' rated power, users' preferences in terms of indoor temperature set points and deadband width, thermal capacitance and thermal resistance of the households. At the end of the simulation, we obtain the nominal power time series to estimate the equivalent storage parameters in equations (7.2).

**EV equivalent storage model**

For the EV equivalent energy storage model, the flexibility signal $U^{ev}$ is defined as the overall charging requirements of a collection of electrical vehicles supply equipment (EVSE). For each EVSE, the flexibility is achieved by redistributing the charging schedule. By default EVSEs use a constant power charge strategy that aim at fully charge the battery as fast as possible. By knowing the expected final user's departure time, EVSE can delay the completion of the charging process acting on the charging schedule, still ensuring that the battery is fully charged by the expected departure time. The flexibility signal $U^{ev}$ is obtained by the sum of the rescheduled charging profile of each of the EVSEs of the collection. It is function of a series of 5 parameters which can be predicted by studying the historical charging sessions of the aggregated EVSEs collection $U^{ev} = f(E^{ev}, \delta_a^{ev}, \delta_d^{ev}, P_+^{ev}, P_-^{ev})$ Equations (7.5) to (7.8) show how these parameters are related to each other and to historical charging patterns.

$$C^{ev}(t) = C^{ev}(t-1) + \alpha_E^{ev}(t) + \beta_E^{ev}(t) \tag{7.5}$$

$$\eta_+^{ev}(t) = \eta_+^{ev}(t-1) + \sum_{i=1}^{M} P_{+,i}^{ev} \cdot \delta_{a,i}(t) + \sum_{i=1}^{M} -P_{+,i}^{ev} \cdot \delta_{d,i}(t) \tag{7.6}$$

$$\alpha_E^{ev}(t) = \sum_{i=1}^{M} E_i^{ev} \cdot \delta_{a,i}(t) \tag{7.7}$$

$$\beta_E^{ev}(t) = \sum_{i=1}^{M} -E_i^{ev} \cdot \delta_{d,i}(t) \tag{7.8}$$

The storage capacity $C^{ev}$ represents, at each time step, the amount of energy that should be collectively delivered by the distributed EVSEs to satisfy the charging requirements of all the EVs plugged into the system (equation 7.5). $\eta_+^{ev}$ and $\eta_-^{ev}$ are the equivalent storage maximum charging and discharging rates, they are estimated summing the maximum charging rates $P_+^{ev}$ and discharging rates $P_-^{ev}$ over each active EVSE. Equation 7.6 shows how to estimate the maximum charging rate; a similar expression can be derived for the the maximum discharging rate substituting $P_+^{ev}$ with $P_-^{ev}$. Using this formulation a non-zero $\eta^{ev}$ value assumes a EVSE with vehicle-to-grid (V2G) capabilities. While this storage model can be applied to study V2G interactions, we consider V2G applications and value discussion beyond the scope of this work. $\alpha_E^{ev}$ and $\beta_E^{ev}$ are respectively the capacity boosting and dissipation rate (equations (7.7) and (7.8)). $\alpha_E^{ev}$ is the amount of capacity added to the equivalent storage at time $t$. This capacity represents the sum of the energy requested during the whole session by each EV plugged into the system at time $t$. $\beta_E^{ev}$ is the amount of capacity removed from the equivalent storage at time $t$, representative of the amount of energy leaving the system when a car is unplugged. For each EVSE, $E^{ev}$ represents the amount of energy to charge during each charging session. $\delta_a$ and $\delta_d$ are Kronecker impulse functions respectively centered at the EV arrival and departure times.

### 7.3.3 Convex formulation for flexibility assets optimal dispatch problem

In this section we show how to formulate the flexible asset's optimal dispatch problem in convex form. We first present a general formulation for the objective function and the constraints set, highlighting the rationale behind it. Then, we present two different aggregators' problems that can be addressed as particular cases of the general convex formulation. We define the problem as a standard form convex optimization problem, in which the cost function is convex, inequalities constraints are convex and equality constraints are affine.

**Objective**

The aggregator goal is to enforce a specific behaviour to the aggregate portfolio net-load in order to satisfy the requirements for a specific service. At any given

time, we define the portfolio net-load as the algebraic sum of the aggregate Load
(L), generation (G) and all the flexible assets available in the portfolio (7.9). This
definition of the net-load can be stretched to assume different meaning depending
on the level of aggregation. For a microgrid, it represents the actual net-load at the
point of connection with the main grid. For a zone aggregator, it represents the
regional balance and it is not necessarily related to a a specific feeder/sub-station.

$$\text{net-load}_{(t)} = L_{(t)} + G_{(t)} + \sum_k U_{(t)}^k \tag{7.9}$$

Equation (7.10) represents the general formulation of the convex optimization prob-
lem's cost function. It consists of three components that aim at penalizing different
aspects of the problem. In this general form, the decision variables are the flexibility
dispatch signal U and the equivalent storage capacity C of each flexibility asset.

$$\underset{U^k, C^k}{\text{minimize}} \qquad f_1(\text{net-load}_{(t)}, p_{(t)}) + \sum_k f_2(\|U^k\|_1, p_{ope}^k) \tag{7.10}$$
$$+ \sum_k f_3(C^k, p_{ena}^k, f_{amo}^k)$$

The first component attributes a value to the usage of the portfolio flexible
assets. It is a function of the net-load and of a penalizing price vector p that can be
representative of an actual market or be fabricated to enforce specific behaviours.
Depending on how we define $f1$, we can use the flexibility assets to correct the
net-load and unlock different kind of service. The second component attributes a
cost to the usage of the k different kind of flexibility assets of the portfolio. We use
an l1-norm to quantify the usage of each asset during the simulated time frame.
This component penalizes the different assets associating different operative costs
$p_{ope}^k$, in $\$/kWh$ of throughput, to their usage. The third component attributes
an enablement cost $p_{ena}^k$ to each flexibility asset. The larger the equivalent storage
capacity selected by the optimization, the higher the relative enablement costs. The
enablement cost can assume different meanings depending on the kind of flexibility
asset and the available data. For a Li-ion EES it simply represents the investment
cost in $\$/kWh$ of storage capacity. For TCLs and EVSE it can represent the cost
of enabling a single unit. The amortization factor $f_{amo}$ scales the enablement cost
depending on the expected asset lifetime and the simulated period. We need the
second and third components to enforce an optimal trade-off between the value
of the service we want to provide, evaluated by the first component, and the cost
of using the flexibility assets. It is worth noticing that we define the cost factors
$(p, p_{ope}, p_{ena})$ to convert the cost function to US dollars.

**Constraints set**

In this paragraph, we present the general constraints set that, together with the general cost function, completes the convex formulation. Constraints (7.11) to (7.20) model the behaviour of a Li-ion EES. The first three constraints, (7.11) to (7.13) allow us to split the control signal for the electrical energy storage into positive semi-definite charging and discharging signals. This is necessary to accurately model the impact of the storage efficiency during both charging and discharging phases. The second component of the cost function (7.10) penalizes both the charge and discharge signal, so that, at any given time, only one of the two variables are different from zero: the storage can either charge or discharge. Constraint (7.14) is the state-equation. At every given time, the internal energy of the storage is effected by the current charging/discharging signal and the relative efficiency. Constraints (7.15) and (7.16) bound respectively the charging and discharging signal between the storage maximum charging/discharging rate. Constraint (7.17) bound the internal energy between two values. The maximum is represented by the total storage capacity, while the minimum is usually related to the characteristics of the batteries and can vary from one producer to another. Constraint (7.18) allow the problem to dynamically set the maximum charging/discharging rate depending on the selected storage capacity. Depending on the characteristics of the storage, the ratio ($C_{ratio}$) between the maximum charging/discharging rate and the capacity can vary: we can use lower ratio for energy intensive applications ($C_{ratio}$ of 0.5,1) and higher ratio for power intensive applications ($C_{ratio}$ of 2,3). Constraints (7.19) and (7.20) directly control the shape of the resulting net-load profile. The former uses the first derivative of the final net-load to limit the ramp rate under a predetermined threshold $L_{(t)}^{ramp}$. The latter uses the second derivative of the final net-load to limit the curvature and enforce an overall smoother, easier, profile to follow. Constraints (7.21) to (7.26) model the behavior of the equivalent energy storage for TCLs and EV assets, using parameters and definitions introduced in section 7.3.2. Constraints (7.21) and (7.24) represent the state-equations respectively for TCLs and EV assets. They track the internal energy of the equivalent energy storage systems. Constraints (7.22) and (7.25) bound the relative flexibility control signals between the maximum discharging ($P_{min}^{tcl}$,$P_{min}^{ev}$) and charging ($P_{max}^{tcl}$,$P_{max}^{ev}$) rates. Constraints (7.23) and (7.26) limit the internal energy of the equivalent storage between zero and the maximum

available capacity.

$$U^{st} = U_c^{st} - U_d^{st} \tag{7.11}$$

$$U_c^{st} \geq 0 \tag{7.12}$$

$$U_d^{st} \geq 0 \tag{7.13}$$

$$x^{st}(t) = x_{(t-1)}^{st} + \eta^{st} U_c^{st}(t)dt - \frac{U_d^{st}(t)dt}{\eta^{st}} \tag{7.14}$$

$$0 \leq U_c^{st} \leq P_{max}^{st} \tag{7.15}$$

$$0 \leq U_d^{st} \leq P_{max}^{st} \tag{7.16}$$

$$c_{min}C^{st} \leq x^{st} \leq C^{st} \tag{7.17}$$

$$P_{max}^{st} = c_{ratio}C^{st} \tag{7.18}$$

$$\frac{d(\text{net-load}_{(t)})}{dt} \leq L_{(t)}^{ramp} \tag{7.19}$$

$$\frac{d^2(\text{net-load}_{(t)})}{dt^2} \leq L_{(t)}^{curv} \tag{7.20}$$

$$x^{tcl}(t+1) = x_{(t)}^{tcl} - \alpha^{tcl}x_{(t)}^{tcl} - U_{(t)}^{tcl}dt \tag{7.21}$$

$$P_{min}^{tcl}(t) \leq U_{(t)}^{tcl} \leq P_{max}^{tcl}(t) \tag{7.22}$$

$$0 \leq x_{(t)}^{tcl} \leq C_{(t)}^{tcl} \tag{7.23}$$

$$x^{ev}(t) = x_{(t-1)}^{ev} - U_{(t)}^{ev}dt\alpha_{t-1}^{ev} \tag{7.24}$$

$$P_{min}^{ev}(t) \leq U_{(t)}^{ev} \leq P_{max}^{ev}(t) \tag{7.25}$$

$$0 \leq x_{(t)}^{ev} \leq C_{(t)}^{ev} \tag{7.26}$$

**The aggregator bidding problem**

We show the capabilities of our framework by addressing the aggregator bidding problem. An aggregator is an entity that buys energy in the day ahead market for a portfolio of clients. The aggregation of the energy assets of these clients is modeled as a virtual power plant and it is not necessarily limited to a specific feeder or a single district area. The aggregator aims at minimizing its cost of operation by optimally bidding in the day ahead market according to its load and generation forecasts. In this work, we refer to the optimal bid profile as the tracking signal $Tr$, because the aggregator portfolio is committed to follow it during real time operations. Due to the uncertain nature of both load and generation, day ahead predictions and commitments can be erroneous. Therefore, in real time operations the aggregator have to adjust its position bidding in the real time market, where energy tend to be more expensive. Such an aggregator can use its available flexibility assets to adjust the aggregate net-load and reduce the gap with the tracking signal. Aggregators

can apply our optimal portfolio management formulation with historical data to optimally size an EES that will serve as their main flexibility asset to correct the portfolio net-load during real time operations. They can also estimate the value of integrating more TCLs and EVs in their portfolio, assessing how the optimal EES capacity vary for different penetration levels. To address this problem we define a specific objective function (equation 7.27 extending the formulation presented in the previous chapter.

$$\underset{U^{tcl},U^{ev},U^{st},C^{st}}{\text{minimize}} \qquad p^{T}_{(t)}|\text{net-load}_{(t)} - Tr_{(t)}| + p^{st}_{ope}\|U^{st}_{c}\|_{1} + p^{st}_{ope}\|U^{st}_{d}\|_{1} \qquad (7.27)$$

$$+ p^{st}_{ena}f^{st}_{amo}C_{st}$$

The first component penalizes the absolute value of the difference between the portfolio net-load and the tracking signal. The price vector $p$ is a function of time and penalizes the bidding error differently depending on the hour of the day, following the real time market trend. The second and third components penalize the l1-norm of the EES charging and discharging control vectors using the EES operative cost $p^{st}_{ope}$ as a regularization coefficient. Their effect is two-folds. First, they limit the usage of the EES so that the optimization strategy treat it as a scarce resource and choose to dispatch the other available flexibility assets first: in this study TCLs and EVs are considered free to enable and dispatch. We assess their value by quantifying how much we reduce the EES size by integrating them in the portfolio. Second, they act as an implicit constraint that limit the search space to cases where $U_{c}$ or $U_{d}$ cannot be different from zero simultaneously.

**The ramp rate control problem**

In this case we want to show how an aggregator can use the same formulation to address a different problem related to ramp rate control. Specifically we aim to limit net-load ramp rates under a predetermined threshold. We know that during spring afternoons solar generation decreases and residential demand increases co-incidentally, creating a steep ramp that is difficult, thus expensive, to follow with conventional generators. This problem is also known as the duck curve problem due to the shape of the resulting net-load. This problem at the national grid level can start being addressed locally forcing districts and microgrids to use their flexibility assets to control their net-load and reduce the ramp rates as a new class of grid service. We simulate this scenario for a district level aggregator, using our optimal portfolio management formulation to obtain the optimal flexibility resource

allocation and the optimal EES capacity to limit the portfolio ramp rate under a predetermined threshold. With respect to the first case study, the objective function (equation (7.28) looses the first component, which means that the net-load behaviour is enforced only by the set of constraints. Specifically constraints (7.19) and (7.20) limit the net-load ramp rate and ensure a easier to follow profile.

$$\underset{U^{tcl}, U^{ev}, U^{st}, C^{st}}{\text{minimize}} \qquad p_{(t)}^T \|U_c^{st}\|_1 + p_{ope}^{st} \|U_d^{st}\|_1 + p_{ena}^{st} f_{amo}^{st} C_{st} \qquad (7.28)$$

We apply a sensitivity analysis over the penetration level of flexible loads, both TCLs and EVs, to study their impact on the optimal EES sizing. Using this methodology we are also able to assign an economic value to the flexible loads, assessing how much money the aggregator can save by avoiding extra EES capacity. We also establish a limit to the necessary enabling costs for TCLs and EVs to become economically competitive to battery energy storage systems.

### 7.3.4 Dataset description

In this study we simulate the prospective of a residential district aggregator, simulating an urban district of 233 households. In the next few sections we describe the dataset and the main set of assumptions used to study both the aggregator bidding and the ramp rate control problems.

**Residential district data**

We use the publicly available Pecan Street dataset to retrieve 15 minutes consumption and generation data for the 233 households. The Pecan Street dataset consists of 1000 residences, including single houses, apartments, small commercial properties and three public schools. These residences include home energy monitoring systems, distributed generation, electric vehicles with level 2 charge systems, smart thermostats, smart water and smart gas meters [72]. We pick all the 233 houses of the dataset for which both load and generation data are available. Figure 7.3 shows 4 days of 15 minutes aggregated load, generation and net-load data for our district.

**TCL data**

As discussed in section 7.3.2, we build a simulation to estimate the necessary TCL equivalent storage parameters. The characteristics of each simulated TCL are defined by a set of five parameters: the initial temperature, the thermal resistance,
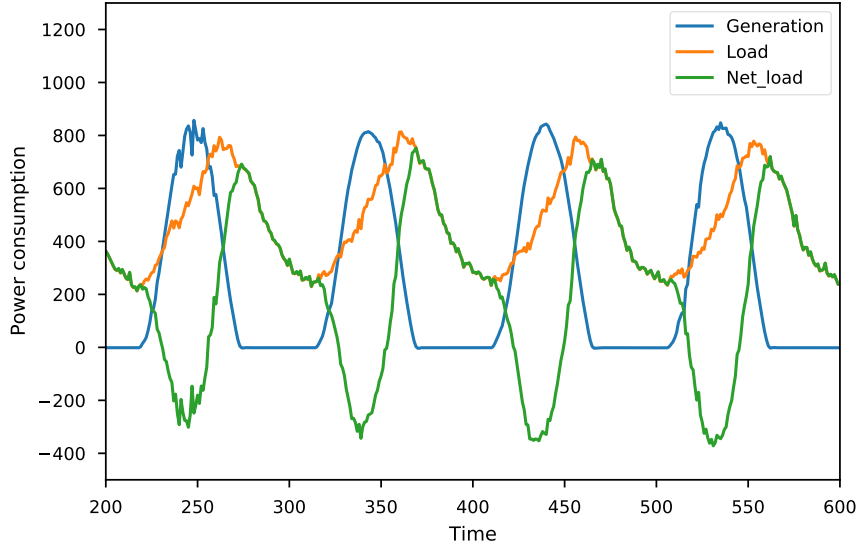
FIGURE 7.3: The simulated district original Net-load

thermal capacitance, air conditioning system rated power and their coefficient of performance. In order to simulate the behavior of an heterogeneous group of TCLs, we simulate a population of 233 households and we sample the required parameters from uniform distributions, using the approach and values presented in [71]. Using hourly outdoor air temperature data from 2016 [44], we evaluated the median temperatures for each hour in summer for the city of Austin, Texas. We use the temperature profile of the resulting median day as an input to the TCL model.

**EV data**

We use a dataset provided by ChargePoint to extract data from residential charging sessions and estimate the relative equivalent energy storage parameters. This dataset includes 1341 EVSEs throughout 75 zip code regions in Northern California with 451.999 charging sessions covering the full year of 2013. We use the charging sessions data from this Northern California dataset even if the rest of the district data we use is from Austin, Texas. Doing this we hypothesize that the charging pattern obtained from residential EVSEs installed in different areas must be similar. For each charging session the following data is reported: plug-in and departure time stamps, average and peak power every 15 min, charged energy every 15 min, Charging port type, zip code and the building category. More than 99 % of the charging sessions in the dataset are from Level 2 EVSEs with a capacity between
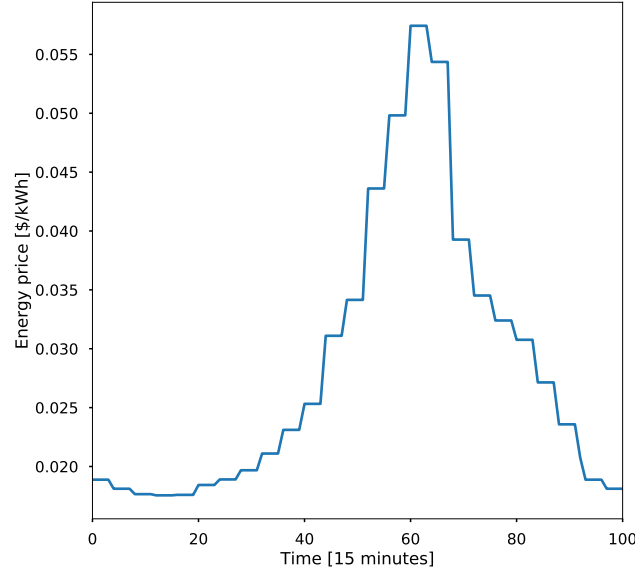
FIGURE 7.4: Price vector from the ERCOT Real-time energy market

4 - 7 kW unidirectional. About two thirds of the EVSEs are located at workplaces and the rest is distributed over hospitals, parking areas, universities, airports and a residential areas. A more detailed description of the dataset is available in [61]. For each EVSE, the 15 minutes averaged power consumption profile is used to estimate the equivalent storage parameters. From the power consumption profile, we can infer the arrival and departure times that are required to use the model we described in section 7.3.2. We use 233 home data sampled from Chargepoint data.

**Storage cost and energy market assumptions**

For the aggregator bidding problem, we need a mechanism to penalize the erroneous day ahead bid. We introduce a dynamic price vector that penalizes this error differently during the day depending on almost real time evaluated grid constraints and resources availability. This mechanism is representative of real time markets, sometimes called imbalance markets. In this study, we use one day of energy price data from the real-time market managed by the Electric Reliability Council of Texas [38]. Figure 7.4 shows the price profile we use in all our simulations. Another set of assumptions are related to both investment and operative costs of running a Li-Ion EES. These assumptions are particularly critical since they directly impact the objective function trade-off between the benefits of integrating

more EES and the relative enabling costs. In this work we use data from a recent report published by the Energy Transition Lab (University of Minnesota), where they perform a techno-economic analysis of storage integration in Minnesota's grid using. First they analyze the all-in cost for a 100MW/4hours EES considering the storage medium, power conversion system, engineering, procurement and construction costs. Then they present three coefficients that are linear function of the installed EES energy and power capabilities: installed cost 1600$/$kW$, Fixed O&M 16$/$kW$ per year and variable O&M 4$/$MWh$. We use these coefficients in our simulations, assuming a 4 year project duration to evaluate fixed O&M cost and the amortization factor in the objective function.

## 7.4 Results

In this section we present the main set of results obtained applying the optimal portfolio management framework to the aggregator bidding and ramp rate management problems. We also present the effect of a sensitivity analysis over two of the critical assumptions we made: EES price and flexibility assets' penetration level.

### 7.4.1 The aggregator bidding problem

Figure 7.5 shows the effect of the optimal flexibility assets dispatch strategy on the district net-load, considering two different set of assumptions. Figures 7.5.a and 7.5.c use the assumptions presented in 7.3.4, while figures 7.5.b and 7.5.d assume reduced cost for the EES. Figure 7.6 shows how, for the reduced cost case, the equivalent storage internal energy varies during the simulation for the different flexibility assets. We obtain the results assuming penetration levels of 80% and 30% for controllable TCLs and EVs. Results show how the optimal dispatch algorithm tries to use the available flexibility assets to correct the net-load and approach the tracking signal. In certain hours of the simulation the two profiles are perfectly superimposed, while in others the final net-load is still identical to the original one. This behavior derives from the problem objective function which implicitly enforces a trade-off between the cost of installing an EES and the benefits derived by reducing the gap with the reference signal. Since flexibility assets represent a scarce resource, way scarcer then what the simulated district would need to follow the reference signal at all time, the optimal dispatch logic chooses to use them when the energy price $p$ in the real time market is higher. With the original set of assumptions the optimal portfolio management strategy chooses not to install an EES and uses the

other available flexibility assets to correct the net-load. Figures 7.5.b and 7.5.d show how the optimal dispatch changes along with the EES cost assumptions. In this case, capital and operative EES costs are reduced by 4 times and the optimal portfolio management strategy chooses to install a 732 kWh EES. Due to the cost reduction is now convenient for the system to reduce the gap with the tracking signal using an EES, instead of adjusting the bidding in the real time market. The EES installation adds flexibility to the portfolio, therefore the final district net-load is able to better track the reference signal. It is worth noticing that TCLs and EVs flexibility usage seems to be affected by the EES cost reduction.

Since the EES cost plays such an important role in the optimal portofolio building and management, we further study its effect on the optimal sizing of the EES by performing a sensitivity analysis over the assumptions presented in section 7.3.4. We simulate multiple scenario reducing both capital and operative costs of EES while keeping the rest of the assumptions set valid. Figure 7.7 shows the effect of the cost reduction on the selected storage capacity. We notice that the storage is introduced in the portfolio after a 30% discount over today's cost. Using this results we can estimate how much today's cost should drop or how much the technology should be subsidized to make it viable, this assuming that the simulated period is able to represent the service we want to provide and the value of using the EES appropriately. The optimal EES size keep increasing with the discount rate, following a piece-wise linear trend. As shown in figure 7.5, an increase in the EES capacity corresponds to better performances in terms of how much we are able to close the gap between the district net-load and the tracking signal.

### 7.4.2 The district's ramp rate control problem

Figure 7.8.a shows the effect of the optimal flexibility assets dispatch strategy on the district net-load, assuming penetration levels of respectively 80% and 30% for controllable TCls and EVs. Due to the effect constraints (7.19) and (7.20) the final net-load is smoother and ramp rates are visibly reduced. Specifically, in this case we limit the net-load ramp rate to 20 $kW/s$ and the second derivative, that control the curve smoothness, to 4 $kW/s^2$. Figure 7.8.b shows how the different flexibility assets are dispatched to effectively control the district net-load within these thresholds. Using the selected portfolio of flexibility assets, we are able to reduce the district ramp rate by up to 9 times, considering that the original Net-load ramp rate reach peaks of 180 $kW/s$. Figure 7.9 highlight this result reporting the ramp rate distribution for both original and final net-loads. The objective function
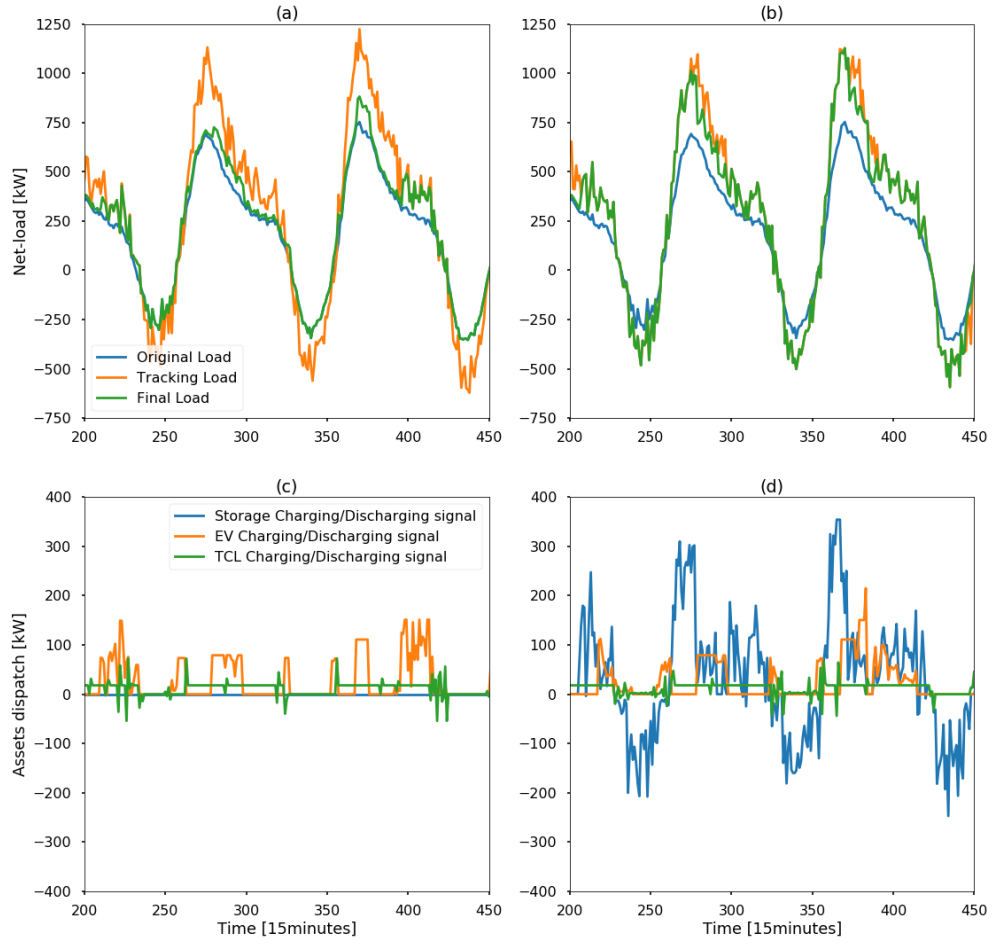
FIGURE 7.5: (a) and (b) shows the original and final net-load, together with the tracking profile. (c) and (d) the relative optimal flexibility assets dispatch profile.
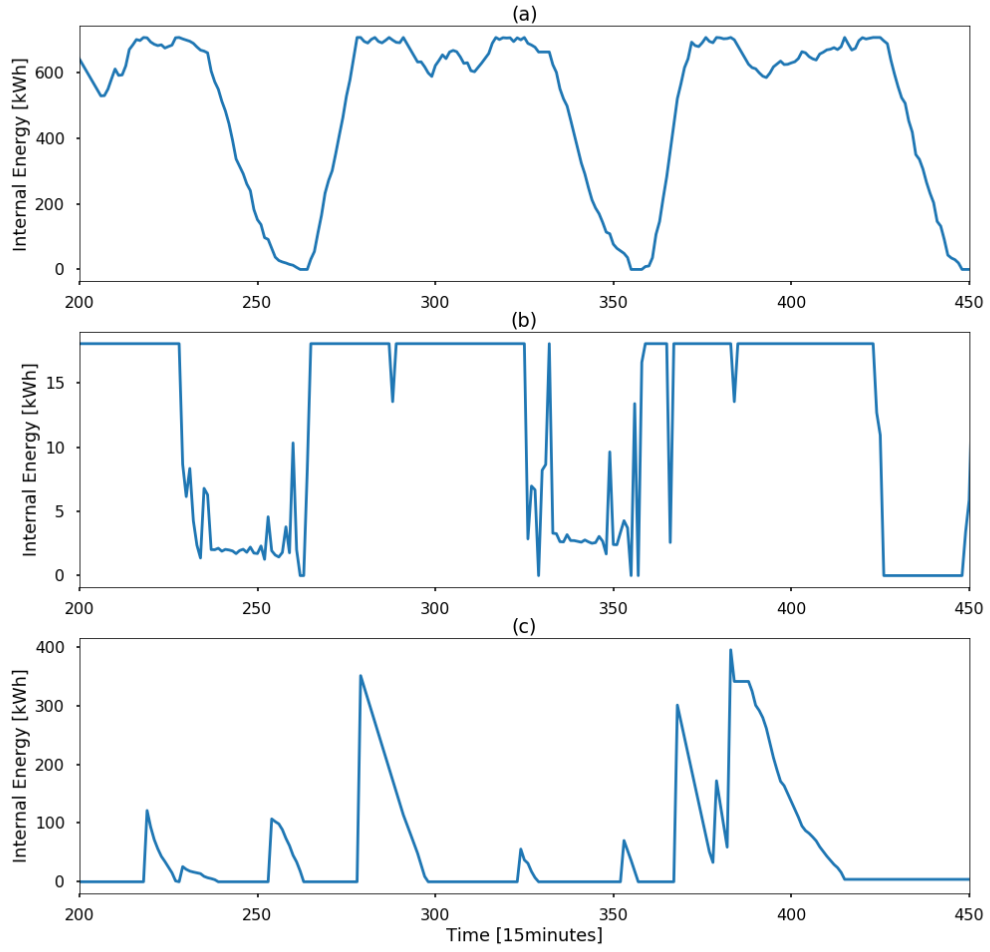
FIGURE 7.6: Internal energy trend for the EES (a), TCL equivalent energy storage (b) and EV equivalent energy storage (c)
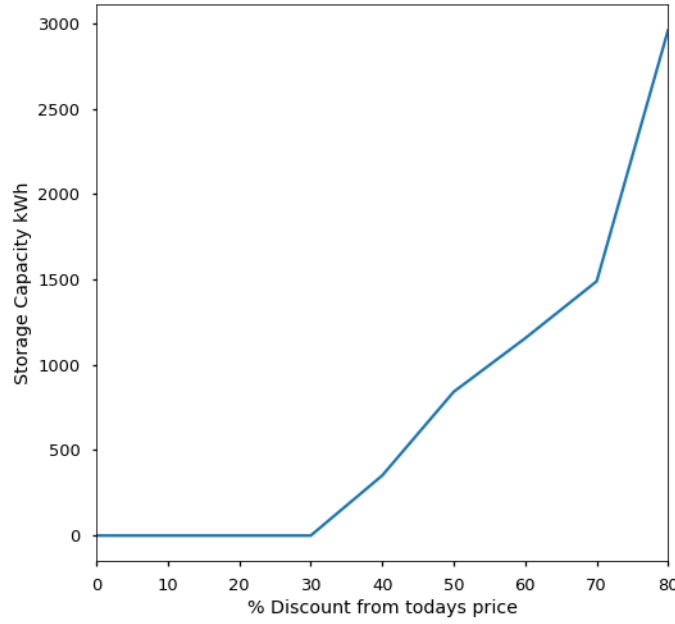
FIGURE 7.7: Sensitivity Analysis over EES cost

penalizes the EES capacity and the EES charging/discharging variables to ensure
that the other available assets (TCLs and EVs) are dispatched first and that the
algorithm selects the minimum EES capacity to achieve the ramp rate limitation
goal. However the regularization coefficients $(p^{st}_{ena}, p^{st}_{ope})$ are not relevant to the
final result: regardless of how hard we penalize it, the algorithm is still going to
select the right capacity to enforce the constraints set. For this reason, this problem
setup is appropriate when we want to simulate a strategy and estimate the optimal
assets capacity regardless of its economic viability. We further study the effect
of the flexible loads on the optimal dispatch problem, by performing a sensitivity
analysis over both TCLs and EVs penetration. Figure 7.10 highlights their effect
on the optimal sizing of the EES. It shows how integrating more flexible loads can
reduce the required EES capacity while enforcing the same service quality.TCLs'
flexibility have a positive effect on the storage capacity and considerably reduces
the required EES capacity. As shown in Figure 7.10.a, this reduction follows a
monotonically decreasing piece-wise linear function with respect to the increase in
TCLs penetration. EVs's flexibility have a slightly positive effect until we reach
a penetration level of 40%, after that we end up increasing the storage capacity
requirements. The EVSEs we are studying does not allow vehicle-to-grid interaction,
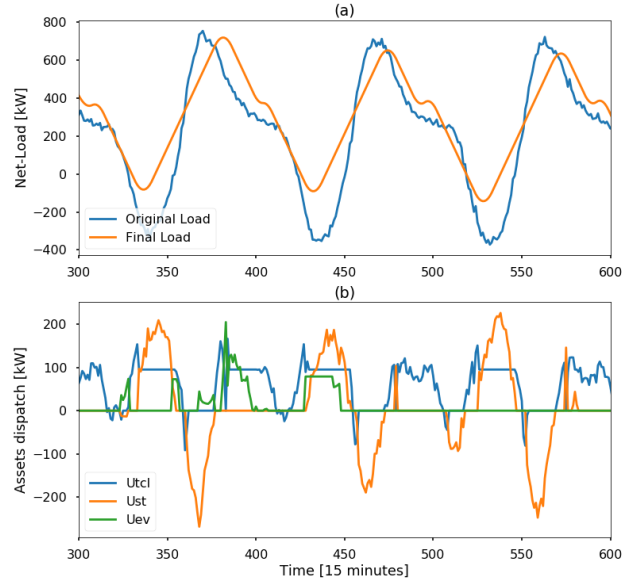
FIGURE 7.8: (a) shows the original and final net-load. (b) shows the relative optimal flexibility assets dispatch profile.
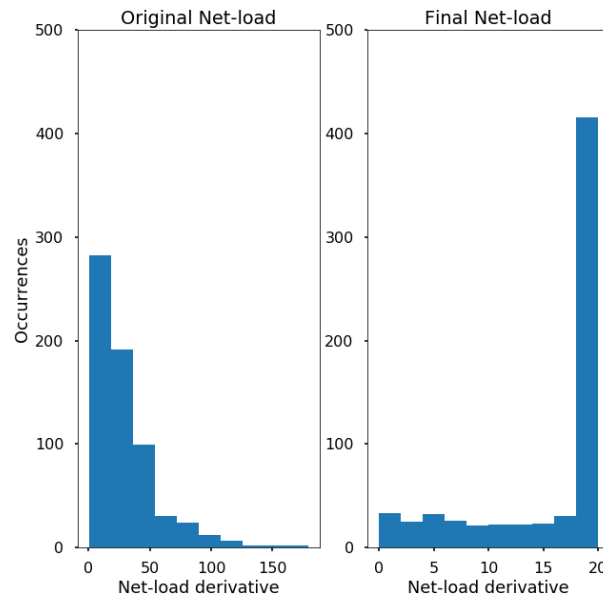


FIGURE 7.9: The two histograms highlight the effect of the flexible loads in limiting the ramp rates

thus the benefits related to EVs integration are limited to the requests of positive flexibility during the charging sessions. The 40% penetration level is a threshold above which the positive effect of integrating EVs are discouraged by the new loads end up increasing the ramp rates and has to be managed by installing a bigger EES. The integration of controllable EVs in the district can have positive or negative effects depending on the characteristics of the service we want to provide. The timing and magnitude at which the flexibility is required are key aspects that can offset the impact of EVs in the portfolio. Also the charging sessions schedule is critical. For example residential and office/commercial EVSEs have complementary schedules, and they are more effective when integrated to provide different services that require flexibility in different portions of the day. Using these results we can estimate the value of integrating extra TCLs and EVs units in the portfolio in terms of how much we can reduce the required EES capacity to deliver the same level of service. For example increasing from 0 to 60 percent the penetration level of TCLs, which for our 233 houses districts means to integrate almost 140 units, we estimate a reduction of about $250kWh$ in the required storage capacity. From here we can estimate how much money the aggregator should invest to enable each TCL unit or, depending on the aggregator prospective, how much should this technology should be subsidized to make the integration of flexible loads economically attractive.
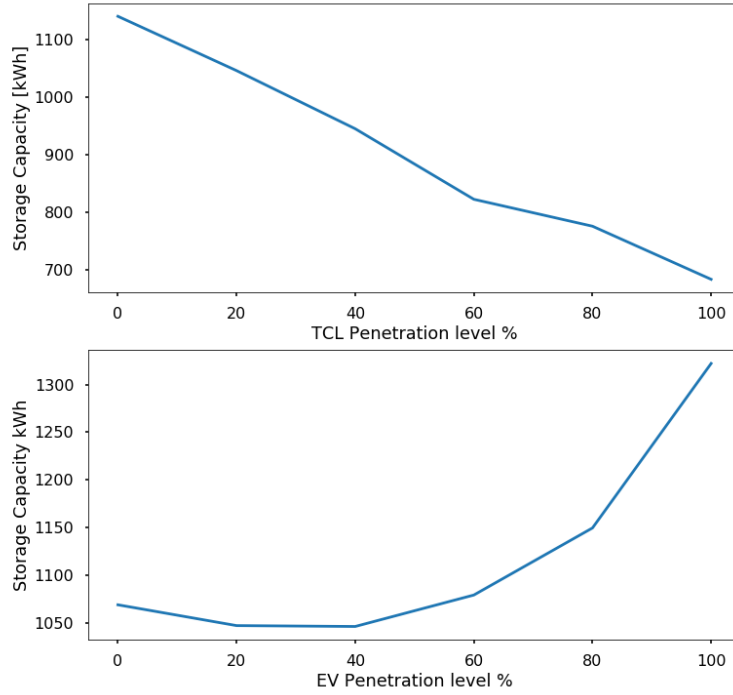
FIGURE 7.10: Sensitivity analysis plots showing how the optimal storage size varies with controllable TCLs (a) and EVs (b) penetration level

## 7.5   Conclusions

In this chapter we presented a framework for the optimal management of a portfolio of flexibility assets, from the perspective of an aggregator of urban districts. The framework can be used to build and optimally manage a portfolio of flexibility loads depending on the service to provide, the aggregation scale and their technical potential. We focused on three main sources of flexibility: thermostatically controlled loads, electrical vehicles and energy storage systems.We introduced a modeling approach to analyze and control each of these flexibility assets as equivalent energy storage, mapping their behaviour into a set of convex and affine constraints. These constraints are part of a convex formulation we developed to solve the optimal portfolio management problem. The convex cost function consists, in its general form, of three components which aim at balancing the benefits achieved by reshaping the net-load of the aggregator's portfolio and the cost of enabling and dispatching the

different assets. We built two case studies to showcase the capabilities of the framework, using historical data from private and publicly available datasets to simulate a residential district. The first case study is related to the aggregator bidding problem and the flexibility assets are used to improve the bidding strategy of an aggregator in a real time market. The second case study offers a distributed approach to solve the californian's grid ramp rate problem, using the available flexibility assets to control the district's net-load and reduce the late afternoon ramp. Results show that the framework is capable to cope with the characteristics of both problems, enabling several layers of analysis. For each case study, we indicate the optimal size of energy storage to install and, for each of the flexibility assets, the optimal dispatch profile. Furthermore, through a sensitivity analysis, we are able to define the impact on the optimal storage sizing of both the technology expected price point and the penetration level of each of the alternative flexibility assets (TCLs and EVs). Results show that the storage is introduced in the portfolio after a 30% discount over today's cost. Using this results we can estimate how much today's cost should drop or how much the technology should be subsidized to make it viable, this assuming that the simulated period is able to represent the service we want to provide and the value of using the EES appropriately. In relation to the alternative assets penetration level, results show that TCLs flexibility have a positive effect on the optimal portfolio since it considerably reduce the required EES capacity. On the other hand, the integration of controllable EVs in the district can have positive or negative effects depending on the characteristics of the service we want to provide. The timing and magnitude at which the flexibility is required are key aspects that can offset the impact of EVs in the portfolio. Residential and office/commercial EVSEs have complementary schedules, and they are more effective when integrated to provide different services that require flexibility in different portions of the day. Future studies will be dedicated to explore different kinds of interaction between the flexibility assets and the distribution grid. We will polish, expand and use the framework to support such studies. We plan to integrate a model to consider TCLs and EVs enabling costs as part of the optimal portfolio building problem. We also plan to improve the modeling capabilities of the framework by using stochastic programming and probabilistic constraints to model the uncertain nature of several variables of interested for the optimal portfolio management problem, such as user's load, RES generation or EVs charging patterns.

# Chapter 8

# A multi-agent based control architecture for flexibility assets in industrial microgrids

## 8.1 Preface to chapter 8

In the last chapter we talked about the optimal portfolio management problem for aggregators of flexibility assets. We introduced a convex formulation to model and solve the problem from the prospective of an aggregator which is capable of taking centralized optimal decisions, having access to perfect information related to the assets of its portfolio. In this chapter we discuss an alternative, distributed, approach to the control of flexibility assets. We introduce a multi-agent based control architecture designed to manage the flexibility assets of an industrial microgrid. In this case the aggregation level is limited to a single industrial microgrid and the aggregator is interested in the optimal control of the different flexibility assets to reduce operational costs and limit consumption peaks during critical hours. Together with eng. Stefano Longo and Dr. Paolo Sernani which implemented the control architecture using Jade, i contributed to the modeling tasks, the design of the control architecture, the definition of the different case studies, the simulation scenarios and of appropriate comparison metrics. Professors Gabriele Comodi and Aldo Franco Dragoni provided help with technical support, ideas and editorial assistance.

## 8.2 Introduction

Many countries are pursuing ambitious goals in terms of renewable shares in their energy portfolio. The intermittent, uncontrollable, nature of renewable generation is making harder to balance energy demand and offer at grids level. This trend will eventually pose new challenges to the entire distribution system in terms of reliability, costs and service quality. Demand response (DR) represents an opportunity for end users to play an active role in mitigating these effects [10]. End users can make available their own assets, a set of thermostatically controlled loads, a residential energy storage system and/or electric vehicle, to dispatch services to the grid.

Microgrids will play an important role in this transition. Microgrids are small scale distribution systems formed by the interconnection of distributed generation, both traditional and renewable, loads and energy storage systems. A microgrid is such that all its entities are coupled with the distribution grid through a single point of common coupling. An intelligence ensures that all the assets are coordinated to deliver power in the most efficient and reliable way. Exploiting their inherent controllable and flexible nature, microgrids can be designed to provide demand response services (e.g. frequency regulation using electrical energy storages systems), to maximize local renewable self-consumption and, in case of grid fault or voltage fluctuation, to operate in islanded mode [78]. Microgrids can be classified, depending on the application, in utility microgrids, industrial/commercial microgrids and remote/isolated microgrids [35]. Each category has its own motivation, benefits and challenges. They are significantly different in terms of consumption magnitude, variance and periodicity. Different kind of microgrids can be used to provide different kind of services to the grid, or aggregated to form a more relevant portfolio of controllable loads to leverage [104].

Industrial microgrids are driven by the potential reduction in operational cost due to self-generation and the promise of higher power quality and reliability. Due to the magnitude and nature of their loads, and the ability to invest in distributed generation and storage, industrial microgrids are perfect candidate to work as Virtual Power Plant (VPP), providing services to the distribution grid or actively playing in balancing electricity markets or day-ahead planning [7]. On the other hand, the flexibility associated with industrial controllable loads is usually more complex to predict, requiring deep knowledge of the specific production processes, and more constrained to high reliability and safety standards. Studies and projects are now focusing on how to quantify the potential benefits of flexible loads in industrial sites, tackling the problem from both the technical (flexible load assessment)

and economic (development of business model and policy recommendation) point of views. As an example, IndustRE is a project financed by the Horizon 2020 program which aims at developing a framework to study the technical potential of different industrial facilities in providing flexibility, proposing a modular approach based on specific case studies and simulation techniques[52]. In [89], the interested reader can find an extended overview of Smart Grid technologies for the industrial sector, with a special focus on automatic demand response applications in specific industries. In [101], authors describe and test a methodology to optimally operate a demand-side management strategy, using the flexibility granted by an industrial air-separation plan to reduce operational costs and provide power reserve to the national grid. In [106], authors develop resource task network models to optimally reschedule the activities of steel plants to minimize operational costs leveraging energy price variability: different models are tested and results show how operational costs can be reduced even if the computational burden of the optimization tasks can be heavy.

Multi-Agent Systems (MASs) are emerging as a promising tool in a wide range of applications in the microgrid, such as decentralizing the infrastructure, giving more weight to society wishes, as well as facilitating maintenance, reducing costs and opening doors for the development of low-cost devices embedded with AI tools [41]. In the scientific literature, autonomous agents and Multi-Agent Systems have been used to support humans, for example controlling home heating by managing uncertainty and user preferences [91], using mathematical modeling [85] to incentivize agents (representing home consumers) to shift their loads when green energy is available and proposing gamified and economic incentives [2] to incentivize users to accept such shifts and promote renewable energy usage. Differently from these traditional approaches, the multi-agent control architecture proposed in this chapter has a different main goal, and is applied and tested into a different scenario: the systems aim at reducing the operational cost of an industrial microgrid, modeling the available assets and their flexibility with autonomous software agents which schedule and regulate the power exchange with the national Distributor System Operator.

Centralized control has been feasible in grids with limited numbers of controllable components, but it becomes increasingly complicated, costly, and computationally intensive, as the quantity and complexity of grid elements grows [26]. In fact, distributed control architecture based on agents, being able to operate without external intervention, communicating through messages, and acting via goal-

directed behaviors [100], are ideal to model and regulate the autonomous physical elements and components of power systems [65]. The agent-based architecture proposed here is composed of multiple agents, as usual for agent-based systems [11], being a Multi-Agent System (MAS): the implemented agents interact with each other via communication, composing a cooperative society to achieve a mutual benefit, i.e. lower operational costs of the microgrid.

This chapter presents a multi agent control architecture designed for industrial microgrids. The control mechanism aims to reduce operational costs while maintaining the same production goals. To do so, it leverages the flexible assets in the microgrid, optimally scheduling the power exchange with the national grid, based on a 24 hours-ahead price signal. A threshold based peak shaving is implemented to allow advanced control strategies and more complex interactions among microgrids assets. The architecture effectiveness is tested using real data coming from Loccioni Leaf Community, an industrial microgrid comprising controllable loads, renewable distributed generation and energy storages. Two different electricity market frameworks are simulated to test the sensitivity and the robustness of the control architecture to different conditions. The main contributions of this work are the followings:

- A new multi agent control mechanism is designed over the needs of future industrial microgrid, robust to different microgrids topology and assets availability;

- New metrics to analyze the effectiveness of a control mechanism are suggested;

- The impact of electricity price variance is analyzed, using the control mechanism effectiveness as a metric.

The rest of this chapter is organized as follows: Section 8.3 contains the methodology; in Subsection 8.3.1, the multi agent control mechanism is described; in Subsection 8.3.2, the industrial microgrid is presented; in Subsection 8.3.3, the test case scenarios, the set of assumptions and the electricity market of reference are presented; in Subsection 8.3.4 the metrics to assess the proposed control mechanism are described. In Section 8.4, simulation results are discussed in terms of algorithm effectiveness and the impact of electricity price over its performances; Subsection 8.4.1 is left to discuss actual implementation related concerns, possible improvements and future research steps. Finally, Section 8.5 draws the conclusions of the chapter.

## 8.3 Methodology

A multi-agent control architecture is designed to respond to the needs of industrial microgrids in terms of varying topology, assets availability, and integration with existing systems. In addition to mapping a microgrid, composed of multiple distributed components, with a distributed architecture, the multi-agent control ensures the modularity of the microgrid: thanks to the standards of the Foundation for Intelligent Physical Agents (FIPA) [42] simply adding new agents in the architecture (registering their services) is enough to wrap different kinds of components and extend the capabilities of the system. Moreover, designing wrapping agents for any instance of the legacy information systems of the microgrid makes the architecture a fully interoperable software layer.

The multi-agent control architecture proposed in this work consists of several agents modeling the available assets of an industrial microgrid, cooperating to reduce day-ahead operational costs, given one day ahead perfect information over the expected load consumption, renewable generation and market energy price. To test the control architecture an actual Italian industrial microgrid serves as test case using real consumption and generation data in simulation scenarios. To study the control mechanism sensitivity to different energy markets, in terms of price magnitude and volatility, two different scenarios are simulated. Simulation are carried out using historical data from different reference markets.

### 8.3.1 The Multi-agent based control architecture

Figure 8.1 depicts the multi-agent control architecture for the microgrid. The DSO Agent represents the Distribution System Operator (DSO): it is not an actual part of the microgrid, but, during the simulations, it allowed sending messages to the microgrid, in order to test the designed architecture. In particular, the proposed architecture assumed that the message sent by the DSO agent to the microgrid is composed by three information: $< \$, P, T >$; where $\$$ is the price of electricity in a certain time frame $P$ defined by contract, under a power threshold $T$, after which the peak-price is used.

Five agents are implemented to model every kind of microgrid, independently from the topology and the specific components available. Such agents model the basic structure of the system:

**Grid Agent.** It is the interface of the microgrid with the DSO. It receives the message sent by the DSO agent and elaborates the $< \$, P, T >$ triple for all the

future calendar day's hours. Depending on the application and the reference energy market, these values can be either deterministic or stochastic. In the latter case the Grid Agent uses the updated information it receives to predict the future states of the $< \$, P, T >$ triple. This data is sent to all the microgrid agents via the control agent and the aggregators, waiting for the response with the electric power (kWh) requested to the national grid for that period. The Grid Agent is then responsible to communicate to the DSO the final decision of the control architecture for the $P$ time frame, sending the amount of electric power that the microgrid will need in $P$.

**Control Agent.** It covers the role of the supervisor of the microgrid, forwarding to all the nodes, via the Aggregator Agents, the price of electricity for the given time-frame and the power threshold. The Control Agent is responsible to process the replies from all the nodes: it collects the requests, in terms of needed power, from all the agents of the microgrid, processing the received data and taking the final decision, informing the Grid Agent as well as the entire microgrid. The single agents can also reject his decision if it goes outside the limits (to prevent cases of error).

**DER Aggregator Agent.** It acts as the interface between the Control Agent and all the Distributed Energy Resources (DERs) of the microgrid, aggregating all the data related to the energy production of each available resource, represented by a DER Agent. The DER aggregator makes the Control Agent and the architecture independent from the actual number of DERs of the microgrid.

**Battery Aggregator Agent.** As it happens with the DER Aggregator, the Battery Aggregator Agent collects the data related to Battery Agent requests (in terms of needing to recharge or discharge), making the Control Agent independent from the actual numbers of Batteries available.

**Load Aggregator Agent.** It aggregates the data of the energy loads of the microgrid, making the Control Agent independent from the number of loads. In addition, since each Load Agent representing a load can perform its loads shifting without being aware of the choices of the other Load Agent, the Load Aggregator is responsible to check each agent's shifting proposal, in order to avoid consumption peaks due to the shifting.

In addition, the DERs, batteries or loads available in the microgrid are modeled by three types of agents:

**DER Agent.** It models a single Distributed Energy Resource in the microgrid. Its goal is to produce the amount of energy that allows reducing the production costs. For example, in case an agent models a diesel generator, the goal would be

to work at the point of maximum efficiency (e.g. 80% of the maximum workload).

**Battery Agent.** It models a single battery in the microgrid. Its goal is to keep the battery at the desired State of Charge (SOC).

**Load Agent.** It is the agent that represents a consumption source. For example, it could be the thermal load of a department or an entire building, as well as single light in a room, depending on the granularity desired in the multi-agent architecture. The consumption profile associated with the each Load Agent consists of critical and non-critical loads. Critical loads cannot be shifted, offering no flexibility to the system (e.g. a test bench that have to run to keep up with a production schedule). On the other hand, non-critical loads can be shifted, offering some flexibility to the control system (e.g. HVAC system in a office space)

The number of DER, Battery, and Load Agents depends on the number of components available in the microgrid.
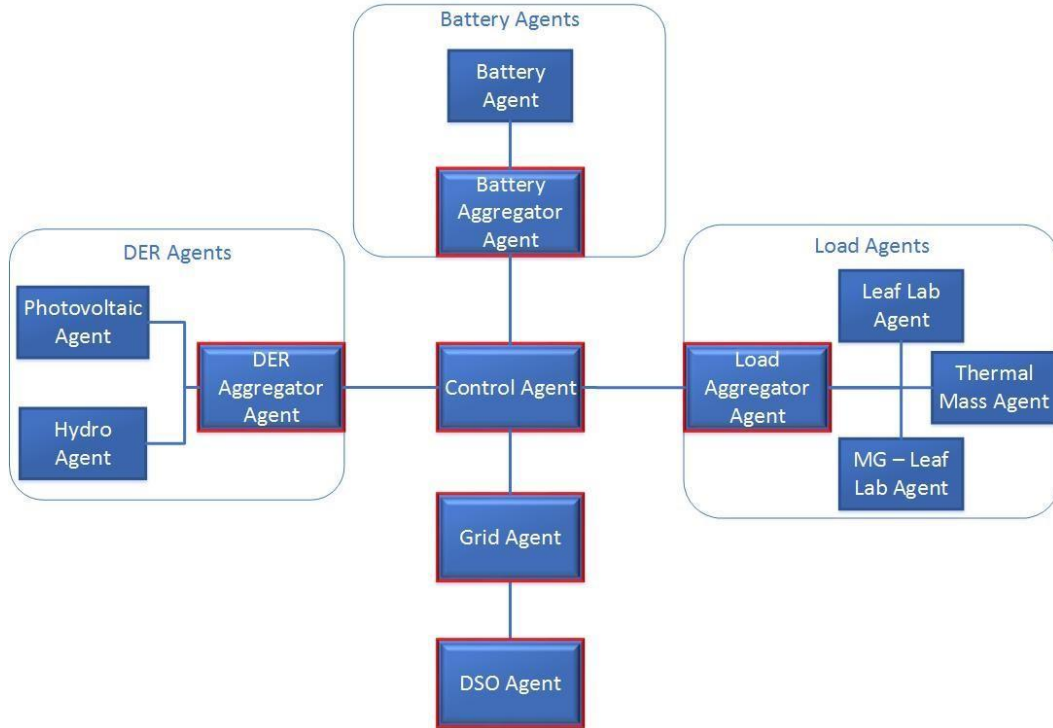


FIGURE 8.1: Multi-agent based control architecture.

The workflow to schedule the consumption and production of the microgrid is as follow.

**Step 1.** Once the Grid Agent receives the price valid in a specific time frame from the DSO, it will add such price to a data structure. If necessary it will forecast the energy price values and the power thresholds for all the remaining time-frames

of the day, producing an array of data for the control agent:

$$[< \$, P, T >, < \$1, P1, T1 >, < \$2, P2, T2 >, ...] \quad (8.1)$$

**Step 2.** The Control Agent forwards such message to all the Aggregator Agents, which forward the message to all the available Loads, Battery, and DER Agents.

**Step 2.a** Processing such data, each Load Agent sends to the Load Aggregator Agent, for each time frame, the minimum amount of power needed for critical, non-deferrable , activities, the maximum amount of power it could use in that time frame in case no loads are shifted, and the desired choice for the requested power, moving some of the non-critical loads in other time frames. In fact, when the minimum and maximum value of power differ, the Load Agent decided to shift its load consumption in the future, since a more convenient price is expected based on the data received from the Grid Agent. In such case, the requested power will be enclosed between the minimum and maximum power needed. By receiving such data for all the future time-frames in the day by the Load Agents, the Load Aggregator Agents is responsible to check whether the load shift can cause an energy consumption peak in the future: in fact, all the agents might decide to shift their loads in a more economically convenient time frame. To perform such check, the Load Aggregator Agent monitor the messages it receives from Load Agents as soon as they send it, summing up the amount of requested power for each time frame. In case in one or more time frame the peak threshold is reached, the Load Aggregator Agent asks to all the agent who sent their message after the peak was reached, to send their second best choice. This process continues until the peak is smoothed, or the minimum power, the maximum power and the desired power of the Load Agents are equal, which means that nothing is shifted. Once a schedule with no peaks or no shifts is agreed, the Load Aggregator Agent aggregate all the data to have a unique minimum consumption, maximum consumption, and desired consumption for each time frame, to send such information to the Control Agent.

**Step 2.b** Once DER Agents receive the message containing the price information for the future time frames, they send to the DER Aggregator Agent, for each time frame, the minimum amount of energy they will produce, the maximum amount of energy they can produce and the amount of energy they want to produce to achieve their own production goal, based on the prices received from the Grid Agent. In addition, the DER Agents send to their Aggregator the average cost for the production of 1 kWh. The DER Aggregator Agent aggregates such data to provide the control agent a unique value for the minimum production, maximum production, and desired production for each time frame.

**Step 2.c** After receiving the price information from the Grid Agent, Battery Agents send to the Battery Aggregator Agent, for each time frame, the maximum amount of power they can distributed to the microgrid, the maximum amount of energy batteries can absorb during charging, and their desired power (the amount of energy Battery Agents are willing to give or to take from the microgrid depending on the sign). In addition, Battery Agents send to their Aggregator the cost of providing 1 kWh to the microgrid, evaluated considering battery's cost per cycle. The Battery Aggregator Agent aggregates such data, to send it back to the Control Agent.

**Step 3.** The Control Agent collects the aggregated data from the Load Aggregator, the DER Aggregator, and the Battery Aggregator, to take the final decision of the microgrid on how much energy should be bought from the DSO in the time frame P in order to satisfy loads request from Load Agents. Three cases can occur:

1. The energy price is among the 30% lowest price of the past week (i.e. price is low). Hence, the Control Agent asks to DER to produce the minimum power they can, communicating to the DER Aggregator that the minimum production is chosen. The energy from the batteries of the microgrid is not needed as well, hence the Control Agents communicates to the Battery Aggregator that Battery Agents that expressed the willing to recharge (through the desired power value) can do so.

2. The energy price is among the 30% highest price of the past week (i.e. price is high). The Control Agent asks to DER Agents, via their Aggregator, to go for the maximum production. Available Battery agents are used to supply energy to the Load Agents, minimizing the energy purchase from the main grid.

3. The price is in between historical high and low prices. The Control Agent make a comparison between the DSO's price for energy, and the production cost of DERs and batteries, and decides if to ask for maximum production from DER and batteries (usual choice, since is almost always more convenient than buy from the network) or not, to satisfy Load agents' requests.

**Step 4.** Once the Control Agent takes the final decision, it might happen that, if price is low or average, the amount of energy requested would exceed the power threshold T indicated by the DSO. In such cases the Control Agent tries to perform a peak shaving action, executing the following steps:

1. DERs are forced to maximize their power output;

2. If the peak is not eliminated yet, all the available Battery Loads are used to discharge energy;

3. If the peak is not eliminated yet, the Control Agent asks to the Load Agents to shift some or all the non-critical loads even if it is not convenient for them, asking for the minimum power consumption.

**Step 5.** After this process is complete, the Control Agent sends a message to the Grid Agent confirming the amount of kWh requested for the time frame P. The Grid Agent communicates such information to the DSO.

### 8.3.2 Test case: the industrial microgrid

The case study considered in this work is the Loccioni's industrial grid-connected microgrid located along the Esino river in Angeli di Rosora (AN). The microgrid is a living lab dedicated to applied research in the energy field. Controllable and non-controllable loads, renewable generation and storage systems are interconnected in low voltage, behind a single meter. The microgrid runs only on electricity, even the HVAC system has been revamped with high efficient heat pumps.

Five buildings are connected to the microgrid: two of them are dedicated to light industrial activities, one to office activities; one to electrical and thermal engine testing; the last one is residential. The resulting load profiles are representative of such a variety of uses, each of them characterized by their own magnitude and periodicity. The overall microgrid consumption profile (Figure 8.2.a) shows a stationary behavior, with strong daily and weekly seasonality. It reflects the periodicity of the working schedule: the company is active 5 days a week, from 8 am until 18 pm.

Only the HVAC share of the overall load is deferrable, considering that heat pumps can be regulated to accommodate different demand management strategies. Almost 60% of the energy consumed along the year is produced by microgrid's DERs. The renewable generation mix consists of multiple rooftop photovoltaic systems (> 400 kWp) and four micro-hydro electric plants (> 200kW). Figures 8.2.b and 8.2.c show the micro-hydro and pv systems production profiles, respectively. Some additional degrees of freedom are granted by two energy storage systems: a 224 kWh li-ion EES and a 450 m3, water based, sensible heat thermal energy storage.

All these assets are managed by a proprietary EMS, whose main functions are the balance of local consumption and generation, the actuation of DSM strategies (e.g. peak shaving) and constant monitoring of systems status.



FIGURE 8.2: Loccioni's microgrid consumption (a) and generation profiles (b,c), May 2016.

### 8.3.3 Simulation setup

Three different scenarios are simulated to stress the characteristics of the control mechanism, while testing performance and robustness in different conditions. The period to simulate has been arbitrarily set to May 2016, with hourly time steps. A primary set of constraints and assumptions are shared by all scenarios, being dependent from the microgrid characteristics: the energy demand and local generation

TABLE 8.1: Batteries specifications.

| Battery Agent | Capacity (kWh) | Type | Maximum Power output (kW) | Round Trip Efficiency |
|---|---|---|---|---|
| Batt1 | 250 | Li-ion | 80 | 0.85 |
| Batt2 | 250 | Li-ion | 80 | 0.85 |

profiles, the share of critical/non-critical loads and the available energy storage

Figures 8.3.a, 8.3.b and 8.3.c show the given consumption profile for the different load agents. For each agent both the critical and non-critical loads are reported. The Leaf Lab agent represents the consumption profile of the most advanced smart building of the microgrid, the Leaf Lab, for which a fixed-share of non-critical, deferrable, loads are available. This non-critical share of the total load is constant during working hours and zero during outside of them. This agent considers just the production related loads: office equipment, illumination, working machines and test benches. On the other hand, the Thermal Mass agent represents the Leaf Lab HVAC system consumption profile. In this case, the whole load is considered non-critical but only in specific hours of the day, for which the HVAC system can potentially be shut down to shift loads ahead. The "Rest of the Microgrid" agent includes all the other buildings with offices and laboratories. This latter agent does not have access to non-critical loads. Table 8.1 reports the available energy storages' characteristics which are used to define the behavior of the battery agents: maximum charging/discharging rate, maximum/minimum state of charge, round trip efficiency and capital cost. The first parameters are used to enforce operational constraints related to the machine characteristics, the latter is necessary to the control mechanism to evaluate when is convenient to use the energy storage.

A second set of assumptions is used to characterized the different scenarios. These assumptions are related to different energy price input vectors and, for scenario 2, to the forcing of a peak shaving strategy (Table 8.2). The energy price vectors considered are representative of two different markets. Figure 8.4.a shows the Italian "Prezzo Unico Nazionale" (PUN). PUN is calculated as the day-ahead wholesale market, zonal demand weighted, price. PUN data can be retrieved from GME's, "Gestore mercati energetici", website [46].

Usually, PUN is not directly applied to end users, which rather sign contract with an energy providing companies: these companies trade their daily capacity in the wholesale market while guaranteeing to the end users a constant tariff. Depending

FIGURE 8.3: The Leaf Lab (a), Thermal Mass (b) and Rest of the microgrid (c)
agents' consumption profiles. Figure shows both critical (in red) and non-critical
(in yellow) share of loads.

on the nature of the end user, the contracted tariff can have different characteristics.
For the sake of this study, end user's tariffs are not taken into consideration. Indeed,
due to the limited spread between peak and off peak prices, they are not able to
incentivize energy arbitrage strategies, neither to highlight the characteristics of the
presented control strategy.

Figure 8.4.b shows the Czech Balancing market (BM) trend in May 2016. This
market trades electricity used to maintain the balance within the Czech power grid.
It is a short-term market, operating in 30 minutes long sessions, opening one hour
before the required time of delivery. Balancing market data can be retrieved from
CEPS website [21]. These price vectors have been selected to represent two different

market schemas. The PUN comes from day-ahead trades, its nature is reflected in less variance and a more stationary behavior. On the other hand, the BM is a faster regulation framework, characterized by high variance and wide daily price swings. Price values showed in figures 4 are the final ones used in the analysis. They reflect the actual PUN and BM trends in terms of variability, while magnitude has been adjusted to account for fees and make the two markets comparable.

As described in Subsection 8.3.1, the grid agent is in charge to receive the updated data from the market and forecast the future energy prices for the next 24 hours' block. To test the effectiveness of the control mechanism, this study assumes perfect information over energy market data. This means that the price forecasts are substituted with the actual energy price vectors.

In scenario 2, peak shaving is activated every day from 15 pm to 17 pm. This means that the control mechanism will try to reduce the microgrid's power consumption down to a predetermined threshold, which, in this study, is arbitrarily set to 100 kW.

<div align="center">TABLE 8.2: Scenarios definition.</div>

|  | **Input price vector** | **Peak shaving status** |
|---|---|---|
| **Scenario 1** | PUN | OFF |
| **Scenario 2** | PUN | ON |
| **Scenario 3** | BM | OFF |

### 8.3.4   Comparison metrics

This study aims to assess the capabilities of the proposed control mechanism and its response to different sets of input conditions. For this reason, results in terms of absolute values are not quite interesting, neither significant. A series of assumptions were made to simplify assets models, knowing that an actual economic is beyond the scope of this work. Two comparison metrics are defined to highlight the relative effectiveness of the control mechanism when facing different scenarios.

Operating Costs Reduction (OCR) is defined as the percentage ratio between the simulated scenarios operating costs and the Baseline's ones (Equation 8.2). The Baseline scenario represents the "business as usual" case, operating costs are evaluated using the actual consumption profile of the microgrid ($P_i^b$), considering the PUN as price vector ($Pr_i^{PUN}$). OCR is a measure of the economic saving potential of the control mechanism. Shifted Energy Ratio (SER) is defined as the percentage

FIGURE 8.4: Energy price input vectors representing the PUN (a) and the BM (b) in May 2016.

ratio between the scenario's shifted energy and the Baseline energy consumption (Equation 8.3). Positive definite, it is a measure of how active, how effective, the control mechanism is under specific simulated conditions.

$$OCR = 100 \cdot \frac{\sum\limits_{i=1}^{744} P_i \cdot pr_i}{\sum\limits_{i=1}^{744} P_i^b \cdot Pr_i^{PUN}} \tag{8.2}$$

$$SER = 100 \cdot \frac{\sum\limits_{i=1}^{744} |P_i - P_i^b|}{\sum\limits_{i=1}^{744} P_i^b} \tag{8.3}$$
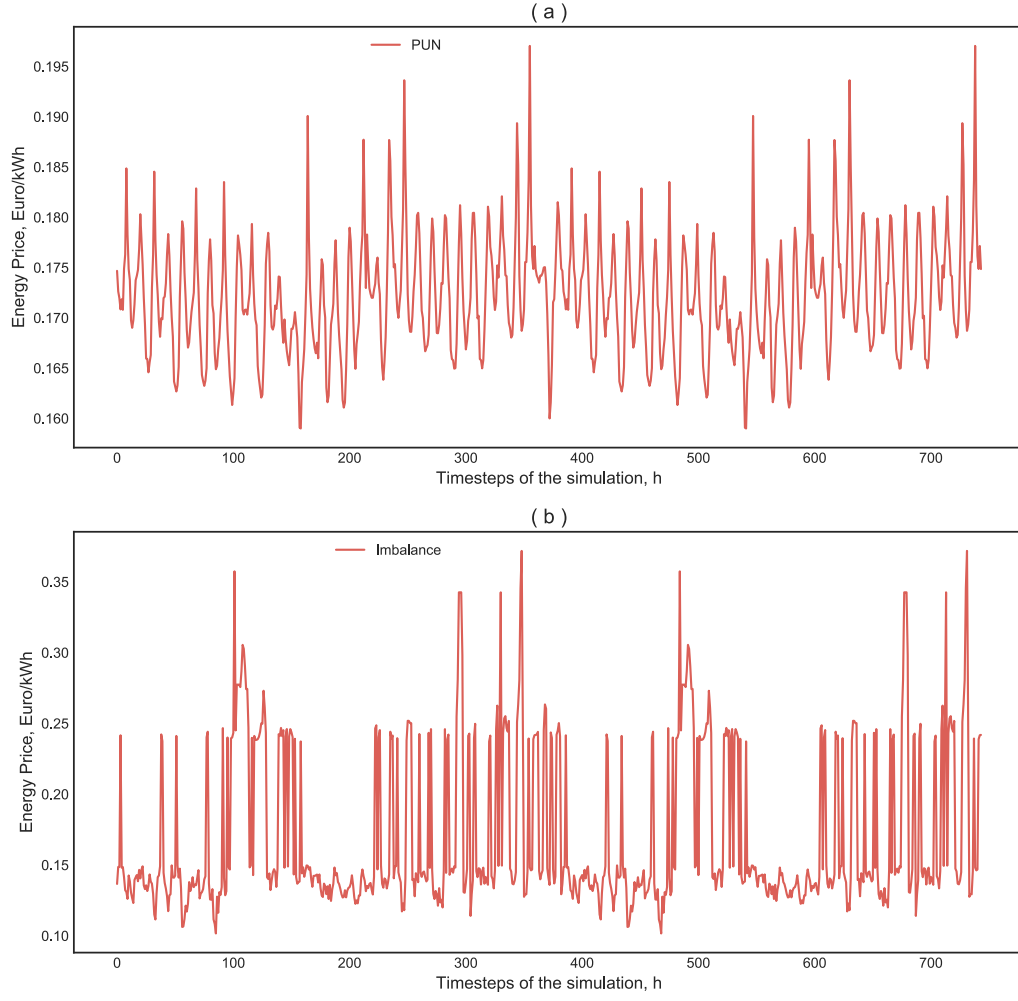
## 8.4 Results and discussion

Results, obtained simulating the different scenarios, confirm the ability of the proposed control method to adjust the microgrid consumption profile in accordance with an external price vector.

Figure 8.5 highlights this aspect, showing the control mechanism response to BM's trend (Shifted load), the original microgrid consumption profile (Baseline load) and BM's price vector. It is possible to distinguish three peak moments in the daily price vector (dashed red curve), to which the control mechanism responds reducing part of the power consumption using the available flexible assets of the microgrid. Loads are shifted to the end of the day (after time step 330), when BM values approach a local minimum.



FIGURE 8.5: Focus on the control mechanisms response to a dynamic price vector

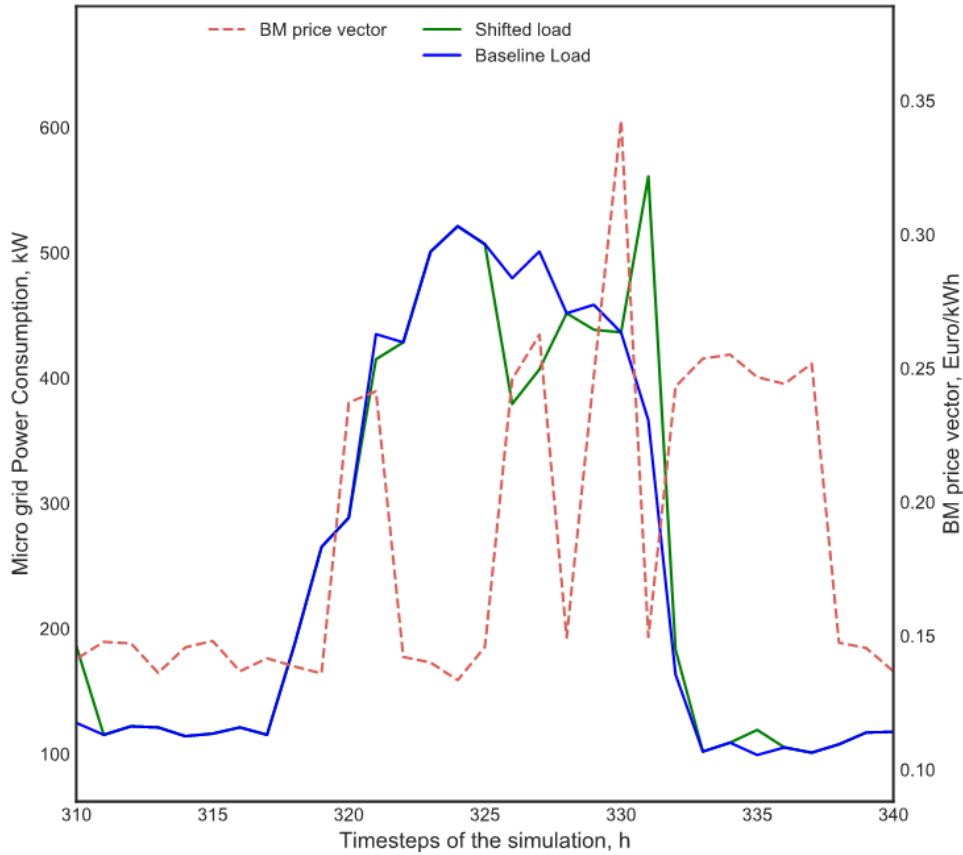Figures 8.6 graphically capture the control mechanism effect on microgrid's consumption profile, reporting three, arbitrarily chosen, simulated days. Figures 8.6.a, 8.6.c and 8.6.e show the microgrid load profile for the different simulated scenarios (see table 8.2), in red, against the baseline profile, in yellow. Figures 8.6.b, 8.6.d and

8.6.f report the input energy prices which forced the control system to shift the consumption. It is easy to appreciate how the control mechanisms impact is different depending on the simulated scenario. Before exploring each of these scenarios, it is worth noting how there is almost no difference in terms of Total Energy Consumption between the Baseline and the different scenarios ($\tilde{0}.01\%$, data in Table 8.3). This proves that the control mechanism is merely reshaping the microgrid's load profile.

In Scenario 1 (figure 8.6.a) the shifted load profile is, for the most part, superimposed with the baseline one, which means that the control mechanism cannot find arbitrage opportunities. This aspect is reflected in Table 8.3 results: Scenario 1 got the lowest shifting capabilities (SER of 4.2%) and non-significant savings opportunities (OCR 0.04%). Part of the daily load from peak hours is consistently shifted in the late evening using the available storage capacity. This shifting pattern exploits the daily seasonality of PUN values, which are consistently higher during specific hours of the day and lower in the night (figure 8.6.b).

Figures 8.6.c and 8.6.d are related to Scenario 2. As in Scenario 1, PUN is used as energy price input vector, however the activation of a peak shaving strategy forces a reduction in the microgrid power consumption every day, between 15 pm to 17 pm. The adopted control mechanism can consistently shred up to 100 kW during peak hours using a combination of electrical storage and deferrable loads. The shredded loads are recovered later in the afternoon, this aspect is visible as the red line start diverging from the yellow one in the descending section of the daily curves (Figure 8.6.c). Results in Table 8.3 prove how the control mechanism is forced to shift a relevant portion of the load (7% of SER) regardless of PUN price, due to the peak shaving strategy. OCR goes negative, which means that, for Scenario 2, the control mechanism increases microgrid's operational costs. This result was to be expected considering that the peak shaving strategy was enforced without considering any form of economic incentive.

Figures 8.6.e and 8.6.f are related to Scenario 3. The BM is used as price input vector of reference, no additional demand management strategies are enforced. The effects of the highly volatile BM are demonstrated by the Shifted load curve which shows an irregular pattern, way divergent from the baseline one. This irregular pattern is shaped by the control mechanism which tries to follow, and exploit, the BM.
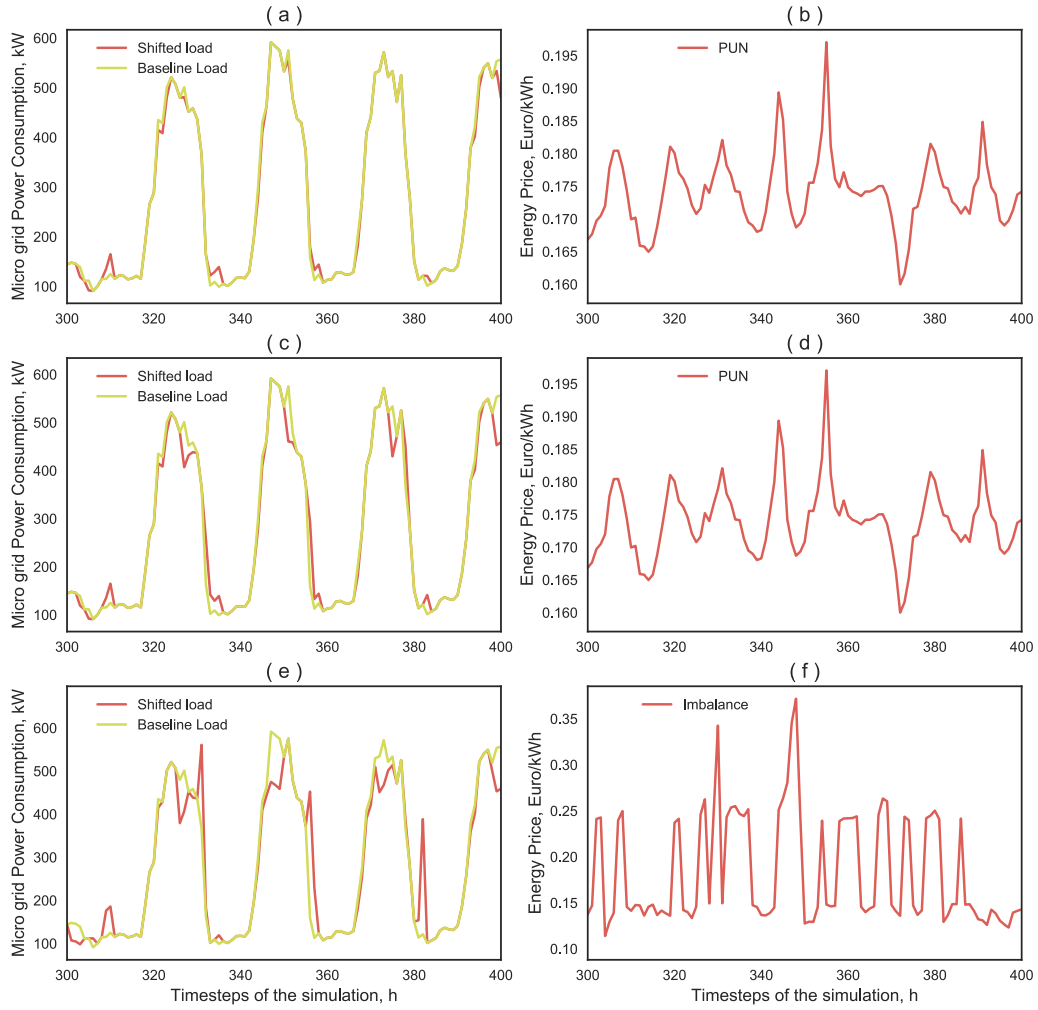
FIGURE 8.6: Baseline power, shifted power and energy price profiles for scenario 1 (a, b), scenario 2 (c,d) and scenario 3 (e, f)).

### 8.4.1 Possible improvements and future steps

The software developed in this study can be further improved under several aspects. When it was designed, many assumptions were done to create a first version of the software that can be always improved with the addition of new functions and the enhancement of the existing ones.

Load-shifting functions can be designed to enable different demand-response programs. For this reason, a basic version of the load-shifting method was implemented and embedded in both the Leaf Lab and Thermal Mass agents. It permits the shift of loads only in the future hours of the day. It is not possible to shift backwards, operating more complex strategies (e.g. offices pre-cooling). Future work

could implement more advanced models to capture the behavior of thermostatically controlled loads and their ability to increase the flexibility of a building. This feature would add more degrees of freedom to the shifting algorithm, enabling more complex and cost-effective decisions.

The control mechanism implemented in the load aggregator agent can be further improved. In the current version, once the loads communicate to the aggregator when they would like to shift the actual amount of power, the aggregator elaborates the new schedule and run a check to avoid the creation of new consumption peaks. When a new consumption peak is generated, the aggregator prioritizes the loads which answered first, allowing them to shift their consumption, while the last ones are forced to re-evaluate their schedule. This mechanism makes the aggregator prioritize always certain loads. To overcome this limit different ranking mechanisms, based on load's value or some comfort criteria, can be implemented to evaluate the schedule after all messages are received.

The battery agents can be improved by adding machine learning capabilities to learn their optimal usage pattern from historical time series. The battery agents can change their objective state of charge at every time step to maintain the reserve of energy necessary to regulate the power stability of the microgrid during the day and to enable highly cost-effective load management strategies.

Finally, in the current version of the software the control mechanism works having "perfect information" regarding the future energy prices: for each day of the simulation, and for each hour of the day, it knows in advance what the energy price will exactly be. Due to this assumption, results from Table 8.2 can be considered ideal, since they do not take into account the uncertainty related to energy price forecasts. In the real case, it is safe to assume that there will be a trade-off between higher margins, achievable in a more volatile market, and the rise in prediction complexity, which would result in the algorithm re-scheduling the load in a sub-optimal way. Future studies will explore this trade-off, while also modelling the impact of the uncertainty related to all the other stochastic variables involved, DER production and microgrid's consumption.

## 8.5   Conclusions

This chapter presented a multi agent control architecture designed for advanced energy management in industrial microgrids. The control mechanism uses the available flexibility assets available in a microgrids (distributed generation, energy stor-

TABLE 8.3: Simulation results.

|  | Total energy consumption (kWh) | Total operating costs (EUR) | OCR (%) | SER (%) |
|---|---|---|---|---|
| **Baseline** | 190220.9 | 32734.7 | - | - |
| **Scenario 1** | 190200.9 | 32721.2 | 0.04 | 4.2 |
| **Scenario 2** | 190220.9 | 32736.1 | -0.004 | 7 |
| **Scenario 3** | 190205.2 | 31126.1 | 1.26 | 6.4 |

age systems and non-critical loads) to reduce operational costs while maintaining the same production goals. Operational costs are reduced optimally scheduling the power exchange with the national grid, based on a 24 hours-ahead price signal. More complex control strategies are possible enforcing a peak shaving regime while maintaining the price arbitrage capabilities. Two comparison metrics were introduced to analyze the results and quantify the effectiveness of the control mechanism under different scenarios. The architecture effectiveness was tested using real data coming from Loccioni's Leaf Community, an industrial microgrids comprising controllable loads, renewable distributed generation and energy storages. Two different electricity market frameworks were simulated to test the sensitivity and the robustness of the control architecture to different conditions.

Results confirm the ability of the proposed control method to adjust the microgrid consumption profile, reducing operating costs while trying to maintain the consumption peak under a specified level. The effectiveness of the control mechanisms is strongly related to the input energy price vectors used to run the simulation. Specifically, the higher the variance in the input energy price vector, the higher the margin for arbitraging and the ability of the control mechanism to create value. All the results collected seem to point towards this general rule. In future studies, different market frameworks should be tested to further validate this hypothesis and identify the optimal market conditions to deploy this kind of control mechanisms.

# Chapter 9

# Conlusions

## 9.1 Key findings and impact

In this dissertation, we developed models, methodologies and tools that now contribute to the state of the art, helping us imagine the role that flexibility assets and aggregators will have in the future energy distribution network.

In chapter 2, we introduced the virtual flexibility plant framework for aggregators. The framework can be adapted for aggregators which are interested in either direct and indirect control strategies. The framework we presented is based on two operation levels: the "Local assets level", where the aggregator interacts with the end users collecting data to estimate and control their flexibility, and the "Flexibility Aggregator level", where it interacts with the energy market to buy/sell energy and provide different services. For each level we presented the aggregators objectives, its activities and we listed the main open questions/challenges from both the research and industry worlds. We explained the reasons behind the need for a generalized modeling methodology to describe and control the flexibility assets, presenting a suitable equivalent storage formulation. This formulation allow us to aggregate the contribution of thousands of heterogeneous assets by simply summing the equivalent storage parameters. Thus, we are able to describe and control radically different kinds of portfolio using the same set of modeling and optimization tools.

In chapter 3, we talked about energy storage systems. Specifically, we presented a simulation methodology to test the impact of integrating a thermal energy storage with an existing HVAC system. As a case study we used the School of Art, Design and Media building located within the NTU campus in Singapore. We designed different management strategies to address different area of interventions. The storage was used to reduce/remove partial load operations, to reduce peaks loads prioritiz-

ing the usage of the most efficient chillers and to perform price arbitrage, exploiting the difference between peak and off-peak electricity rates in Singapore. Results we obtained indicate how the extra flexibility introduced by a thermal energy storage can sensibly improve the building performances, reducing operational costs while improving the cooling system efficiency. The technology seems to be particularly effective when used to remove partial load operations by shifting part of the energy demand.

In chapter 4, we talked about the intrinsic flexibility of the residential cooling energy demand and introduced thermostatically controlled loads. We modeled a heterogeneous population of 1000 households using a specific set of parameters sampled from uniform distributions. Using this population, we ran several simulations testing the effect of different climate conditions and setpoint/deadband variations. We observed that human behavior, expressed through thermostat control preferences, has a critical effect on the estimated demand response potential. Specifically, we demonstrated how moving from a dynamic setpoint strategy towards a dynamic deadband one, consumers could trade energy saving potential to increase their load flexibility. Relaxing the thermostats control's deadband, aggregators can replace more storage capacity integrating the same number of residential costumers. Results show how temperate climates get the most benefits from a dynamic deadband strategy, giving us precious indications to build targeting recommendations: given a fixed number of households that we can aggregate in our portfolio, we get more flexibility in Sacramento than in Los Angeles. To the best of our knowledge, this is the first work that perform a direct comparison between these two strategy simulating their impact on both demand efficiency and flexibility.

In chapter 5, we introduced a modeling approach to describe an aggregation of Electric Vehicles System Equipments (EVSEs) as an equivalent energy storage. The model is based on five parameters that can be estimated using historical charging data. These parameters should be evaluated for each single EVSE and summed up to aggregate their contribution. We explained how the model can be used by referring to a trivial case of an aggregation of two EVSEs. We also discussed about the impact of mobility patterns on the aggregate flexibility. Specifically, the flexibility associated with each EV driver depend on arrival and departure time, the energy consumed driving and the charging frequency. EVs integration in a flexibility resource portfolio can have either positive, neutral or even negative effect depending on the smart charging strategy and the kind of service the aggregator seeks to provide.

In chapter 6, we talked about the challenges related to the actual implementation of a demand side management strategy in an industrial microgrid. We reported data collected during a test campaign showing how we can exploit the existing flexibility assets to implement simple strategy and reshape the energy demand profile. Specifically, we used a sensible heat thermal energy storage and the existing HVAC system, proving that the peak load can be substantially reduced. However, when the strategy is revoked and the original temperature setpoint is restored, the chillers turn on again at maximum power to push the temperature within the acceptable deadband, generating a new peak in terms of energy demand. The data we collected also proves that sampling electricity consumption with a 15 minutes time granularity is adequate to identify the activation of a load shedding strategy, giving us an important feedback when it comes to choose the appropriate metering infrastructure for such applications.

In chapter 7, we defined a methodology to address the optimal portfolio management problem for flexibility aggregators. Using this methodology we can estimate the flexibility portfolio of a generic urban district by describing the different flexibility resources using the equivalent storage models. We presented a convex formulation that is designed to solve the optimal portfolio management problem for flexibility aggregators. The goal of this formulation is to optimally manage the available flexibility resources, leveraging the energy price variability to reduce operational costs, while producing valuable services for the national grid. We tested the methodology in two alternative scenarios, simulating the characteristics of an urban district which has access to controllable residential TCLs, controllable EVSEs and energy storage systems. Both scenarios aimed to show how aggregators could enhance their control over the aggregated energy demand by optimally using the available flexibility resources, while integrating extra storage capacity to supply specific services to the national grid. Results show how enabling residential TCLs can reduce aggregators investment in extra storage capacity by up to 30%, while providing the same level of services to the end users and the national grid. On the other hand, EVs integration can have a positive or neutral effect depending on the smart charging strategy and the required services.

In chapter 8, we introduced a multi-agent based control architecture designed to manage the flexibility assets of an industrial microgrid. In this case the aggregation level is limited to a single industrial microgrid and the aggregator is interested in the optimal control of the different flexibility assets to reduce operational costs and limit consumption peaks during critical hours. Two comparison metrics were

introduced to analyze the results and quantify the effectiveness of the control mechanism under different conditions: the operating cost reduction is an economic index that compares the operative costs before and after the introduction of the control strategy; the Shifted energy ratio is an energy index that measures how active, effective, the control mechanism is, regardless of the economic benefits. The control mechanism effectiveness was tested using real data coming from an industrial microgrids comprising controllable loads, renewable distributed generation and energy storages. Results confirm the ability of the proposed control method to adjust the microgrid consumption profile, reducing operating costs while operating a peak shaving strategy. The potential of the control mechanisms is strongly related to the input energy price vectors used to run the simulation. Specifically, the higher the variance in the input energy price vector, the higher the margin for arbitraging and the ability of the control mechanism to create value.

## 9.2   Future research topics

We believe the methods introduced and the results discussed in this dissertation to represent a starting point for several others research opportunities, including:

- Starting from the Virtual Flexibility Plant architecture developed in chapter 2, to define the necessary data infrastructure, the data exchange protocols and a functional, scalable and secure database architecture

- To demonstrate how aggregators can coordinate large numbers of TCLs and EVSEs implementing different DR services and smart strategies in an urban scale pilot

- To identify targeting metrics for households and areas with the highest value flexibility

- To identify optimal targeting strategy for investing in EVSEs given the mobility patterns of a population

- To integrate the flexibility estimates and modeling techniques introduced in this dissertation with models of future grid emissions

- To implement and test the optimal portfolio management method, presented in chapter 7, in an urban scale pilot

- To implement and test the multi-agent based control architecture, presented in chapter 8, in a microgrid pilot

- To explore how blockchain technologies can facilitate the vision for Smart Grids and aggregators of distributed flexibility resources

- To further analyze the potential social role and the business opportunities for aggregators of distributed flexibility resources

# Bibliography

[1] F. A.Ipakchi. Grid of the future. *EEE Power and Energy Magazine*, 7(2): 52–62, 2009.

[2] C. Akasiadis, K. Panagidi, N. Panagiotou, P. Sernani, A. Morton, I. A. Vetsikas, L. Mavrouli, and K. Goutsias. Incentives for rescheduling residential electricity consumption to promote renewable energy usage. In *2015 SAI Intelligent Systems Conference (IntelliSys)*, pages 328–337, Nov 2015. doi: 10.1109/IntelliSys.2015.7361163.

[3] M. Alcázar-Ortega, C. Álvarez-Bel, G. Escrivá-Escrivá, and A. Domijan. Evaluation and assessment of demand response potential applied to the meat industry. *Applied Energy*, 92:84–91, 2012. ISSN 03062619. doi: 10.1016/j.apenergy.2011.10.040.

[4] A. Arteconi, N. J. Hewitt, and F. Polonara. State of the art of thermal storage for demand-side management. *Applied Energy*, 93:371–389, 2012. ISSN 03062619. doi: 10.1016/j.apenergy.2011.12.045.

[5] A. Arteconi, J. Xu, E. Ciarrocchi, L. Paciello, G. Comodi, F. Polonara, and R. Wang. Demand Side Management of a Building Summer Cooling Load by Means of a Thermal Energy Storage. In *Energy Procedia*, volume 75, pages 3277–3283, 2015. doi: 10.1016/j.egypro.2015.07.705.

[6] A. Arteconi, E. Ciarrocchi, Q. Pan, F. Carducci, G. Comodi, F. Polonara, and R. Wang. Thermal energy storage coupled with PV panels for demand side management of industrial building cooling loads. *Applied Energy*, 185: 1984–1993, 2017. ISSN 03062619. doi: 10.1016/j.apenergy.2016.01.025.

[7] P. Asmus. Microgrids, virtual power plants and our distributed energy future. *The Electricity Journal*, 23(10):72–82, 2010. doi: 10.1016/j.tej.2010.11.001.

[8] H. Auer and R. Haas. On integrating large shares of variable renewables into the electricity system. *Energy*, 115:1592–1601, 2016. ISSN 0360-5442. doi: 10.1016/j.energy.2016.05.067. URL `http://dx.doi.org/10.1016/j.energy.2016.05.067`.

[9] G. Barbose. U.S. Renewable Portfolio Standards: 2016 annual status report. Technical report, Lawrence Berkeley National Lab, 2016. URL `https://emp.lbl.gov/sites/all/files/lbnl-1005057.pdf`.

[10] S. Behboodi, D. P. Chassin, C. Crawford, and N. Djilali. Renewable resources portfolio optimization in the presence of demand response. *Applied Energy*, 162:139–148, 2016. doi: 10.1016/j.apenergy.2015.10.074.

[11] F. L. Bellifemine, G. Caire, and D. Greenwood. *Developing multi-agent systems with JADE.* John Wiley & Sons, 2007.

[12] J. M. Bert. Ancillary services : Technical and Commercial Insights. *The Orthopedic clinics of North America*, 39(1):1–4, v, 2008. ISSN 0030-5898. doi: 10.1016/j.ocl.2007.08.001. URL `http://www.ncbi.nlm.nih.gov/pubmed/20228656`.

[13] R. J. Bessa, F. J. Soares, J. A. Peças Lopes, and M. A. Matos. Models for the EV aggregation agent business. In *2011 IEEE PES Trondheim PowerTech: The Power of Technology for a Sustainable Society, POWERTECH 2011*, 2011. ISBN 9781424484195. doi: 10.1109/PTC.2011.6019221.

[14] M. Brolin. Aggregator trading and demand dispatch under price and load uncertainty. In *IEEE PES Innovative Smart Grid Technologies Conference Europe*, 2017. ISBN 9781509033584. doi: 10.1109/ISGTEurope.2016.7856228.

[15] S. Burger, J. P. Chaves-Ávila, C. Batlle, and I. J. Pérez-Arriaga. A review of the value of aggregators in electricity systems, 2017. ISSN 18790690.

[16] L. F. Cabeza, L. Miró, E. Oró, A. de Gracia, V. Martin, A. Krönauer, C. Rathgeber, M. M. Farid, H. O. Paksoy, M. Martínez, and A. I. Fernández. CO2 mitigation accounting for Thermal Energy Storage (TES) case studies. *Applied Energy*, 155:365–377, 2015. ISSN 03062619. doi: 10.1016/j.apenergy.2015.05.121.

[17] CAISO. Regulation Energy Management Draft Final Proposal, 2011. URL `http://www.caiso.com/Documents/`

RevisedDraftFinalProposal-RegulationEnergyManagement-Jan13{_}2011.
pdf.

[18] CAISO. What the duck curve tells us about managing a green grid. *California ISO, Shaping a Renewed Future*, Fact Sheet:1–4, 2012. doi: CommPR/HS/ 10.2013.

[19] D. S. Callaway. Tapping the energy storage potential in electric loads to deliver load following and regulation, with application to wind energy. *Energy Conversion and Management*, 50(5):1389–1400, 2009. ISSN 01968904. doi: 10.1016/j.enconman.2008.12.012. URL `http://dx.doi.org/10.1016/j.enconman.2008.12.012`.

[20] C. Calvillo, A. Sánchez-Miralles, J. Villar, and F. Martín. Optimal planning and operation of aggregated distributed energy resources with market participation. *Applied Energy*, 182:340–357, 2016. ISSN 03062619. doi: 10.1016/j.apenergy.2016.08.117. URL `http://dx.doi.org/10.1016/j.apenergy.2016.08.117`.

[21] CEPS. Czech transmission system operator. `https://www.ceps.cz/ENG/Data/Vsechna-data/Pages/Systemova-odchylka-a-zuctovaci-cena.aspx`.

[22] G. Chalkiadakis, V. Robu, R. Kota, A. Rogers, and N. Jennings. Cooperatives of Distributed Energy Resources for Efficient Virtual Power Plants. *The Tenth International Conference on Autonomous Agents and Multiagent Systems (AAMAS-2011)*, (Aamas):787–794, 2011. URL `http://eprints.soton.ac.uk/271950/`.

[23] S. Chanana and M. Arora. Demand Response from Residential Air Conditioning Load Using a Programmable Communication Thermostat. *International Journal of Electrical and Computer Engineering*, 7(12):1670–1676, 2013. doi: scholar.waset.org/1999.5/9996726.

[24] D. P. Chassin, J. Stoustrup, P. Agathoklis, and N. Djilali. A new thermostat for real-time price demand response: Cost, comfort and energy impacts of discrete-time control without deadband. *Applied Energy*, 155:816–825, 2015. ISSN 03062619. doi: 10.1016/j.apenergy.2015.06.048. URL `http://dx.doi.org/10.1016/j.apenergy.2015.06.048`.

[25] W. D. Chvala. Technology potential of thermal energy storage (Tes) systems in federal facilities. *Energy Engineering: Journal of the Association of Energy Engineering*, 99(5):55–80, 2002. ISSN 15460118. doi: 10.1080/01998590209509356.

[26] C. M. Colson and M. H. Nehrir. Comprehensive real-time microgrid power management and control with distributed agents. *IEEE Transactions on Smart Grid*, 4(1):617–627, 2013. doi: 10.1109/TSG.2012.2236368.

[27] E. Commission. 2050 low-carbon economy, November 2017. URL `https://ec.europa.eu/clima/policies/strategies/2050_en`.

[28] G. Comodi, A. Giantomassi, M. Severini, S. Squartini, F. Ferracuti, A. Fonti, D. Nardi Cesarini, M. Morodo, and F. Polonara. Multi-apartment residential microgrid with electrical and thermal storage devices: Experimental analysis and simulation of energy management strategies. *Applied Energy*, 137:854–866, 2015. ISSN 03062619. doi: 10.1016/j.apenergy.2014.07.068.

[29] G. Comodi, F. Carducci, B. Nagarajan, and A. Romagnoli. Application of cold thermal energy storage (CTES) for building demand management in hot climates. *Applied Thermal Engineering*, 103:1186–1195, 2016. ISSN 13594311. doi: 10.1016/j.applthermaleng.2016.02.035.

[30] G. Comodi, F. Carducci, J. Sze, N. Balamurugan, and A. Romagnoli. Storing energy for cooling demand management in tropical climates: A techno-economic comparison between different energy storage technologies. *Energy*, 121, 2017. ISSN 03605442. doi: 10.1016/j.energy.2017.01.038.

[31] N. Daina, A. Sivakumar, and J. W. Polak. Electric vehicle charging choices: Modelling and implications for smart charging services. *Transportation Research Part C: Emerging Technologies*, 81:36–56, 2017. ISSN 0968090X. doi: 10.1016/j.trc.2017.05.006.

[32] N. Deforest, W. Feng, J. Lai, C. Marnay, and M. Stadler. Thermal energy storage for electricity peak-demand mitigation: a solution in developing and developed world alike. *ECEEE Summer Study Proceedings*, pages 1191–1197, 2013.

[33] P. Denholm, M. O'Connell, G. Brinkman, and J. Jorgenson. Overgeneration from solar energy in california: A field guide to the duck chart. *National Renewable Energy Laboratory, Tech. Rep. NREL/TP-6A20-65023*, 2015.

[34] I. Dincer and M. Rosen. *Thermal Energy Storage Systems and Applications.* 2011. ISBN 9780470747063.

[35] J. Driesen and F. Katiraei. Design for distributed energy resources. *IEEE Power and Energy Magazine*, 6(3):30–40, May 2008. doi: 10.1109/MPE.2008. 918703.

[36] E. Efficiency. Energy Efficiency in Buildings. 2015.

[37] C. Eid, E. Koliou, M. Valles, J. Reneses, and R. Hakvoort. Time-based pricing and electricity demand response: Existing barriers and next steps. *Utilities Policy*, 40:15–25, 2016. ISSN 09571787. doi: 10.1016/j.jup.2016.04.001. URL `http://dx.doi.org/10.1016/j.jup.2016.04.001`.

[38] ERCOT. ERCOT Real-Time Market. URL `http://www.ercot.com/mktinfo/rtm`.

[39] I. Ernmenta and L. P. A. Nel. *Climate Change 2014 Synthesis Report.* ISBN 9789291691432.

[40] F. E. R. C. (FERC). Assessment of Demand Response and Advanced Metering. *Department of Energy EEUU*, page 130, 2012. ISSN 13514180. doi: 20426. URL `file:///C:/Users/SATELLITE/GoogleDrive/ReferenciasDoctorado//FederalEnergyRegulatoryCommission(FERC)-2012-AssessmentofDemandResponseandAdvancedMetering.pdf`.

[41] V. M. I. N. F.Guimaraes. Multi-agent systems applied for energy systems integration: State-of-the-art applications and trends in microgrids. *Applied Energy*, 187:820–832, 2017. doi: 10.1016/j.apenergy.2016.10.056.

[42] FIPA. The foundation for intelligent physical agents standards [on-line]. `http://www.fipa.org`, 2017.

[43] D. Fischer, T. Wolf, J. Wapler, R. Hollinger, and H. Madani. Model-based flexibility assessment of a residential heat pump pool. *Energy*, 118:853–864, 2017. ISSN 03605442. doi: 10.1016/j.energy.2016.10.111. URL `http://dx.doi.org/10.1016/j.energy.2016.10.111`.

[44] N. C. for Environmental Information. MS Windows NT kernel description, 2017. URL `https://www.ncdc.noaa.gov`.

[45] M. D. Galus, M. G. Vayá, T. Krause, and G. Andersson. The role of electric vehicles in smart grids, 2013. ISSN 20418396.

[46] GME. Gestore mercati engergetici. `http://www.mercatoelettrico.org/it/Esiti/MGP/EsitiMGP.aspx`.

[47] M. Gonzalez Vaya and G. Andersson. Optimal Bidding Strategy of a Plug-In Electric Vehicle Aggregator in Day-Ahead Electricity Markets under Uncertainty. *IEEE Transactions on Power Systems*, 30(5):2375–2385, 2015. ISSN 08858950. doi: 10.1109/TPWRS.2014.2363159.

[48] T. M. Hansen, R. Roche, S. Suryanarayanan, A. A. Maciejewski, and H. J. Siegel. Heuristic Optimization for an Aggregator-Based Resource Allocation in the Smart Grid. *IEEE Transactions on Smart Grid*, 6(4):1785–1794, 2015. ISSN 19493053. doi: 10.1109/TSG.2015.2399359.

[49] H. Hao, B. M. Sanandajib, K. Poolla, T. L. Vincent, B. M. Sanandaji, K. Poolla, and T. L. Vincent. Aggregate Flexibility of Thermostatically Controlled Loads. *IEEE Transaction on Power Systems*, 30(1):1–10, 2014. URL `http://ieeexplore.ieee.org/xpls/abs{_}all.jsp?arnumber=6832599{%}0Ahttp://plaza.ufl.edu/hehao/papers/TCL{_}IEEE{_}TPS.pdf`.

[50] M. Hu, F. Xiao, and L. Wang. Investigation of demand response potentials of residential air conditioners in smart grids using grey-box room thermal model. *Applied Energy*, 2017. ISSN 03062619. doi: 10.1016/j.apenergy.2017.05.099. URL `http://linkinghub.elsevier.com/retrieve/pii/S0306261917306098`.

[51] J. Ikäheimo, C. Evens, and S. Kärkkäinen. DER Aggregator Business: the Finnish Case. page 38, 2010.

[52] IndustRE. The IndustRE H2020 project. `http://www.industre.eu/the-industre-project/`, 2017. WIP Renewable Energies, accessed April, 2017.

[53] International Energy Agency. Global EV Outlook 2016 Electric Vehicles Initiative. *Iea*, page 51, 2016. doi: EIA-0383(2016).

[54] International Energy Agency (IEA). Technology roadmap: Electric and plug-in hybrid electric vehicles. *International Energy Agency, Tech. Rep*, (June):

52, 2011. ISSN 1557-170X. doi: 10.1109/IEMBS.2004.1403974. URL `http://scholar.google.com/scholar?hl=en{&}btnG=Search{&}q=intitle:Technology+Roadmap+-+Electric+and+plug-in+hybrid+electric+vehicles{#}0`.

[55] International Energy Agency (IEA). Renewables 2017, 2017. URL `https://www.iea.org/publications/renewables2017/`.

[56] A. Ipakchi and F. Albuyeh. Grid of the future, 2009. ISSN 15407977.

[57] Y. Kabalci. A survey on smart metering and smart grid communication, 2016. ISSN 18790690.

[58] S. Kakran and S. Chanana. Smart operations of smart grids integrated with distributed generation : A review. *Renewable and Sustainable Energy Reviews*, 81(July 2017):524–535, 2018. ISSN 1364-0321. doi: 10.1016/j.rser.2017.07.045. URL `http://dx.doi.org/10.1016/j.rser.2017.07.045`.

[59] E. C. Kara. Data-Driven Approaches to Demand Response : Studies on Thermostatically Controlled Loads and Electric Vehicles. 2014.

[60] E. C. Kara, M. D. Tabone, J. S. MacDonald, D. S. Callaway, and S. Kiliccote. Quantifying flexibility of residential thermostatically controlled loads for demand response. *Proceedings of the 1st ACM Conference on Embedded Systems for Energy-Efficient Buildings - BuildSys '14*, pages 140–147, 2014. doi: 10.1145/2674061.2674082. URL `http://dl.acm.org/citation.cfm?doid=2674061.2674082`.

[61] E. C. Kara, J. S. Macdonald, D. Black, M. Bérges, G. Hug, and S. Kiliccote. Estimating the benefits of electric vehicle smart charging at non-residential locations: A data-driven approach. *Applied Energy*, 155:515–525, 2015. ISSN 03062619. doi: 10.1016/j.apenergy.2015.05.072.

[62] S. Kiliccote, P. Price, M. A. Piette, G. Bell, S. Pierson, E. Koch, J. Carnam, H. Pedro, J. Hernandez, and A. Chiu. Field Testing of Automated Demand Response for Integration of Renewable Resources in California ' s Ancillary Services Market for Regulation Products. *Lawrence Berkeley National Laboratory*, 1(April 2012), 2012.

[63] K. Knezović, M. Marinelli, P. Codani, and Y. Perez. Distribution grid services and flexibility provision by electric vehicles: A review of options. In *Proceed-*

*ings of the Universities Power Engineering Conference*, volume 2015-Novem, 2015. ISBN 9781467396820. doi: 10.1109/UPEC.2015.7339931.

[64] R. Leszczyna. Cybersecurity and privacy in standards for smart grids - A comprehensive survey, 2017. ISSN 09205489.

[65] T. Logenthiran, D. Srinivasan, A. M. Khambadkone, and H. N. Aung. Multiagent system for real-time operation of a microgrid in real-time digital simulator. *IEEE Transactions on Smart Grid*, 3(2):925–933, June 2012. doi: 10.1109/TSG.2012.2189028.

[66] D. Madjidian, M. Roozbehani, and M. A. Dahleh. Emulating Batteries with Deferrable Energy Demand: Fundamental Trade-offs and Scheduling Policies, 2016. ISSN 07431619. URL https://arxiv.org/abs/1611.03765.

[67] Y. V. Makarov, C. Loutan, J. Ma, and P. de Mello. Operational impacts of wind generation on California power systems, 2009. ISSN 08858950.

[68] T. Malinick, N. Wilairat, J. Holmes, and L. Perry. Destined to Disappoint: Programmable Thermostat Savings are Only as Good as the Assumptions about Their Operating Characteristics. *ACEEE Summer Study on Energy Efficiency in Buildings*, 1(7):162–173, 2012.

[69] S. Martinenas, K. Knezovic, and M. Marinelli. Management of Power Quality Issues in Low Voltage Networks Using Electric Vehicles: Experimental Validation. *IEEE Transactions on Power Delivery*, 32(2):971–979, 2017. ISSN 08858977. doi: 10.1109/TPWRD.2016.2614582.

[70] J. L. Mathieu, M. Dyson, and D. S. Callaway. Using Residential Electric Loads for Fast Demand Response : The Potential Resource and Revenues , the Costs , and Policy Recommendations. *Proceedings of the ACEEE Summer Study on Buildings*, 1(Ccst 2011):189–203, 2012.

[71] J. L. Mathieu, M. E. H. Dyson, and D. S. Callaway. Resource and revenue potential of California residential load participation in ancillary services. *Energy Policy*, 80:76–87, 2015. ISSN 03014215. doi: 10.1016/j.enpol.2015.01.033. URL http://dx.doi.org/10.1016/j.enpol.2015.01.033.

[72] G. McCracken, Brewster; Tom. Pecan Street Smart Grid Demonstration Project_Final Technology Performance Report. Technical Report February, Pecan Street Inc, Department of Energy, 2015.

[73] MITEI;, R. Schmalensee, V. Bulovic, and R. Armstrong. The Future of Solar Energy. An interdisciplinary MIT study. Technical Report 3, 2015.

[74] M. Motalleb, M. Thornton, E. Reihani, and R. Ghorbani. Providing frequency regulation reserve services using demand response scheduling. *Energy Conversion and Management*, 124:439–452, 2016. ISSN 01968904. doi: 10.1016/j.enconman.2016.07.049. URL `http://dx.doi.org/10.1016/j.enconman.2016.07.049`.

[75] L. M.S.Andersen, J.Dahl. Cvxopt: A python package for convex optimization, 2013. URL `http://cvxopt.org`.

[76] M. Muratori, B.-a. Schuelke-leech, and G. Rizzoni. Role of residential demand response in modern electricity markets. *Renewable and Sustainable Energy Reviews*, 33:546–553, 2014. ISSN 1364-0321. doi: 10.1016/j.rser.2014.02.027. URL `http://dx.doi.org/10.1016/j.rser.2014.02.027`.

[77] F. Nagele, T. Kasper, and B. Girod. Turning up the heat on obsolete thermostats: A simulation-based comparison of intelligent control approaches for residential heating systems. *Renewable and Sustainable Energy Reviews*, 75 (January):1254–1268, 2017. ISSN 18790690. doi: 10.1016/j.rser.2016.11.112. URL `http://dx.doi.org/10.1016/j.rser.2016.11.112`.

[78] New York State Energy Research and Development Authority. *Microgrids: An Assessment of the Value, Opportunities and Barriers to Deployment in New York State, Final Report*. NYSERDA report. None, 2010.

[79] S. M. Nosratabadi, R. A. Hooshmand, and E. Gholipour. A comprehensive review on microgrid and virtual power plant concepts employed for distributed energy resources scheduling in power systems, 2017. ISSN 18790690.

[80] E. Oró, V. Depoorter, N. Pflugradt, and J. Salom. Overview of direct air free cooling and thermal energy storage potential energy savings in data centres, 2015. ISSN 13594311.

[81] E. Parliament. Directive 2009/28/ec, 2009. URL `http://eur-lex.europa.eu/LexUriServ/LexUriServ.do?uri=OJ:L:2009:140:0016:0062:EN:PDF`.

[82] N. G. Paterakis, O. Erdinç, and J. P. Catalão. An overview of Demand Response: Key-elements and international experience, 2017. ISSN 18790690.

[83] M. Pritoni, J. M. Woolley, and M. P. Modera. Do occupancy-responsive learning thermostats save energy? A field study in university residence halls. *Energy and Buildings*, 127:469–478, 2016. ISSN 03787788. doi: 10.1016/j. enbuild.2016.05.024. URL `http://dx.doi.org/10.1016/j.enbuild.2016.05.024`.

[84] PSERC. Challenges in Integrating Renewable Technologies into an Electric Power System. Technical report, 2010.

[85] S. D. Ramchurn, P. Vytelingum, A. Rogers, and N. R. Jennings. Agent-based homeostatic control for green energy in the smart grid. *ACM Transactions on Intelligent Systems and Technology (TIST)*, 2(4):35:1–35:28, 2011.

[86] T. Ribera and J. Sachs. DEEP decarbonization. pages 1–58, 2015. URL `papers2://publication/uuid/E7622E05-580D-4FEC-9AB7-DFE70AA5D572`.

[87] j. H. M. Robert H. Miller. *Power System Operation*. McGraw-Hill, 1993.

[88] A. Y. Saber and G. K. Venayagamoorthy. Plug-in vehicles and renewable energy sources for cost and emission reductions. *IEEE Transactions on Industrial Electronics*, 58(4):1229–1238, 2011. ISSN 02780046. doi: 10.1109/TIE.2010.2047828.

[89] T. Samad and S. Kiliccote. Smart grid technologies and applications for the industrial sector. *Computers & Chemical Engineering*, 47:76–84, 2012. doi: 10.1016/j.compchemeng.2012.07.006.

[90] H. Schreiber, S. Graf, F. Lanzerath, and A. Bardow. Adsorption thermal energy storage for cogeneration in industrial batch processes: Experiment, dynamic modeling and system analysis. *Applied Thermal Engineering*, 89: 485–493, 2015. ISSN 13594311. doi: 10.1016/j.applthermaleng.2015.06.016.

[91] M. Shann and S. Seuken. Adaptive home heating under weather and price uncertainty using gps and mdps. In *Proceedings of the 2014 International Conference on Autonomous Agents and Multi-agent Systems*, AAMAS '14, pages 821–828. International Foundation for Autonomous Agents and Multi-agent Systems, 2014.

[92] M. H. Shoreh, P. Siano, M. Shafie-khah, V. Loia, and J. P. Catalão. A survey of industrial applications of Demand Response, 2016. ISSN 03787796.

[93] S. M. Sirin and M. S. Gonul. Behavioral aspects of regulation: A discussion on switching and demand response in Turkish electricity market. *Energy Policy*, 97:591–602, 2016. ISSN 03014215. doi: 10.1016/j.enpol.2016.08.005. URL `http://dx.doi.org/10.1016/j.enpol.2016.08.005`.

[94] G. Strbac. Demand side management: benefits and challenges. *Energy Policy*, 36(12):4419–4426, 2008.

[95] W. Surles and G. P. Henze. Evaluation of automatic priced based thermostat control for peak energy reduction under residential time-of-use utility tariffs. *Energy and Buildings*, 49:99–108, 2012. ISSN 03787788. doi: 10.1016/j.enbuild.2012.01.042. URL `http://dx.doi.org/10.1016/j.enbuild.2012.01.042`.

[96] Z.-e. Vehicles. ZEV Action Plan. (February):32, 2013. URL `http://opr.ca.gov/docs/Governor's{_}Office{_}ZEV{_}Action{_}Plan{_}(02-13).pdf`.

[97] I. S. Walker and A. K. Meier. Residential Thermostats : Comfort Controls in California Homes Iain S . Walker and Alan K . Meier Lawrence Berkeley National Laboratory Berkeley , California March 2008 LBNL-938E. *None*, 2008.

[98] J. Wang, H. Zhong, W. Tang, R. Rajagopal, Q. Xia, C. Kang, and Y. Wang. Optimal bidding strategy for microgrids in joint energy and ancillary service markets considering flexible ramping products q. *Applied Energy*, 205:294–303, 2017. ISSN 0306-2619. doi: 10.1016/j.apenergy.2017.07.047. URL `http://dx.doi.org/10.1016/j.apenergy.2017.07.047`.

[99] J. H. Williams, A. DeBenedictis, R. Ghanadan, A. Mahone, J. Moore, W. R. Morrow, S. Price, and M. S. Torn. The Technology Path to Deep Greenhouse Gas Emissions Cuts by 2050: The Pivotal Role of Electricity. *Science*, 335 (6064):53–59, Jan. 2012. ISSN 0036-8075, 1095-9203. doi: 10.1126/science.1208365. URL `http://www.sciencemag.org/content/335/6064/53`.

[100] M. Wooldridge and N. R. Jennings. Intelligent agents: Theory and practice. *The knowledge engineering review*, 10(2):115–152, 1995.

[101] D. P. Xenos, I. M. Noor, M. Matloubi, M. Cicciotti, T. Haugen, and N. F. Thornhill. Demand-side management and optimal operation of industrial elec-

tricity consumers: An example of an energy-intensive chemical plant. *Applied Energy*, 182:418–433, 2016. doi: 10.1016/j.apenergy.2016.08.084.

[102] R. Yin, E. C. Kara, Y. Li, N. DeForest, K. Wang, T. Yong, and M. Stadler. Quantifying flexibility of commercial and residential loads for demand response using setpoint changes. *Applied Energy*, 177:149–164, 2016. ISSN 03062619. doi: 10.1016/j.apenergy.2016.05.090. URL `http://dx.doi.org/10.1016/j.apenergy.2016.05.090`.

[103] Yixing Xu, Le Xie, and C. Singh. Optimal scheduling and operation of load aggregator with electric energy storage in power markets. *North American Power Symposium 2010*, pages 1–7, 2010. doi: 10.1109/NAPS.2010.5619601.

[104] C. Yuen, A. Oudalov, and A. Timbus. The provision of frequency control reserves from multiple microgrids. *IEEE Transactions on Industrial Electronics*, 58(1):173–183, Jan 2011. doi: 10.1109/TIE.2010.2041139.

[105] K. K. Zame, C. A. Brehm, A. T. Nitica, C. L. Richard, and D. S. Iii. Smart grid and energy storage : Policy recommendations. *Renewable and Sustainable Energy Reviews*, (July 2016):1–9, 2017. ISSN 1364-0321. doi: 10.1016/j.rser.2017.07.011. URL `http://dx.doi.org/10.1016/j.rser.2017.07.011`.

[106] X. Zhang, G. Hug, and I. Harjunkoski. Cost-effective scheduling of steel plants with flexible eafs. *IEEE Transactions on Smart Grid*, 8(1):239–249, Jan 2017.

[107] P. Zhao, G. P. Henze, S. Plamp, and V. J. Cushing. Evaluation of commercial building HVAC systems as frequency regulation providers. *Energy and Buildings*, 67:225–235, 2013. ISSN 03787788. doi: 10.1016/j.enbuild.2013.08.031. URL `http://dx.doi.org/10.1016/j.enbuild.2013.08.031`.

[108] D. Zhou, C. Y. Zhao, Y. Tian, M. C. Lott, S.-I. Kim, P. Eames, D. Loveday, V. Haines, P. Romanos, European Commission, F.-m. Advantage, N. Term, B. Post, IRENA, ETSAP, and DNV KEMA Energy and Sustainability. Technology Roadmap. *SpringerReference*, 92 (January):24, 2013. ISSN 03062619. doi: 10.1007/SpringerReference_7300. URL `http://www.springerreference.com/index/doi/10.1007/SpringerReference{_}7300`.